Investigation on Switching Technologies for Hybrid Wireless Networks (RF and FSO)

Dissertation submitted by

FARUKH NADEEM

to the Faculty of Electrical Engineering and Information Technology

Graz University of Technology, Austria

in partial fulfillment of the requirements for the degree of

Doctor of Philosophy (Dr. Technische)

at the

Institute for Broadband Communication

Supervisor and Reviewer: Prof. Dr. Erich Leitgeb

Second Reviewer: Prof. Dr. Gorazd Kandus, IJS, Ljubljana

Graz, May 2010

Declaration - EIDESSTATTLICHE ERKLÄRUNG

Ich erkläre an Eides statt, dass ich die vorliegende Arbeit selbstständig verfasst, andere als die angegebenen Quellen/Hilfsmittel nicht benutzt und die den benutzten Quellen wörtlich und inhaltlich entnommenen Stellen als solche kenntlich gemacht habe.

Graz, am:————- (Unterschrift)————————..

STATUTORY DECLARATION

I declare that I have authored this thesis independently, that I have not used other than the declared sources / resources and that I have explicitly marked all material which has been quoted either literally or by content from the used sources.

Graz, dated:————- Signature————————..

Dedication

To my parents.

CONTENTS

LIST OF FIGURES

LIST OF TABLES

Acknowledgements

This thesis finds me indebted to many colleagues and scientists, who have helped me in numerous ways in the completion of this task. The first acknowledgement is for all the co-workers at the Institute of Broadband Communications (IBK) who ensured in providing a relaxed and very friendly working environment. Many thanks are due to my colleagues who have helped me by discussions and guidance. They include Muhammad Saleem Awan, Muhammad Saeed Khan, Benno Flecker, Michael Gebhart, Paul Brandl, Thomas Plank, Pirmin Pezzei.

My advisor for the PhD work, Prof. Erich Leitgeb has always provided me the necessary guidance and help. His encouragement in different aspects of the work contributed to my personal and professional development. He has helped me in numerous ways during the course of this work, and provided me all required resources to accomplish the task. His dedication to his work was always exemplary, and he was the main driving force behind most of the research accomplished during the course of the thesis. I would also like to thank Prof. Gorad Kandus for agreeing to act on my examination committee, and his valuable suggestions helped refine the work.

The masters students who worked with me, provided many important inputs and were a great helping hand, namely Bernhard Geiger and Maximilian Henkel. Both have been extremely supportive during the emotionally exhaustive intense research. I would also like to thank Dr. Markus Loeschnigg for his financial support for experimental setup.

I would also like to acknowledge the financial support of the Higher Education Commission of Pakistan which made this work possible. The Europe-wide network of excellence in Satellite Communications (SatNEx) played a vital role in the dissemination of the research results.

Thanks to my wife and other family members, who have remained the binding force in my life all through this work. Thanks to my Lord, Allah who gifted me with this life and all its surprises.

Abstract

Free Space Optics (FSO) or optical wireless systems provide high data rate solution for bandwidth hungry communication applications. Carrier class availability is a necessity for wide scale acceptability which is extremely difficult to achieve in the case of optical wireless links. FSO links are highly weather-dependent and different weather effects reduce the link availability. Employing a hybrid network consisting of an FSO link and a back up link in the GHz frequency range renders high availability besides providing comparable data rates.
The thesis proposes different switch over algorithms for hybrid FSO/RF and analyses their performance under different weather conditions. After a short description of the available technologies in this thesis, first the different weather influences on FSO and GHz links are analysed. In the following part merits and demerits of useful Switch-Over technologies of FSO-RF-Hybrid-Networks are analysed and discussed. Considering the results of these investigations, the best suited solution (Algorithm) is proposed which has been evaluated in practice. After the implementation and realisation of this Switch-Over technology, some applications are considered. At the end as a special application, the performance of hybrid wireless networks has been analysed for power optimisation of wireless sensor networks.

Zusammenfassung

Free Space Optics (FSO) oder optische Freiraumübertragungssysteme bieten eine hohe Datenrate und somit eine Lösung für bandbreitenintensive Kommunikationsanwendungen. Die von den Telekomprovidern klassifizierte und geforderte Verfügbarkeit ist im Fall der optischen drahtlosen Verbindungen eine Notwendigkeit, aber schwer erreichbar, weshalb die Akzeptanz der Systeme äuSSerst gering ist. FSO-Verbindungen sind sehr witterungsabhängig und verschiedene Wetter-Effekte reduzieren die Zuverlässigkeit und Verfügbarkeit der Übertragungsstrecke. Durch die Verwendung eines Hybrid-Netzwerkes, bestehend aus einer FSO-Verbindung und einer Back-Up-Verbindung im GHz-Frequenzbereich (RF) wird eine hohe Verfügbarkeit mit vergleichbaren und brauchbaren Datenraten erreicht.
In der vorliegenden Arbeit, werden verschiedene Umschalt-Algorithmen für Hybrid-Verbin-dungen (realisiert mit RF und FSO) vorgeschlagen, wobei deren Leistungsfähigkeit unter diversen Wetterbedingungen analysiert wird. In der Arbeit werden nach einer kurzen Darstellung der vorhandenen Technologien zuerst die unterschiedlichen Witterungseinflüsse auf FSO und GHz Links untersucht und miteinander verglichen. Im folgenden Teil der Arbeit werden sinnvolle Möglichkeiten der verschiedenen Switch-Over-Technologien eines FSO-RF-Hybrid-Netzwerks analysiert und diskutiert, sowie deren Vor- und Nachteile erarbeitet. Auf Grund dieser Untersuchung wird die geeignetste Lösung (Algorithmus) vorgeschlagen, welche auch praktisch getestet wurde. Nach der Implementierung und Realisierung dieser Switch-Over-Technologie wurden noch Anwendungsfälle betrachtet. AbschlieSSend wurde als spezielle Anwendung die Leistung eines Hybrid-Wireless-Netzwerkes zur Leistungsoptimierung von Wireless Sensor Networks analysiert.

1 INTRODUCTION

The thesis presents the weather influences analysis of Free Space Optics/ RF hybrid network so that hybrid FSO /RF combination with highest availability can be selected. As fog is the major concern for FSO, the comparative analysis of different fog attenuation predicting models is also presented. Different switch over algorithms are proposed and their performance is analysed in terms of availability. The traffic data requirement and availability of FSO/RF network have been comparatively analysed. Power Consumption efficient Wireless sensor networks employing FSO/RF hybrid networks are analysed.
The thesis analyses the performance of hybrid FSO/RF hybrid network under conditions of fog, rain, snow and cloud. This analysis can help the selection of FSO wavelength and back up links for achieving high availability.

1.1 Overview

Line of sight optical wireless high-bandwidth transmission links have tremendous potential to serve for the future huge data transmission requirements. The concept of transmitting information through the air by means of modulated light signal is quite simple: a narrow beam of light is launched at a transmission station, transmitted through the atmosphere, and subsequently received at the receive station Inherent high carrier frequency (in 20 THz - 375 THz range) enables Free Space Optics (FSO) to provide communication with highest data rates. License free communication, easy installation, avoiding electromagnetic pollution and wiretapping safety are few other advantages. Additionally, FSO communication provides solution to problems like first / last mile access connectivity, broadband internet access to rural areas and disaster recovery etc. Next generation high speed optical networks can employ FSO links in point-to-point as well as optical multi-input multi-output (MIMO) configurations [26, 56]. Some of the possible implementation scenarios are delay free web browsing and data library access, electronic commerce, streaming audio and video, video on demand, video teleconferencing, real time medical imaging transfer, enterprise networking, work-sharing capabilities and high speed interplanetary internet links [5]. FSO communication is recently investigated for ground-to-ground (short and long distance line of sight (LOS) terrestrial links), satellite uplink/downlink, inter-satellite, satellite or deep space probes to ground, ground-to-air (e.g., Unmanned Area Vehicle (UAV), High Altitude Platforms (HAP) etc.) / air-to-ground terminal. This endeavour has resulted in some successful experiments by European Space Agency (ESA) like SILEX (Semiconductor intersatellite link) - the link between Optical Ground Station (OGS) and ARTEMIS

(Advanced Relay Technology Mission Satellite) and the earth reconnaissance low earth orbit (LEO) satellite SPOT-4 [36]. The performance of RF and optical links has been compared for deep space communication and optical communication link has been found suitable for high data rate near earth satellite links [101].

1.2 Motivation

The widespread growth of the technology has been held back by reliability and availability issues [55, 20] related to weather influenced attenuations like fog, snow and rain. The fog is the major attenuating factor as it causes significant attenuation for non negligible time [38, 59]. Consequently FSO short fall of the desired carrier grade availability of 99.999%. The alternate solution is to use back up RF link in order to cope the weather effected reduced availability of FSO link [47]. Different combinations of FSO and back up transmission links had been proposed for various application scenarios like hybrid link for airborne applications [105], ad-hoc mobile networks [31, 30] and terrestrial and space applications [15, 32, 47, 96]. The idea behind using such a hybrid network is to utilize the potential of other link when main link is not fully functional.
However, the availability analysis in the presence of weather influenced attenuations can be helpful for selecting the optimum FSO/RF hybrid network. This analysis can provide a way out to achieve the required carrier grade availability. The performance analysis of different switch over algorithms can enhance the utilisation of potential provided by two technologies while maintaining the availability of hybrid network.

1.3 Different back up link technologies

The two technologies Millimeter Wave (mmW) system and IEEE 802.11 generally used and installed in Graz University of Technology as back up link are discussed here.

1.3.1 Millimeter Wave (mmW) system

Due to their high carrier frequencies ranging from several tens of GHz up to more than 100 GHz Millimeter Wave communication systems also offer very high data rates comparable to FSO. Operated at the diffraction limit, high directivity can be achieved even with small antenna dishes in the range of 20 cm. Although the frequency range up to 375 GHz is governed by Frequency Control Commissions worldwide, there are some license-free bands available like 77 GHz with limitations in power and other properties.
The most promising technology for a cost-effective market solution is based on integrated semiconductor amplifiers. For this new technology however, several technical challenges

exist. Temperature drift of oscillators and filter stages, noise , low available output power and device aging under thermal stress are critical points today. As the price increases much for Millimeter Wave semiconductor amplifiers, system costs would increase much with link distance, for a given bit rate and availability.
The channel for terrestrial outdoor mmW communication links has different characteristics as compared to wireless optical communication. Rain causes the main attenuation contribution. Fog on the other hand is less important (except for wavelengths which are absorbed by water vapours, as in the 22 GHz range). This complementary behaviour gives rise to the concept of a hybrid system, combining advantages of FSO and mmW to a wireless communication link offering high data rates and high availability at reasonable costs.
The mmW equipment at Graz university of Technology was a prototype designed for an LMDS experimental setup operating at 10 - 100 Mbit/s (depending on modulation scheme and symbol rate) at a carrier frequency in the 40.5 - 43.5 GHz band.

1.3.2 IEEE 802.11 standards

The IEEE 802.11 [29] is an international standard of physical and MAC layer specifications for wireless local area networks in the 5 GHz and 2.4 GHz public spectrum bands. The original version supports data rates of 1-2 Mbps but this initial specification was extended by the amendment IEEE 802.11a which specifies the operation in the 5 GHz band with a nominal data rate of 54 Mbps.
The IEEE 802.11 standard has many features that motivate to use it as a back up link. The major goal of a back up link is to withstand fog attenuation when the main link (FSO) is strongly affected by fog. Research studies have shown that links below 10 GHz frequency are optimal back up links for highly available hybrid wireless networks as these links show negligible attenuation due to fog. The IEEE 802.11a back up link does not cause an abrupt performance decline but rather provides soft degradation of the data rate during a fog event. Another reason to support IEEE 802.11a as back up link is license free usage.
The preference of 802.11a as back up link over 2.4 GHz link is favoured due to the absence of radio interference caused by microwave ovens or an overcrowded band with overlapping channels. Thus 802.11a should provide an increased reliability regarding the bandwidth or a total link failure. Moreover concerning the regulatory conditions in Europe it is possible to operate 5 GHz equipments outdoors with far higher output levels compared to the widely used IEEE 802.11b/g standard (2.4 GHz). This transmit power level is only allowed if transmission power control (TPC) and dynamic frequency selection (DFS) is enabled to avoid interference with other equipment operating in this frequency range [28]. The latter also helps against interference on specific channels. Additionally suitable antennas which give a narrower beam are used to provide behaviour comparable to the FSO link. This results in an even more robust link between the two points except the uncertain event of an interfering system inside the beam.

1.4 Thesis structure and Research contributions

The combined FSO/RF hybrid network can achieve high availability. However efficient switch over algorithm is required to avoid redundant transmission on both links. Different switch over algorithms are proposed. These algorithms improve the performance of the hybrid FSO/RF hybrid network while maintaining the availability achieved by redundant transmission on both links. Implementation of self synchronising algorithm and load balancing algorithms are also presented. The link loss during switch operation required forward attenuation prediction. Forward attenuation prediction algorithm is analysed.
As an application, Power consumption efficient Wireless sensor networks employing FSO/RF hybrid networks are analysed. Switch over algorithm for such Wireless sensor network is proposed that improves the life time of Wireless sensor network.
The detailed availability analysis under different weather conditions was required for FSO/RF hybrid network. The intention was to evaluate the existing FSO/RF hybrid network so that the optimal hybrid network with highest availability can be selected. As fog is the major attenuating factor, the comparison of existing fog attenuation predicting models was important so that the most accurate attenuation prediction can support the availability analysis. This analysis required the attenuation measurements. Previous results showed that different fog types can produce different attenuations. The data was collected from different locations Nice, Graz and Prague with the motivation of analysing location dependent attenuation behaviour.
The state of the art literature survey of the FSO/RF hybrid networks is discussed in Chapter 2. The main contributions of the thesis are the simulation for weather effect analysis of FSO/RF hybrid network, different FSO wavelength attenuation comparison analysis, different fog attenuation predicting models comparison analysis, availability analysis of different FSO/RF hybrid network combinations presented in Chapter 3; proposing of different switch over algorithms, their performance analysis in terms of throughput and bandwidth utilisation, implementation of self synchronising approach, and load balancing algorithms in chapter 4. The implementation and measurement based on implementation, comparison of traffic data and availability data of FSO/RF hybrid network, proposal and analysis of switch over algorithm for power efficient Wireless sensor network employing FSO/RF hybrid network and Forward attenuation prediction and future application of hybrid network for Satellite and HAPs are discussed in Chapter 5. Chapter 6 conclude the thesis with summary of results. The originality and significance of the above thesis contributions is reflected by publication of parts of this thesis in several refereed conference proceedings and journals (End of the thesis "Own Publications").

2 HYBRID NETWORK- STATE OF THE ART REVIEW

The benefits of FSO motivates to use it for high data rate demanding communication applications. However FSO also poses some important challenges such as sensitivity to misalignment between transmitter and receiver, atmospheric turbulence induced fading, and severe signal attenuation caused by adverse weather conditions such as fog. This makes the achievement of carrier class availability of 99.999% a great challenge. The addition of back up link can provide the solution. This approach has created significant interest in hybrid FSO/RF hybrid networks.

2.1 Earlier Hybrid networks

Kim and Korevar [47] analysed that FSO can meet the required carrier class availability with reduced range depending upon the link budget. For instance they observed that FSO links should be less than 140 m with link budget of 54 dB and less than 286 m for a link margin of 100 dB. To achieve much larger metro access, they proposed FSO/RF hybrid network with RF link of 2.4 GHz and concluded that carrier class availability can be achieved with some compromise on bandwidth.
Scot Bloom [15] proposed FSO/RF hybrid network with 60 GHz back up link for last mile access. He observed that in majority of the cities in the world FSO can obtain carrier class availability only within 500 m. He quoted one plus one equals 5 nines for hybrid FSO/RF network.

2.2 First FSO/RF hybrid network implementations

Ahmet Akbulut et al. [32] presented the results for 1550 nm FSO/ 2.4 GHz RF (802.11b) hybrid network at Ankara University Turkey. He first time explained the design procedure for hybrid network. He showed that Laser link was up for much higher availability 99.98% as he used longer wavelength of FSO 1550 nm.
Wolfgang Kogler et al. [49] used mmW as back up link for FSO/RF hybrid network at Graz University of Technology, Austria. The FSO link was 850 nm used for 2.7 km and back up link was operated at 40-43 GHz. The ping test was used as a measure of availability and yearly availability of 99.926 % was achieved despite the low individual link availability of 97%.

Erich Leitgeb, Michael Gebhart et al. extended the work of Kogler and presented the results in [52]. They showed that despite 80% FSO availability in December and overall 93.6% average yearly FSO availability, hybrid network achieved 99.926% availability.

2.3 Tactical and Earlier Air borne applications of hybrid network

Milner and Davis [58] presented hybrid FSO/RF network application for tactical operations. They discussed the topology and diversity control, pointing, acquisition and tracking (PAT) and joint FSO/RF transceiver with PAT. It was shown that Flexible, hybrid FSO/RF wireless networks with topology control have the ability to provide high availability with performance that can be optimized in the competing problems of link physics, traffic flows, and network management.
Tzung-Hsien Ho et al. [41] extended the work of Milner and Davis and came up with testbed in order to conduct studies of the performance of FSO/RF links under various atmospheric conditions; and investigate network performance using discrete event simulation. In order to make their network simulations realistic, they incorporated the real-world performance of FSO and RF links through the atmosphere, including attenuation of FSO by clouds, FSO degradation by turbulence and the effects of rain. The results confirmed that the hybrid link provided reliability through redundancy.
Kashyap and Shayman presented routing framework for FSO/RF backbone networks in [46]. They addressed the issue of providing obscuration tolerant paths (paths having instantaneous backup) to traffic on a hybrid RF/FSO backbone network, given a traffic profile. As FSO links offer higher bandwidth and security, while RF links offer more reliability, so they introduced the concept of criticality index for traffic profile entries, which was used in determining the fraction of traffic for each profile entry which is routed on obscuration tolerant paths. They provided optimal algorithms for the case where traffic can be split over multiple paths.
Wu et al. [104] focused on examining availability of an airborne hybrid RF/FSO links. The channel model was established based on factors such as scattering, absorption, scintillation, etc. Based on the channel model, along with cloud information acquired from the ISCCP database, they produced the probability distribution of capacity for both the RF and FSO channels. From the results, it was shown that FSO alone can only achieve a very small availability, due to its strong sensitivity to cloud blockage. But with a backup RF link, availability can be significantly increased due to the immunity of RF signals to cloud attenuation. However, if backup RF links is used during FSO down time, capacity is still significantly reduced due to bandwidth limitations on the RF channel.

2.4 Further details of first proposed switch over

Akbulut et al. extended their work of [32] and presented new results in [8]. They presented the results of two years availability measurement. As they used the longer wavelength of FSO 1550 nm, they measured the average availability of 99.986%. They observed that snow storms are the most destructive for the availability of FSO.

2.5 Other hybrid networks

Llorca et al. [54] presented methodologies for modeling and simulation of hybrid FSO/RF networks. Individual link propagation models were derived using scattering theory, as well as experimental measurements. Network performance in the form of dropped packets and average end-to-end delay was measured for low, medium and high obscuration scenarios. The results conclusively showed performance improvement with topology control and enhanced link state routing for mobile hybrid FSO/RF networks. They considered FSO 1550 nm and RF 1 mm.
Derenick et al. [31] considered FSO/RF hybrid network for mobile adhoc networks. The primary motivation of using FSO for such networks is the tremendous throughput provided by FSO over long link distances. However, the technology also offers additional advantages such as lower per-bit power consumption and a secure/robust transmission medium. They proposed optimal deployment scheme so that robots can autonomously establish optical links over sufficiently long distances as well as the formulation of a mobile network architecture can exploit high throughput FSO channels. They also provided initial experimental results from autonomous deployments of a hybrid FSO/RF MANET with real-time video data routed across both optical and RF links [30].
Sana et al. [96] proposed a novel Ethernet-based wired/wireless broadband access networking architecture that utilizes the existing wired trunk feeder fiber of either passive optical network (EPON) infrastructure along with a hybrid FSO/RF reliable wireless connectivity to the end-users Optical Network Units (ONUs). By combining the benefits of both FSO and RF technologies, the proposed integrated networking solution can provide a downstream bandwidth of up to 2.5 Gbps per wavelength and 99.999% availability at a range of 1 km in all weather conditions fewer packet drops, less delay and better through put.
Jia et al. [42] investigated BER performance of the hybrid FSO/RF system operating atmospheric attenuation channels. The performance was demonstrated using numerical simulations. They concluded that in FSO systems, BER increases sharply with the decreasing visibility through fog while BER increases as the rain rate is growing in RF systems.
Wu and Kavehard [105] focused on examining availability of an airborne hybrid RF/FSO links. A channel model was established, incorporating factors such as scattering, absorption, scintillation, etc. Based on the channel model, along with the cloud information

acquired from the ISCCP database, they produced the probability distribution of capacity for both the RF and FSO channels. From the results, it was shown that FSO-alone can only achieve a very small availability, due to its strong sensitivity to cloud blockage. But with a backup RF link, availability can be significantly increased due to the immunity of RF signals to cloud attenuation. However, if a backup RF link is used during FSO down time, capacity is still significantly reduced due to bandwidth limitations on the RF channel. For relatively thin clouds, multiplexing schemes can be used to significantly improve FSO channel capacity, and thus enhance the FSO subsystem availability.
A patent [3] used an optical, wavelet-based fractal modulation of ultra-short light pulses as part of a high-bandwidth communications system. The preferred embodiment utilizes the scheme as part of a hybrid wireless optical and RF transmission system for broadband communications among fixed and/or mobile platforms. An ultra-short pulse laser, high-power WDM-ARRAY laser or high-power incoherent light sources may be used. Computer-generated hologram techniques are employed in designing the optical transceiver subsystems for spectral encoding and decoding of wavelet patterns. Part of the design goal is to select a diversity receiver Field-of-View (FOV) in a way that the effects of scintillation are reduced by as much as possible. Compared to existing optical wireless systems, the invention offered a much higher average transmission bit rate and a much smaller bit error rate outage value, thus enabling highly available FSO links. Wireless transceiver will be capable of communications with nearly line-of-sight FSO links and will be more tolerant to shadowing. Also, the optical medium is designed to be more secure than counterparts against any intrusion.
Till the start of the thesis work, the state of the art work on hybrid network either did not provide the details of switch over for network or only used redundant transmission on both links. The switch over algorithms were analysed so that potential of both technologies can be optimally utilised while maintaining the availability provided by the hybrid network.
Moreover a detailed analysis of the weather influences on hybrid network was required so that availability optimum combination of FSO/RF network can be selected for implementation of FSO/RF hybrid network. The detailed analysis was required for all the weather influences like fog, rain, snow and clouds. The analysis and results are presented in the next chapters.

3 WEATHER EFFECTS ANALYSIS OF HYBRID FSO/RF NETWORK

Despite the great potential of wireless optical communication, its widespread deployment has been hampered by reliability or availability issues related to atmospheric variations. Research studies have shown that FSO specific attenuation has peak values of 120 dB/km in continental fog conditions in Graz (Austria) and 480 dB/km in maritime fog conditions in La Turbie (France) [59]. In addition to fog, weather effects of rain and snow restricts FSO to achieve the carrier class availability of 99.999%. The alternate solution is to use back up link. The availability for such a hybrid network of FSO and 40 GHz back up link was measured to be 99.92% in spite of 96.8% availability of FSO alone [52]. However, the weather effects on both of the links should be thoroughly investigated in order to fully assess the shortcomings of hybrid network. It is thus important to investigate the appropriate characteristics of such hybrid network and to identify which back up frequency ranges are best suited to overcome weather attenuations of FSO for terrestrial and space networks. In this chapter weather effects on hybrid network of optical wireless link and GHz frequency back up links are analyzed for the most deterrent weather phenomenon like fog, rain, snow and clouds.

3.1 Fog Effects on FSO

The main challenge for the implementation of outdoor short-range optical wireless links is the atmospheric attenuation caused due to absorption and scattering. Water particles and carbon dioxide cause the absorption of optical signals. Scattering takes place in fog, haze, rain and snow and it causes portion of light traveling from a source to deflect away from the intended receiver [1]. Among various atmospheric attenuation effects on FSO communication, fog is the most important factor. It is highly deterrent for achieving high availability in FSO, causing significant attenuation for considerable amount of time. As the size of fog particles is comparable to the transmission wavelength of optical and near infrared waves, it causes attenuation due to scattering. The most accurate way to calculate attenuation in case of fog droplets is based on Mie scattering theory. However, it requires detailed information of fog parameters like particle size, refractive index, particle size distribution etc. which may not be readily available at a particular location of installation. Moreover it involves complex computations.

3.1.1 Fog attenuation models based on visibility

Another approach is to predict specific attenuation due to fog using visibility data. The visibility is the distance to an object where the image contrast drops to 5% of what it would be if the object were nearby instead. The wavelength used to measure the visibility is 550 nm which is used as visibility reference. The transmissiometer in meteorological stations or at airports usually operate at 550 nm center wavelengths with 250 nm bandwidth to collect visibility data.
The models Kruse [37], Kim [48] and Al Nabulsi [61, 17] are discussed here. These models use visibility to predict specific attenuation. The specific attenuation for both Kim and Kruse model is given by

$$\alpha_{Fog} = \frac{10\log V\%}{V(km)}\left(\frac{\lambda}{\lambda_0}\right)^{-q}. \tag{3.1}$$

Here V(km) stands for visibility, V% stands for transmission of air drops to percentage of clear sky, λ in nm stands for wavelength and λ_0 as visibility reference (550 nm). For Kruse model [37].

$$q = \begin{cases} 1.6 & \text{if V} > 50 \text{ km;} \\ 1.3 & \text{if 6km} < \text{V} < 50 \text{ km ;} \\ 0.585V^{\frac{1}{3}} & \text{if V} < 6\text{km.} \end{cases} \tag{3.2}$$

According to Kim [48] the value of the q parameter is,

$$q = \begin{cases} 1.6 & \text{if V} > 50 \text{ km;} \\ 1.3 & \text{if 6km} < \text{V} < 50 \text{ km ;} \\ 0.16V + 1.34 & \text{if 1km} < \text{V} < 6 \text{ km ;} \\ V - 05 & \text{if 0.5km} < \text{V} < 1 \text{ km ;} \\ 0 & \text{if V} < 0.5\text{km.} \end{cases} \tag{3.3}$$

Eqn. 3.2 implies that for any meteorological conditions, there will be less attenuation for higher wavelengths. Therefore, attenuation of 1550 nm is expected to be lesser than attenuations at shorter wavelengths. Kim rejects such wavelength dependency of optical attenuations for low visibility range conditions as in dense fog.
Al-Naboulsi [61, 17] characterizes advection and radiation fog separately and proposed two different models for advection and radiation fog. The advection fog is formed by the movements of wet and warm air masses above the colder maritime surfaces while Radiation fog is related to the ground cooling by radiations over continental surfaces. According to Al-Naboulsi the advection fog model is,

$$\alpha_{ADV}(\lambda) = \frac{0.11478\lambda + 3.8367}{V} \tag{3.4}$$

and for radiation fog model is,

$$\alpha_{RAD}(\lambda) = \frac{0.18126\lambda^2 + 0.13709\lambda + 3.7502}{V}. \tag{3.5}$$

The specific attenuation for both types of fog can simply be calculated as follows,

$$A_{Fog}(dB/km) = \frac{10}{\ln(10)}(\alpha(\lambda)). \tag{3.6}$$

3.1.2 Wavelength Comparison of different FSO wavelengths

The long wavelengths have been found to be more resistant to fog attenuations and it has been analysed that long wavelengths typically have better fog penetration as high as twice (stable fogs) and ten times (selective fogs) the transmission of shorter wavelengths [7]. It has been observed that the 3.5-micron line-of-sight laser communication system can obtain an acceptable quality of service for a line-of-sight propagation [39]. In addition to the advantages of less attenuation under a wide variety of channel conditions long wavelengths also exhibit increased safety and immunity to solar background interference [91]. However, all currently available commercial FSO systems are using wavelengths between 0.78μm to 1.55μm. The key benefit of these wavelengths is that components are readily available since they are similar to the components used in fibre optic communications and other industrial and consumer applications.

3.2 Effect of Fog on GHz Links

The small fog droplets also cause scattering and significant attenuation for backup radio frequencies greater than 10 GHz. While the effect on frequencies lesser than 10 GHz is ignorable. In case of fog droplets with size lesser than 0.01 cm and frequencies below 200 GHz, the Rayleigh approximation is valid. The total water content per unit volume can be used to express attenuation. The specific attenuation γ_{Fog} is given by [89],

$$\gamma_{Fog} = K_l M, \tag{3.7}$$

Eqn. 7 where
γ_{Fog}: specific attenuation in dB/km within the cloud or fog
K_l: specific attenuation coefficient $(dB/km)/(g/m^3)$
M: liquid water density in cloud or fog (g/m^3).

The specific attenuation coefficient can be calculated using mathematical model based on Rayleigh scattering. This model uses double-Debye model for the dielectric permittivity $\varepsilon(f)$ of water, where ε(f)= $\acute{\varepsilon}$ + j$\acute{\acute{\varepsilon}}$. The specific attenuation coefficient is given as,

$$K_l = \frac{0.819f}{\acute{\varepsilon}(1+\eta^2)}. \tag{3.8}$$

where f is frequency in GHz, ε is complex dielectric permittivity (union of real and imaginary parts) andη is,

$$\eta = \frac{2+\acute{\varepsilon}}{\acute{\acute{\varepsilon}}}. \tag{3.9}$$

The complex dielectric permittivity of water is given as,

$$\acute{\acute{\varepsilon}}(f) = \frac{f(\varepsilon_0 - \varepsilon_1)}{f_p(1+(\frac{f}{f_p})^2)} + \frac{f(\varepsilon_1 - \varepsilon_2)}{f_s(1+(\frac{f}{f_s})^2)}. \tag{3.10}$$

$$\acute{\varepsilon}(f) = \frac{f(\varepsilon_0 - \varepsilon_1)}{(1+(\frac{f}{f_p})^2)} + \frac{f(\varepsilon_1 - \varepsilon_2)}{(1+(\frac{f}{f_p})^2)} + \varepsilon_2. \tag{3.11}$$

In the above expressions f_p and f_s are principal and secondary relaxation frequencies in GHz respectively and are expressed as,

$$f_p = 20.09 - 142(\frac{300}{T} - 1) + 294(\frac{300}{T} - 1)^2 \tag{3.12}$$

$$f_s = 590 - 1500(\frac{300}{T} - 1). \tag{3.13}$$

here T is temperature in Kelvin and

$$\varepsilon_0 = 77.6 - 103.3(\frac{300}{T} - 1); \tag{3.14}$$

$$\varepsilon_1 = 5.48; \tag{3.15}$$

$$\varepsilon_2 = 3.1. \tag{3.16}$$

Visibility range can be expressed in terms of liquid water content as [33],

$$V = 0.024M^{-0.65}. \tag{3.17}$$

where V is the visibility range in km and M is liquid water content in g/m^3.

3.3 Rain attenuation of FSO

When the optical signal passes through the atmosphere, it is randomly attenuated by fog and rain. The main attenuation factor for optical wireless link is fog. However, rain also imposes certain attenuation.
When the size of water droplets of rain becomes large enough to cause reflection and refraction process, these droplets cause wavelength independent scattering [100]. Most of the rain drops fall in this category. The attenuation linearly increases with rainfall rate, and

the mean of the raindrop sizes increases with the rainfall rate and is in the order of a few mm [6]. The specific attenuation of wireless optical link for rain rate of R mm/hr is given by [100]

$$\alpha_{Rain} = 1.076R^{0.67}. \tag{3.18}$$

The most general form of raindrop size distribution function Na is given by Weibull [18]

$$N_a = \frac{N_T}{a_0 V_a}\phi(n)n(\frac{a}{a_o})^{n-1}e^{-\phi(n)\frac{a}{a_o}n}. \tag{3.19}$$

such that $a_0 = d(z_a)^b e^{-cz_a}$ and $\phi(n) = \Gamma^n(1+\frac{1}{n})$.

Here z_a is the rainfall rate of raindrops having radius a. The most common rainfall has following values [18]:
d = 0.941, b = 0.336, c = 0.471102 and n = 3.

The overall constant in the above equation N_T represents the total number of raindrops of all sizes in unit volume. The total scattering coefficient by rain can be derived from the following Eq.(3.20) [6]:

$$\beta_{scat}^{rain} = \sum_a \pi a^2 N_a Q_{scat}(\frac{a}{\lambda}). \tag{3.20}$$

Here Q_{scat} is the scattering efficiency, also referred to as the Mie attenuation coefficient.

3.4 Rain attenuation of GHz links

The performance of the microwave communication system is also effected by rain attenuation. Although the propagation of signals is greatly disturbed by fog, clouds and dust particles but rain is the major attenuating factor at frequencies above 10 GHz [94].The relationship between specific attenuation and rain rate is given by

$$\gamma_{Rain} = kR^{\alpha} \tag{3.21}$$

where k and α depend upon the frequency and microstructure of rain. The theoretical back ground of the above relationship is given in [86].The main parameters associated with rain are shape, drop size distribution and temperature of rain drops.
The shape of the rain drops can be spherical, spheroid , oblate or shapes described by [92]. The shape of the drop does not play significant role because the error between specific attenuation by spherical shape and other shapes is less than 10% for mmW [86, 21].
Different raindrop-size distributions have been reported. The earliest paper on the size of raindrops was by Laws and Parsons [50]. Later, Marshall and Palmer proposed the famous exponential raindrop-size distribution [57]. Other distributions include Joss [44],Gamma distribution [13] and Weibull distributions [43]. The temperature is another important

factor. However, the temperature does not effect significantly above 15 GHz. Generally 0 °C. and 20 °C. are used temperatures for attenuation prediction. But 20 °C is a reasonable assumption for attenuation prediction of terrestrial links [34].
There are two popular models for prediction of rain attenuation; ITU [88] terrestrial model and Crane [22, 23, 24] models.
According to ITU-R model, constant k and α in Eq. 3.21 is given as

$$k = \frac{(k_H + k_V + (k_H - k_V)\cos^2\theta\cos 2\tau)}{2}, \tag{3.22}$$

$$\alpha = \frac{(k_H\alpha_H + k_V\alpha_V + (k_H\alpha_H - k_V\alpha_V)\cos^2\theta\cos 2\tau)}{2k}. \tag{3.23}$$

The values of constants k_H, , k_V , α_H and α_V are given in [88]. The values of k and α in Eq. 3.21 are also given in Crane model for different frequencies.

3.5 Snow attenuation on FSO

Fog, rain and other precipitations causes the scattering of the light and the laser beam power is attenuated resulting in reduction of received signal strength. Consequently either complete link failure or bit errors occurs when received signal fluctuations are large and received signal level decreases drastically [10]. The amount of light attenuation is proportional to number and size of fog, rain and snow particles [6, 18]. It is well known that variation in the received signal strength increase with the amount of rainfall [10, 102, 12]. Since snow flakes are generally larger than rain drops, the received signal strength fluctuation will be larger for snow and snow attenuation is not ignorable [9]. The snow flakes as large as 20 mm have been reported [107, 51] and a large snowflake can cause link failure if laser beam is narrow. When a snowflake crosses the laser beam, the receive signal level depends on the diameter of the snowflake and distance from the transmitter, as well as the position of the snowflake relative to the cross section of the beam [9]. The FSO attenuation due to snow has been classified into dry and wet snow attenuations. If S is the snow rate in mm/hr then specific attenuation in dB/km is given by [60].

$$\alpha_{_{Snow}} = aS^b \tag{3.24}$$

If λ is the wavelength, then for dry snow the values of parameters a and b are,
$a = 5.42 \times 10^{-5}\lambda + 5.4958776$ and $b = 1.38$.
The values of same parameters for wet snow are,
$a = 1.023 \times 10^{-4}\lambda + 3.7855466$ and $b = 0.72$.

3.6 Snow attenuation for GHz links

The fog, rain or snow particles affect the GHz link due to scattering. In the calculation of the scattering properties of various kinds of hydrometeors, the knowledge of their dielectric properties is fundamental. Snow particles are the complicated mixtures of ice with air, water, or both. The mixing rate and the shapes of the constituents may vary considerably depending on external meteorological conditions to which snow particles are exposed. In the theoretical treatment of the electrical properties of such a mixture, it is assumed that the component materials are large enough to be able to assign their dielectric functions. Nevertheless, finding the "effective" dielectric function of such a mixture is a quite difficult problem since a large number of interactions can occur among the component materials; the solutions can only be obtained by various approximations. The radio wave attenuation due to snow are difficult to analyze as there is lot of weather dependent variation in shape, dielectric constants and size distribution of snow flakes. It is certain that the attenuation due to dry snow in the microwave region is an order of magnitude less than that due to rain of the same rate of precipitation. However, wet or watery snow gives attenuation comparable to that due to rain in the microwave and millimeter-wave regions. Attenuation often exceeds that of rain; attenuation as large as six to seven times the attenuation due to rain was reported [87]. Measurements made at a wavelength of 0.96 mm by have indicated that, at this wavelength range, the attenuation even by dry snow exceeds by 30 to 40 percent the attenuation due to rain of the same intensity [85]. This indicates that the snow attenuation may be increasingly important as wavelengths get short. The specific snow attenuation γ_{Snow} in terms of snow rate S is given as follows [85]

$$\gamma_{Snow} = 0.00349\frac{S^{1.6}}{\lambda^4} + 0.00224\frac{S}{\lambda}. \tag{3.25}$$

3.7 Experimental Setup

The attenuation measurement campaign at Graz, Austria was carried out in the winter months from 2004 to 2005 and 2005 to 2006. IR link at 850 nm and 950 nm wavelengths was used for a distance of 79.8 m and 650 m. The optical transmitter used has two independent LED based light sources. One operates at 850 nm center wavelength with 50 nm spectral width at a full divergence of 2.4 deg which emits 8 mW average optical power; average emitted power in this case after the lens is about 3.5 mW. Second source operates at 950 nm center wavelength with 30 nm spectral widths at a beam divergence of 0.8 deg using four LEDs each emitting 1 mW to produce the same average power at the receiver. The data was collected and sampled at 1 s. The results were reported in [59, 38]. In year 2004, with the same FSO system the measurement campaign was also carried out in La Turbie, France for dense advection fog conditions. Additionally, the measurement setup

here also included the visibility range transmissiometer operating at 550 nm centre wavelength.
At Prague, Czech Republic two commercially available systems, the NOKIA MetroHopper 57.650 GHz frequency and ELVA-Link PPC-100/STM-1 93.370 GHz systems both using V polarisation are operational since Dec. 2000 and Dec. 2005, respectively. The channel length is about 850 m. Recording margin of 57.650 GHz and 93.370 GHz links is 27 dB and 30 dB whereas the transmit powers are 5 dBm and 17 dBm, respectively. Here an FSO link operating at 850 nm is also used for the same channel length of 850 m. Transmitted power of this FSO system is +16 dBm, divergence angle is 9 mrad, receiver aperture is 515 cm^2 and the recording fade margin is about 18 dB.
The meteorological conditions were recorded using a BW video camera. Weather observation system at the receiver end uses Vaisala PWD11 device for visibility range measurement and the rain rate was measured using two tipping bucket rain gauges with different collecting areas.
The availability of hybrid FSO/RF network system installed at Graz is analysed. This system uses FSO 850 nm system (main link) and 40 GHz mmW (back up link) as two parallel links. The characteristics of this hybrid system are presented in Table 3.1.
The availability of this hybrid system A(t) is the probability that the system works correctly at time t. If the cumulative period of an existing link is T_{UP} and cumulative period of the total time of measurement is $T_{UP} + T_{DOWN}$ then by [62] the availability is,

$$A = \frac{T_{UP}}{T_{UP} + T_{DOWN}} \times 100\% \tag{3.26}$$

By [8], if the received signal strength is 3 dB above the receiver sensitivity then the bit error rate reduces to 10^{-9} with OOK modulation of FSO. This criterion is considered as a measure of correct working of our hybrid system in the availability analysis.

3.8 Results and analysis of Fog Attenuation Effects on FSO Link

Simulation were carried out to compare the measured value of fog FSO specific attenuation under moderate radiation fog conditions in Graz to the fog FSO specific attenuation values for wavelength 850 nm, 950 nm and 1550 nm predicted by three different models of Kim, Kruse and Al Naboulsi. The results were presented in [81, 70].

Figure 3.1 shows comparison of attenuations by different models at 850 nm, 950nm and 1550 nm wavelengths and measured specific attenuation value at Graz (Austria) against a radiation fog event of 25.10.05. In Figure 3.1, the measured value of attenuation has been taken as 120 dB/km against a visibility range of 100 m. This value is closer to attenuation value as predicted by Kruse model. According to [38], the atmospheric attenuations are

Table 3.1: Properties of FSO, mmW and FSO, WLAN Hybrid Systems [76]

System	FSO	mmW	WLAN
Tx Wavelength	850 nm	40 GHz	5.2 to 5.825 GHz
Tx Technology	VSCEL	Semiconductor Amplifier	Semiconductor Amplifier
Tx Power	2mW(+3dBm)	EIRP 16 dBW	1.26 mW 1 dBm
Tx Aperture Diameter	4x25mm Convex lens	Antenna gain 25 dB	Antenna gain 30dBi
Beam divergence	2.5 mrad	10 degree	-
Rx Technology	Si-APD	Semiconductor LNA	Semiconductor Amlifier
Rx acceptance angle	2 mrad	10 degree	30 dBi
Rx aperture	4x25mm Convex lens	-	-
Rx sensitivity	-41 dBm	Noise figure 6 dB	Noise figure -94 dBm
Specific Margin	7 dB/km	2.6 dB/km	14 dB/km

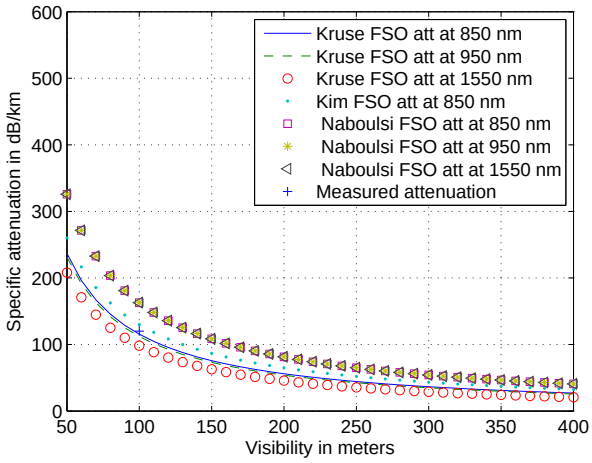

Figure 3.1: Comparison of attenuations by different models for Graz fog event [81].

wavelength dependent that means system operating at longer wavelengths has better range performance than systems at shorter wavelengths. The simulations show that this effect is more prominently observed for Kruse model as the Kim model does not show any wavelength dependent attenuation behaviour against a visibility range lower than 500 m. The Al Naboulsi radiation fog model is also simulated for the two mentioned wavelengths (850 nm and 1550 nm) and it was observed that this model too does not show any considerable wavelength dependent attenuations for moderate continental fog (radiation fog) conditions. A similar comparison was carried out for dense maritime fog (advection fog) conditions at

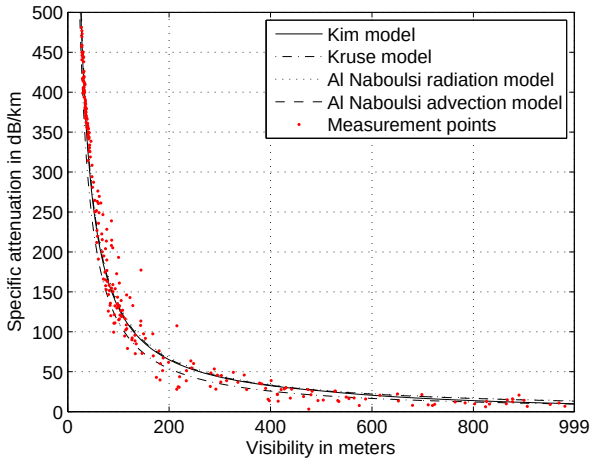

Figure 3.2: Predicted and measured attenuation of 950 nm for Nice fog event [81].

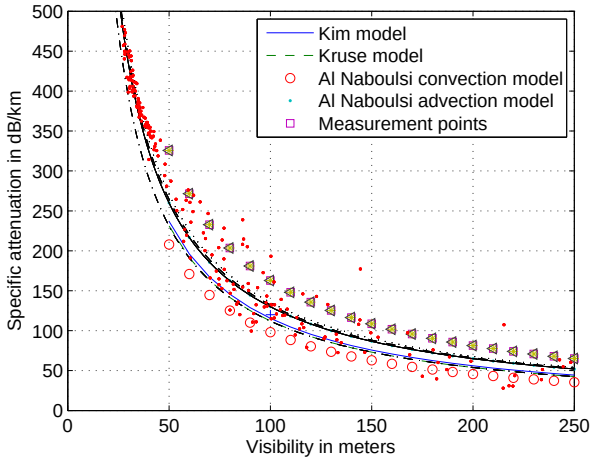

Figure 3.3: Magnified comparison of 950 nm attenuation for Nice fog event [70].

La Turbie (France) The Figure 3.2 plot (taken from [59]) shows a comparison of different models predicted and measured attenuation data of 950 nm for La Turbie (Nice, France) against a fog event of 28.06.04 for a visibility range up to 1000 m . In [59], the magnified view up to 350m visibility was presented and it was concluded that we cannot prefer any particular model over the other since the attenuations in dense maritime fog case are wavelength independent. In [81] a comparison of different models and measured attenuation data for 950 nm for La Turbie (Nice, France) against a fog event of 28.06.04 for a visibility range up to 250 m has been shown in Figure 3.3. Figure 3.4shows a comparison of attenuation predicted by different models and measured attenuation data for 850 nm for La Turbie (Nice, France) against a fog event of 28.06.04 for a visibility range up to 1000

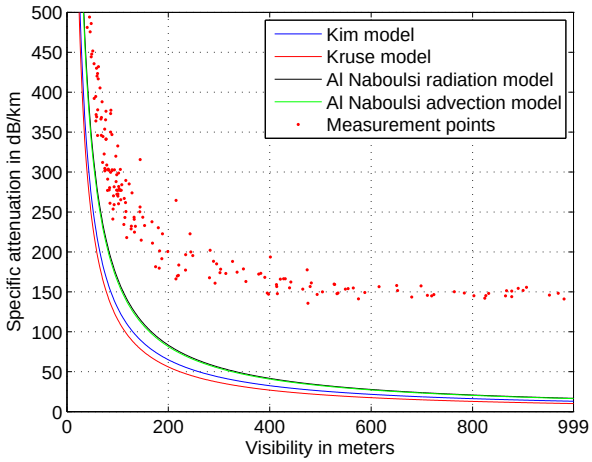

Figure 3.4: Predicted and measured attenuation of 850 nm for Nice fog event [75].

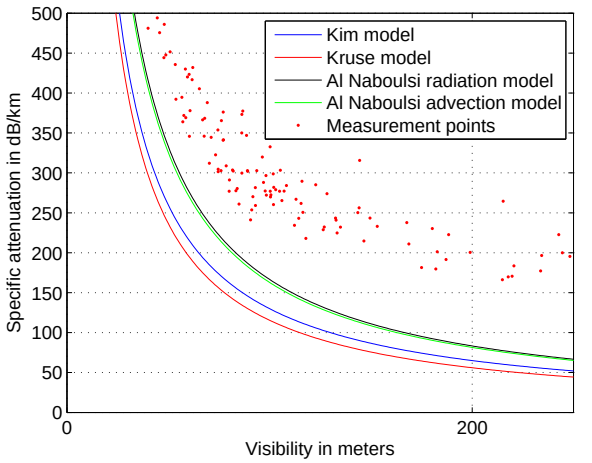

Figure 3.5: Magnified comparison of 850 nm attenuation for Nice fog event [75].

m. The magnified view presented in Figure 3.5 shows a comparison of different models and measured attenuation data for 850 nm for La Turbie (Nice, France) against a fog event of 28.06.04 for a visibility range up to 250 m..

3.8.1 Fog attenuation model comparison

This requires a statistical analysis for the measured attenuation data to qualify the best model. The statistical analysis in terms of Mean square error (MSE) is performed in [75]. The MSE has been computed by dividing the sum of the square of the errors between

model predicted attenuation $Pred_{att}$ and measured attenuation $Meas_{att}$ by the total number of measurements $Total$ as shown in Eq. 3.27.

$$MSE = \frac{\sum(Pred_{att} - Meas_{att})^2}{Total} \tag{3.27}$$

As the measurement was done for 850 nm and 950 nm in Graz, the MSE of the models has been shown for these wavelengths in Figure 3.6. As there was only one measured value for Graz, the MSE for Al Naboulsi model seems to be much higher. Moreover like Kim model, there is no significant difference between MSE of 850 nm and 950 nm for Al Naboulsi model. These results show that MSE for Kruse model seem to be the best for Graz. As this is one value, anything cannot be deducted certainly and it shows only a course estimate.
The mean square error of 950 nm wavelength for this event is shown in Figure 3.7. The mean square error of 850 nm wavelength for this event is shown in Figure 3.8. Figure 3.7 and Figure 3.8 show that advection fog model has the minimum MSE in comparison to other models. The reason may be the existence of Maritime fog in La Turbie and advection model may be better fit for this fog. The higher error in MSE for 850 nm may be due to any measurement error.
The mean square error for Prague is shown in Figure 3.9. As the measurement was done with only 850 nm wavelength, MSE of different models are presented for 850 nm only. These results favour Kruse model. Again like Graz, Prague has continental fog and Kruse model seems to be better fit for Continental fog.

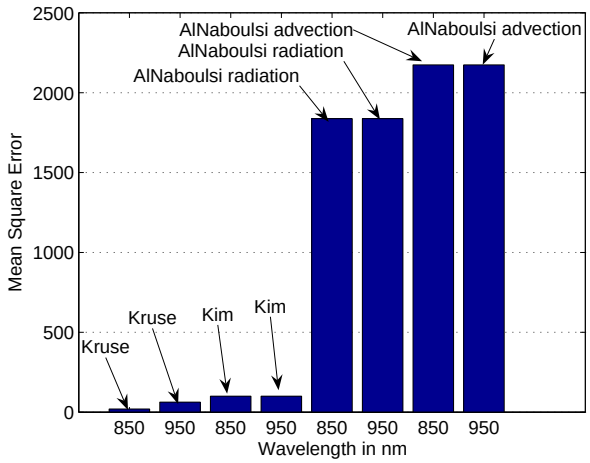

Figure 3.6: Mean Square Error of different models for Graz data [75].

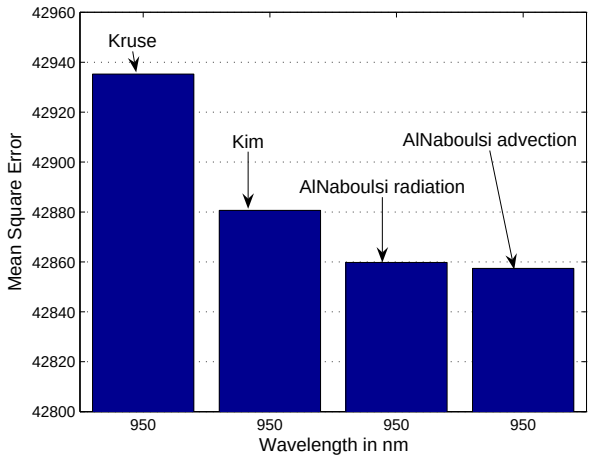

Figure 3.7: Mean Square Error of different models for 950 nm Nice data [75].

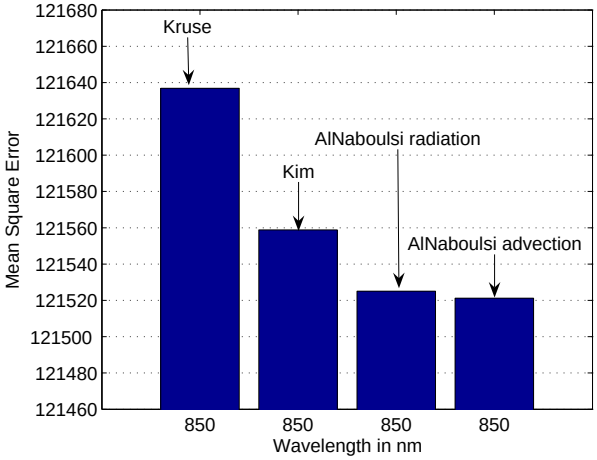

Figure 3.8: Mean Square Error of different models for 850 nm Nice data [75].

3.8.2 Long wavelength fog attenuation comparison

The comparison analysis of long wavelength attenuation has been performed in [77, 78]. As Kruse model has been found better fit for Continental fog, it has been used to show the wavelength comparison of different wavelengths in Figure 3.10. Figure 3.10 shows comparison of the specific attenuation of different wavelengths for visibility up to 500 m using Kruse model. It can be observed that specific attenuation for longer wavelengths is less. At extremely low visibility, the specific attenuation at 850 nm and 950 nm is almost 100 dB/km more than the specific attenuation at 10 μm. This shows that under dense fog with extremely low visibility, 10 μm surpasses the performance of 850 nm and 950 nm.

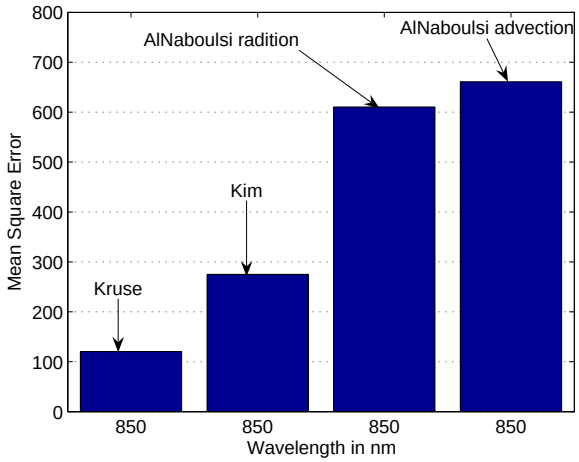

Figure 3.9: Mean Square Error of different models for 850 nm Prague data [75].

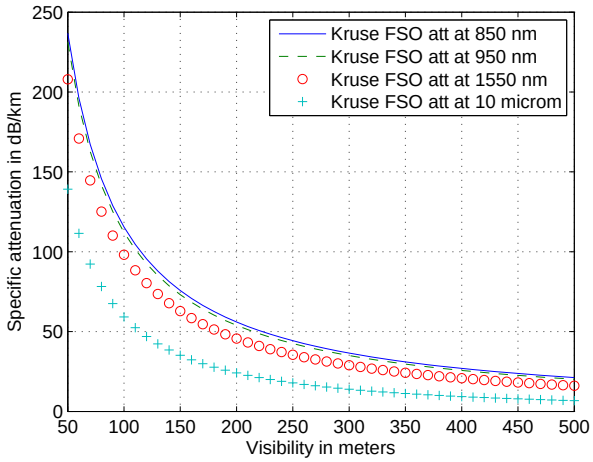

Figure 3.10: Kruse model attenuation comparison of different wavelengths [77].

The comparison of different wavelengths has been simulated using Al Naboulsi radiation model in Figure 3.11for Dense Maritime fog and this figure shows comparison of the specific attenuation of different wavelengths for visibility up to 500 m using Al Naboulsi model . Al Naboulsi model also does not exhibit any wavelengths dependent specific attenuation. It seems also contradictory to the measured results of [91].This shows that Kruse model seems to be better fit for wavelength comparison analysis. Keeping in view, this argument, the comparison of wavelength attenuation has been performed using Kruse model for the fog event of La Turbie, France. Figure 3.12 shows the comparison of the

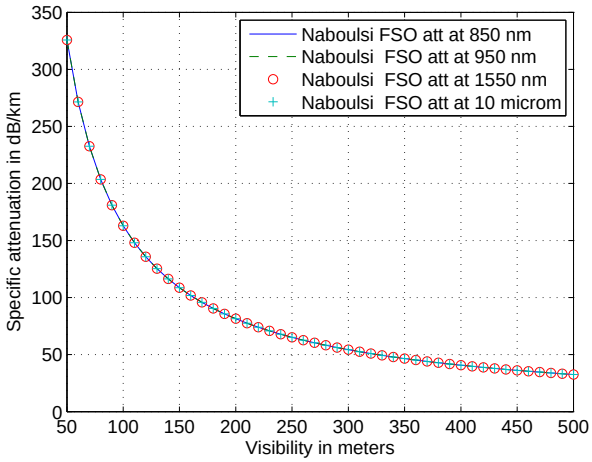

Figure 3.11: Al Naboulsi model attenuation comparison of different wavelengths [77].

specific attenuation of 950 nm and 10 μm wavelengths for fog event of 28.06.04.

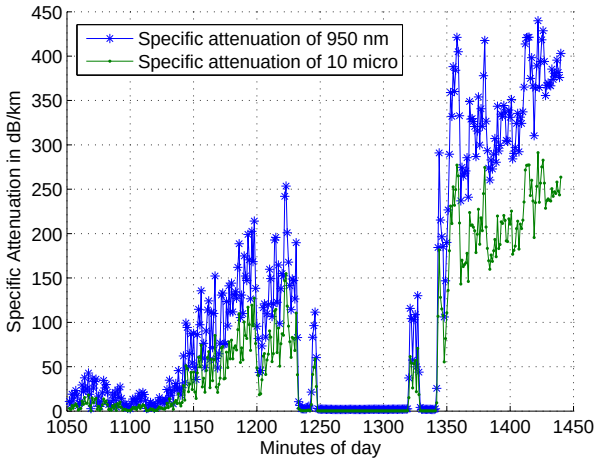

Figure 3.12: Attenuation comparison of 950 nm and 10 μm for Nice fog event. [77].

3.9 Results and analysis of Fog Attenuations on GHz Links and Hybrid Network

The effect of fog attenuations on radio frequencies in the range of 10 GHz up to 200 GHz were simulated. The normal temperature variation at Graz in winter is from $-20\,^{\circ}$C to

10 °C and to simulate the fog attenuation behaviour, the temperatures of −20 °C,−10 °C,0 °C and 10 °C were considered. The liquid water densities of 0.05 g/m^3 and 0.5 g/m^3 that correspond to visibility ranges of 300 m and 50 m, respectively [89] were considered. Figure 3.13 shows specific attenuation for frequencies greater than 10 GHz for liquid water density of 0.05 g/m^3 . Figure 3.14 shows Specific attenuation for frequencies greater than 10 GHz for liquid water density of 0.5 g/m^3. It is clear from Figure 3.13 and Figure 3.14 , that higher the frequencies more the attenuations we can expect under foggy conditions. Additionally, for GHz frequencies below 100 GHz the attenuations are more at −20 °C and −10 °C when compared with attenuations at temperatures of0 °C and 10 °C . This behaviour is reversed for GHz frequencies beyond 100 GHz as the attenuations are more at0 °C and 10 °C than the attenuations at −20 °C and −10 °C observed for the both liquid water density values. It is important to mention here that by increasing the liquid water density 10 times we observe an increase of 10 times in the specific attenuation values. Further, it can also be noticed that for frequencies higher than 200 GHz, there is a difference of 1 dB/km between temperatures of −20 °C and 10 °C. This further implies that temperature difference has insignificant role towards attenuations at GHz range.

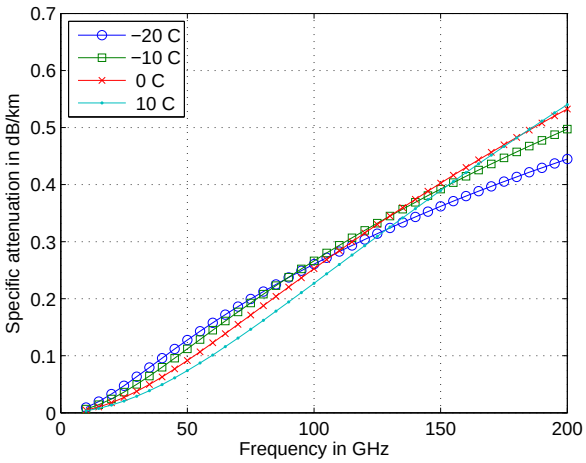

Figure 3.13: Attenuation of GHz frequencies for liquid water density of 0.05 g/m^3 [81].

Simulations were also performed to compare fog attenuations at different frequencies for exaggerated extremely low visibility range. Figure 3.15 shows the comparison of fog attenuations by FSO link operating at 850 nm and different GHz links up to 200 GHz frequency for the visibility range up to 500 m at 10 °C temperature. Kruse model is simulated here for FSO link attenuation at 850 nm. The significance of 850 nm wavelength selection here is that the FSO system used in availability analysis has this wavelength as main link.

Since the attenuation behaviour of GHz frequency link is almost the same for temperatures of 10° C and 0°C, as already mentioned above. So temperature of 10° C is selected for simulations here. It is noticed that a very high difference in fog attenuation levels for the

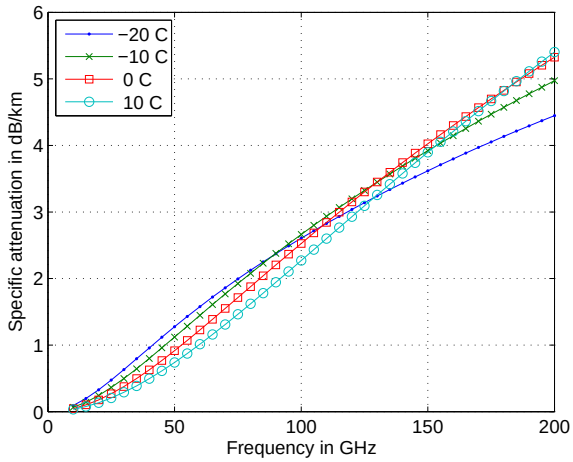

Figure 3.14: Attenuation of GHz frequencies for liquid water density of 0.5 g/m^3 [81].

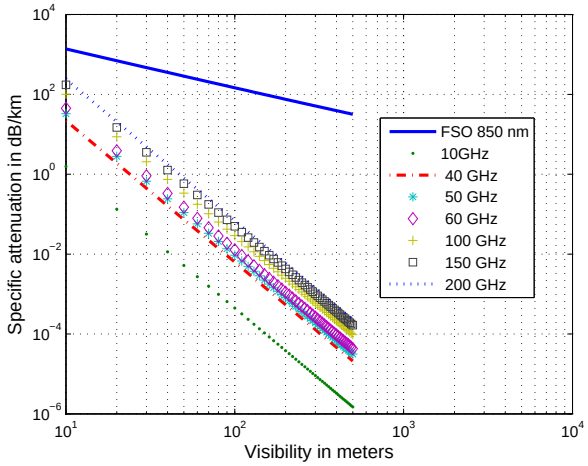

Figure 3.15: Attenuations comparison between FSO and GHz frequencies [70].

FSO and GHz links as the fog attenuation for GHz frequency range is much lesser than for FSO link. However, it is alarming that a back up link operating at 200 GHz frequency may suffer attenuations higher than 200 dB/km for extremely low visibility range.
Furthermore, it is noticeable that for extremely low visibility range the fog attenuations of GHz frequency range are significantly high and are up to such an extent that these frequencies no more complete the requirement of back up link. If availability is the only concern and data rate is insignificant for a certain application, then low frequencies should be preferred for the back up link.
In Figure 3.16, time series of continental fog event recorded on 28.09.2007 at Prague (Czech Republic) and behaviour of 850 nm FSO, 58 GHz and 93 GHz links are presented

by providing the comparison of attenuations for 850 nm FSO link, 58 GHz and 93 GHz links. The specific attenuation suffered by two GHz links is almost same and two curves overlap each other. It can be seen that despite huge variation in visibility range, the attenuation in GHz links remains insignificant whereas FSO link suffers more than 20 dB attenuations on link distance of 850 m. The solid bold line shows the visibility in meters. Now in order to perform availability analysis for combined FSO/40 GHz link, individual

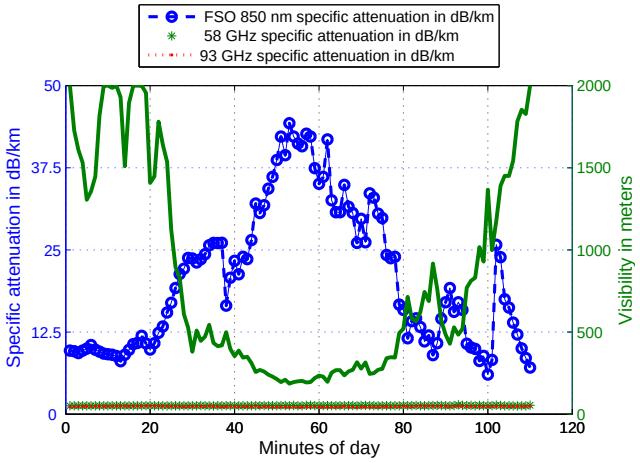

Figure 3.16: Comparing 850 nm FSO, 58 GHz and 93 GHz for Prague fog event [70].

FSO and 40 GHz links a representative dense maritime fog event measured on 28.06.04 on a 28 m channel length at La Turbie is taken. The time series of fog attenuations and the corresponding visibility range variations are shown in Figure 3.17 for the mentioned event. The bold solid line shows the visibility in meters whereas dotted line shows attenuation in dB/km.

The corresponding availability analysis plot that shows specific attenuations and the calculated availabilities is plotted in Figure 3.18. If 3 dB is reduced from fade margin of FSO link using OOK modulation, the specific margin reduces to 5.88 dB/km to achieve BER of 10^{-9} on a link distance of 2.7 km. It means, whenever the specific attenuation exceeds this threshold the FSO link is no more available to maintain a BER of 10^{-9}. The modulation of FSO link is considered as OOK. Similarly, the same specific margin is utilised to maintain a BER of 10^{-9} on a link distance of 2.7 km with 40 GHz link. Due to high specific attenuations the FSO link has only 0.51 % availability while on the other hand the negligible fog attenuations in case of 40 GHz back up link renders 100 % availability. As a result the overall combined availability of this hybrid network goes up to 100 %.

Availability analysis simulations of a combined hybrid (850 nm FSO/40 GHz) link, 850 nm FSO link and 40 GHz link were performed as shown in Figure 3.18 for a dense maritime fog event mentioned in Figure 3.17. Due to fog attenuation any link can be either in operationally active state or down state. The operationally active state of FSO and 40 GHz links are represented by values of 400 and 500, respectively. Whereas the operationally

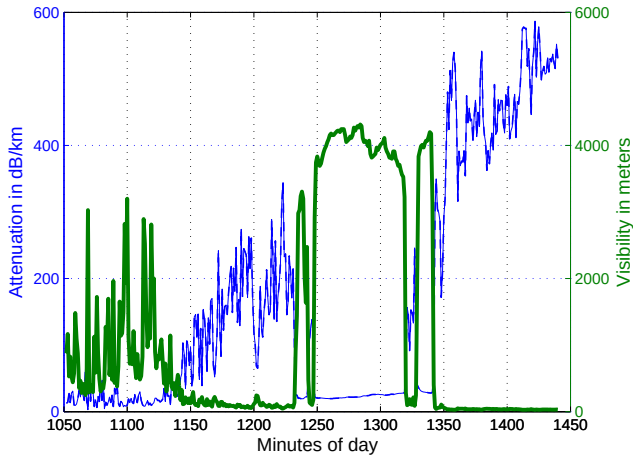

Figure 3.17: FSO 850nm attenuation and visibility for Nice fog event [70].

active state of hybrid network is represented by a value of 600. Similarly the down states of FSO, 40 GHz and combined hybrid network are represented by values of 100, 200 and 300, respectively. It is important to remember that these values are only a representation of operationally active or down states and the availability of any particular link is calculated by the percentage of the time that link had operationally active state. For example, FSO had the operationally active state of only 2 minutes out of total measured 389 minutes, thus making its availability as 0.51%. Therefore, FSO has been represented now for operationally active state by a value of 400 for 2 minutes whereas FSO link down states has been represented by a value of 100 for 387 minutes. The same argument holds for 40 GHz and combined hybrid network availability. The criterion for these link state simulations is that it always satisfies the requirement for a BER of 10^{-9}.

The comparison analysis of FSO 850nm/ 40 GHz hybrid system and FSO 850 nm/WLAN hybrid system was performed in [76]. The comparison does not exhibit any advantage of using WLAN over 40 GHz back up link as both back up links provide the same improvement in availability. The use of 40 GHz back up link seems to be advantageous as it provides higher carrier frequency that can support high data rate demanding applications during fog events.

The immunity of 10 μm to fog motivated to compare the availability achieved by FSO alone with the availability achieved by FSO 850 nm/ WLAN hybrid sytems. The properties of FSO 850 nm/ WLAN hybrid sytems are mentioned in 3.1 where as the link budget summary of FSO 10 μm is based on a 500mW source, OOK modulation, 100mm Rx aperture and a 1km range link with at 155Mbps. The specific margin is 41 dB as mentioned in [91]. The simulation of WLAN attenuation and 10 μm wavelength are performed using [89] and [37] respectively. The results were presented in [78]. Due to high specific attenuation, 850 nm link has only 0.51% availability whereas 100% availability of WLAN link due to it negligible attenuation improves the combined availability of 850nm/WLAN

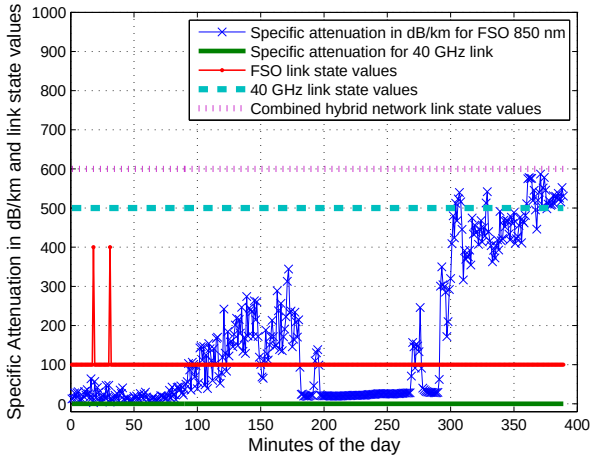

Figure 3.18: Attenuation and link states of FSO 850 nm/ 40 GHz for Nice fog event [70].

hybrid network up to 100%. The negligible attenuation of 10 μm makes the 100% availability of 10 μm link. Availability values of 700, 600 500 and 400 represent when combined 850nm/WLAN , 10 μm link, WLAN link and 850 nm link are available respectively whereas availability values of 350, 300, 200 and 100 represent when combined, 10 μm, WLAN link and 850 nm link are not available respectively depending on 10^{-9} BER criterion. Figure 3.19 shows comparison of the specific attenuation, availabilities for 850 nm, WLAN, 10 μm and Combined 850 nm/WLAN availability for a fog event. Figure 3.19 shows the significant advantage of using 10 μm link over 850 nm/WLAN hybrid network. 10 μm link does not need any fail over or switch over. Although both 10 μm link and 850nm/WLAN hybrid network show 100% availability but 10 μm link provides high data rate link. These observations strongly recommend to prefer 10 μm link over hybrid network of shorter wavelength FSO/RF.

Monte Carlo simulation for FSO availability estimation under fog conditions

The fog attenuation results use measured data. However, the randomly varying visibility motivates to use it as a random variable and perform Monte Carlo simulation to predict attenuation for this random visibility. Kruse model has been used to predict the attenuation from this random variable of visibility as the results of Kruse model were close to the measured data for continental fog. The results were presented in [71]. The random values of visibility between 400m (extremely low visibility) and 10 km were generated using uniform distribution. The number of random values taken is 100000. From these visibility values, the attenuation was evaluated using Kruse model. These 100000 attenuation values and link budget consideration were used to find the status of reception of the optical signal. These 100000 optical signal reception status values were used to evaluate one availability

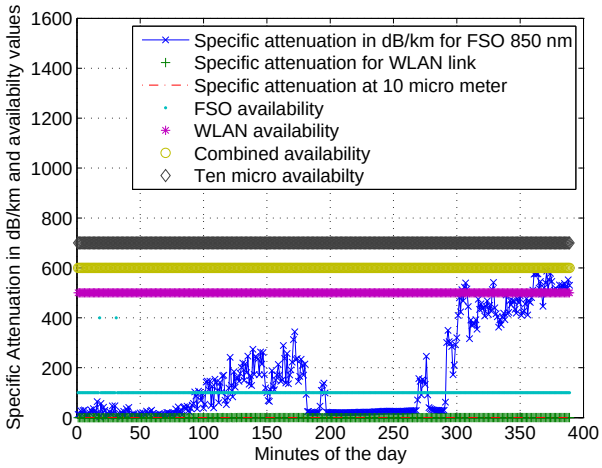

Figure 3.19: Availability of FSO 850 nm/ WLAN and FSO 10 μm for fog event [78].

value. The whole above process was repeated 100000 times to find 100000 availability values. These 100000 different availability values were used to make the histogram. The simulation was performed using Matlab. The results are presented in Figure 3.20. The results show that availability of FSO link remains around 87% during different visibility values of fog conditions.

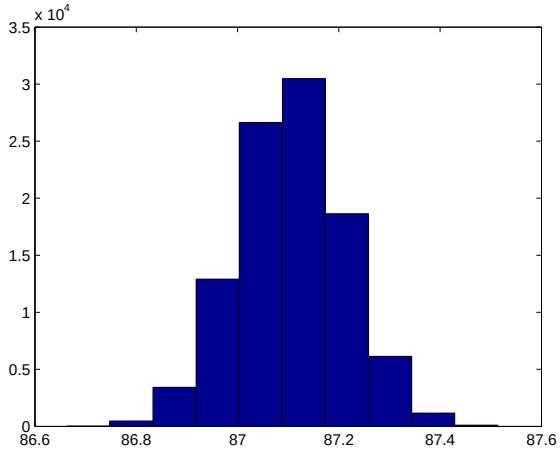

Figure 3.20: Histogram of FSO link availability for different visibility values [71].

3.10 Results and analysis of Rain Attenuations Effect on Hybrid Network

The effect of rain attenuations on the FSO link and GHz links has been simulated by employing ITU-R model [88] and the model as mentioned in Eq. 3.18 that relates specific attenuations with different rain rate. The specific attenuation behaviour of different GHz links has been simulated using ITU model [88] in Figure 3.21. The results were presented in [83, 70]. It is evident through this simulation that the specific attenuation does not change notably for frequencies greater than 60 GHz. However, the GHz links operating below 10 GHz have specific attenuations that are quite lower than 10 dB/km for rain rates up to 155 mm/hr. This information can be useful in selecting a suitable back up link because a back up link for FSO main link in a hybrid system must be chosen in a manner such that it should have the least possible effects of weather attenuations to achieve an overall high availability. Prior to simulating the behaviour of model presented in Eq. 3.18, it is important to recall here that rain attenuations for FSO link are wavelength independent, but this is not the case for GHz frequency link.Figure 3.22 shows Simulations of specific attenuation for FSO and different GHz links at different rain rates. According to simulations as shown in Figure 3.22 based on model mentioned in Eq. 3.18, it is quite clear that for a rain rate of 155 mm/hr FSO attenuation easily exceed 30 dB/km. However, these attenuations are quite less in comparison when compared with attenuations for 40 GHz and 100 GHz links with the same rain rate.

Moreover, for GHz links operating below 40 GHz frequency the rain attenuations are

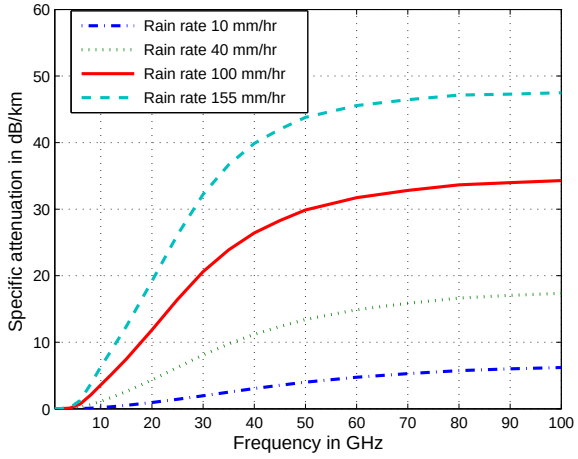

Figure 3.21: Specific attenuation simulation of GHz links for different rain rate [70].

quite low in comparison with the FSO link attenuations. This may create a trade off in the selection of a back up link for the hybrid system. If reliability of hybrid network is the major driving force then links below 10 GHz should be the optimum choice for usage

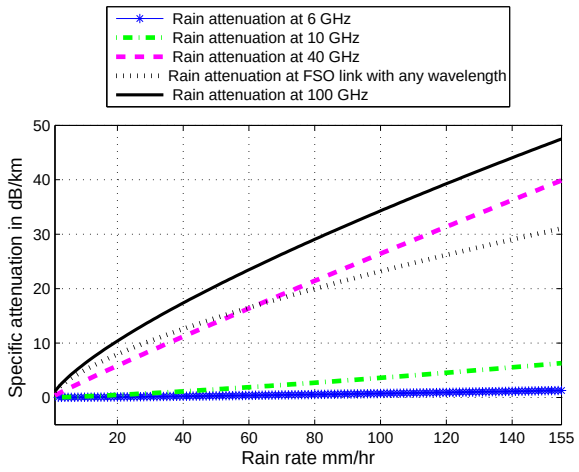

Figure 3.22: Specific attenuation for FSO and GHz links at different rain rates [70].

as a back up link. And also due to the fact that, for the 6 GHz link (ISM band), there are negligible weather dependent attenuations. Similarly, if for the back up link relatively higher data rates comparable to the main FSO link are mainly required and with it slightly lower reliability is acceptable, then a back up link operating just below 40 GHz frequency should be preferred.

The effects of rain on different GHz frequencies have been simulated and are compared with two representative measured rain events that occurred on May 2002 and September 2002 at Graz, Austria . Figure 3.23 shows the time series of measured rain rate and simulated specific attenuations for different GHz links against rain event of May 2002 at Graz (Austria) whereas Figure 3.24 shows time series of measured rain rate and simulated specific attenuations for different GHz links against rain event of September 2002 at Graz (Austria). The rain rates of 102 mm/hr and 113 mm/hr were recorded, and corresponding attenuations on the 40 GHz link were 27 dB/km and 30 dB/km against May 2002 and September 2002 rain events, respectively. For comparison 102 mm/hr and 113 mm/hr rain rates were taken and simulated them for 6, 10, 40, 100 GHz frequency and FSO links. The corresponding plots of rain attenuations are shown in Figure 3.23 and Figure 3.24 separately for the two rain events of May 2002 and September 2002. The bold solid line indicates the rain rate in mm/hr in Figure 3.23 and Figure 3.24. According to these plots, there is no behavioural change related to the two events at different GHz and optical frequencies. However, as expected the specific attenuation of frequencies below 10 GHz is much lesser than optical attenuations for the two rain events.

Hence if data rates can be compromised for locations with very frequent rainfall, then frequencies below 10 GHz, like as in the ISM band, are highly suitable for usage as a back up link frequencies to the main FSO link in a Hybrid FSO/RF communication link. This observed trend of rain attenuations simulated for different frequencies against two representative rain events of Graz can also be complemented through a representative rain

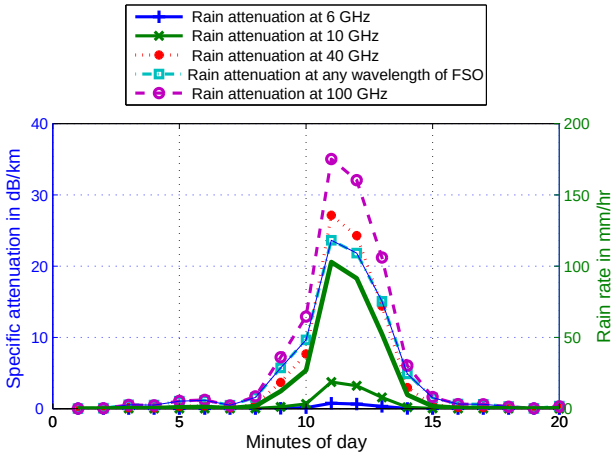

Figure 3.23: Simulated GHz attenuations for Graz rain event of May 2002 [70].

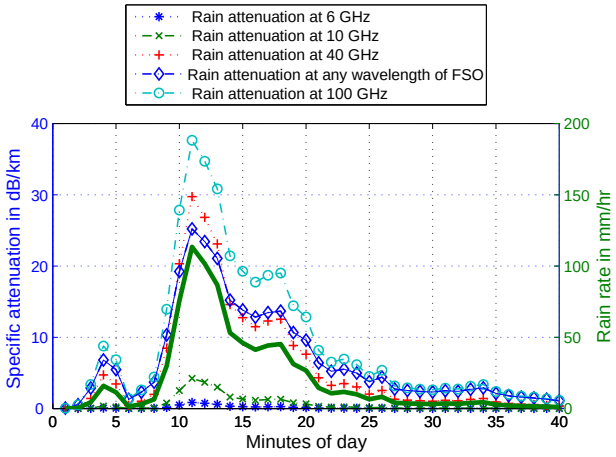

Figure 3.24: Simulated GHz attenuations for Graz rain event of September 2002 [70].

event recorded on 18.09.2007 at Prague (Czech Republic) as Prague just like Graz is a continental location. Rain attenuations were measured on the 850 nm FSO, 58 GHz and 93 GHz links at Prague. Figure 3.25 shows time series of representative rain event at Prague (Czech Republic) on 18.09.2007 and behaviour of FSO 850 nm, 58 GHz and 93 GHz links. In Figure 3.25, the bold solid line in the plot indicates the rain rate in mm/hr. It is easily observable that the two GHz links suffer more rain attenuations when compared with the rain attenuations (max. up to 7 dB/km) recorded on 850 nm FSO link. Moreover, the 93 GHz link has suffered more attenuations than the 58 GHz link. This suggests the need to take appropriate measures, like for example enough link margin, while selecting a particular frequency back up link in order to have acceptable data rates, high availability

and least effect of weather dependent attenuations for certain applications.

Similarly the availability analysis simulations were performed against the representative

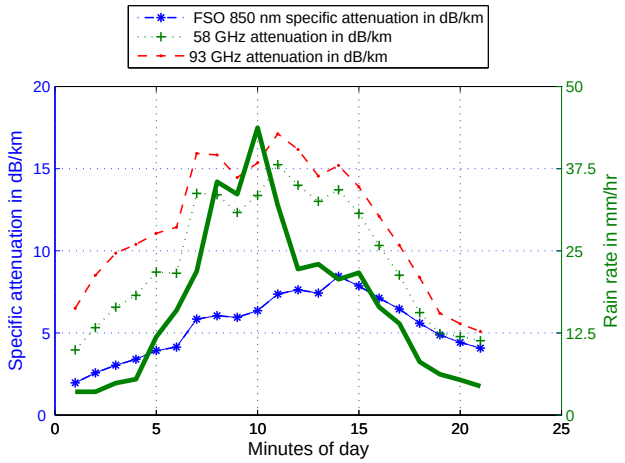

Figure 3.25: Comparing FSO 850 nm, 58 GHz and 93 GHz for Prague rain event [70].

rain event of 18.09.2007 recorded at Prague. Figure 3.26 shows the comparison of the specific attenuations and link state values for FSO 850 nm, 40 GHz and combined hybrid link for a rain event of 18.09.2007. The specific attenuations for 40 GHz link were simulated by applying the model as mentioned in [34]. The criterion for the availability analysis simulations for the rain event is the same as it was for the fog case i.e., BER of 10^{-9} with OOK modulation of FSO.

According to these simulations, availability values of 60, 45 and 30 represent when hy-

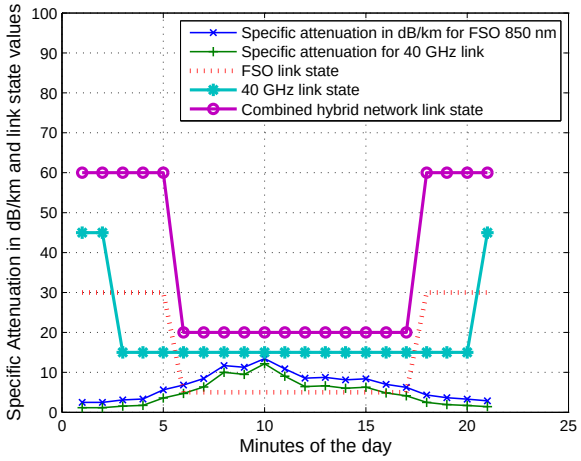

Figure 3.26: Attenuations and link state of FSO /40 GHz for Prague rain event [70].

brid (850 nm FSO/40 GHz) link, 850 nm FSO and 40 GHz links are available, respectively.

While the availability values of 20, 15 and 5 represent when hybrid (850 nm FSO/40 GHz) link, 850 nm FSO and 40 GHz links are not available, respectively. According to the simulations the measured availability by the hybrid link for the representative rain event case was only up to 42.86%, equal to the same value of availability that is achieved through 850 nm FSO link only. This suggests that if improvements in availability are required against rain effects concerning regional locations that have high average probability of rainfall then GHz frequency back up link in the lower frequencies range, preferably below 40 GHz, should be preferred.

The comparison analysis of FSO 850nm/ 40 GHz hybrid system and FSO 850 nm/WLAN

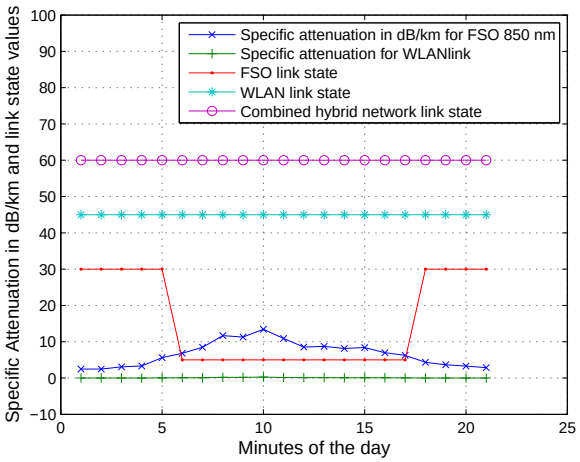

Figure 3.27: Attenuations and link state of FSO / WLAN for Prague rain event [76].

hybrid system was performed in [76]. The availability analysis of FSO 850nm/ WLAN hybrid system is shown in Figure 3.27. Figure 3.27 shows comparison of the specific attenuations and link state values for FSO, WLAN and combined hybrid link for a rain event of 18.09.2007. According to these simulations, availability values of 60, 45 and 30 represent when hybrid (850 nm FSO/WLAN) link, 850 nm FSO and WLAN links are available, respectively.The advantage of using WLAN as back up link over 40 GHz link becomes prominent for rain event. This time the combined availability for FSO/40 GHz hybrid network remains only up to the FSO link availability of 42.86%. The combined availability of FSO/WLAN link on the other hand improves to 100% due to negligible attenuation of WLAN link for rain event. This suggests that if improvement of availability is required for rain event, back up link with lower frequencies should be selected.

3.10.1 Comparison of FSO 10μm availability with the availability of FSO 850nm/WLAN hybrid system for rain event

The properties of FSO 850 nm/ WLAN hybrid sytems are mentioned in Table 3.1 where as the link budget summary of FSO 10 μm is based on a 500mW source, OOK modulation, 100mm Rx aperture and a 1km range link with at 155Mbps. The specific margin is 41 dB as mentioned in [91]. The simulation of WLAN attenuation and 10 μm wavelength are performed using [88] and model as mentioned in Eq. 3.18 respectively. The results were presented in [78]. Figure 3.28 shows comparison of the specific attenuation, availabilities for FSO 850 nm, WLAN, 10μm and Combined 850 nm/ WLAN availability for a rain event of 18.09.2007 at Prague. In Figure 3.28 availability values of 65, 60, 45 and 30 represent when FSO 10 μm, combined 850nm /WLAN, WLAN link and FSO 850 nm link are available respectively whereas availability values of 25, 20, 15 and 5 represent when FSO 10 μm, combined 850nm /WLAN, WLAN link and FSO 850 nm link are not available respectively depending on 10^{-9} BER criterion. The FSO 850 nm has 42.86% availability whereas both WLAN and 10 μm have 100% availability. Again the availability of 850 nm/ WLAN hybrid network is same as the availability of 10 μm FSO link but FSO 10 μm link has the advantage of high data rate.
Figure 3.28 also shows that specific attenuation of both FSO links is same. But due to eye safety concerns, higher power transmission at 10 μm increases the availability at this link.

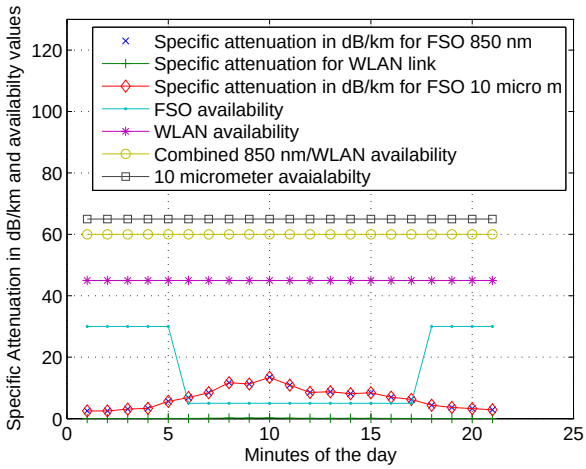

Figure 3.28: Availability of FSO 850 nm/WLAN, FSO 10μm for Prague rain event [78].

3.10.2 Monte Carlo simulation for FSO availability estimation under rain conditions

The rain attenuation results use measured data. However, the randomly varying rain rate motivates to use it as a random variable and perform Monte Carlo simulation to predict attenuation for this random occurrence of rain rate.The results were presented in [71]. The random values of rain rate between 1 mm/hr and 155 mm/hr were generated using uniform distribution. The total number of values taken is 100000. From these rain rate values, the attenuation was evaluated using equation 8. These 100000 attenuation values and link budget consideration were used to find the status of reception of the optical signal. These 100000 optical signal reception status values were used to evaluate one availability value. The whole above process was repeated 100000 times to find 100000 availability values. These 100000 different availability values were used to make the histogram. The simulation was performed using Matlab. The results are presented in Figure 3.29. The results show that availability of FSO link re-mains around 7.6% during different rain rate values.

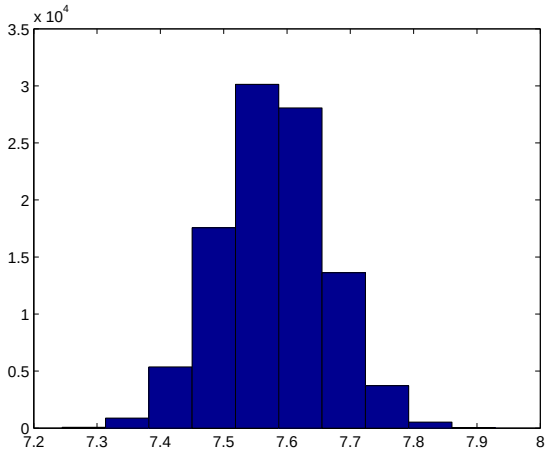

Figure 3.29: Histogram of FSO link availability for different rain rate values [71].

3.11 Results and analysis of Dry Snow Attenuations Effects on Hybrid Network

The snow attenuations on FSO link installed at Graz were measured against a dry snow event that started on 25.11.05 and lasted till 28.11.05. The results were presented in [74, 70]. Figure 3.30 below shows time series of specific attenuations corresponding to

a dry snow event recorded on 25.11.05 to 28.11.05 at Graz (Austria). The changes in specific attenuations corresponding to this snow event were about 10 dB/km measured on a second scale. Keeping in view such rapid changes in specific attenuations on a second scale, it is recommended that the backup link should be used as early as possible upon detection of a snow event in order to avoid any link losses.

The highest value of snow rate S calculated, using the model mentioned in Eq. 3.24, is

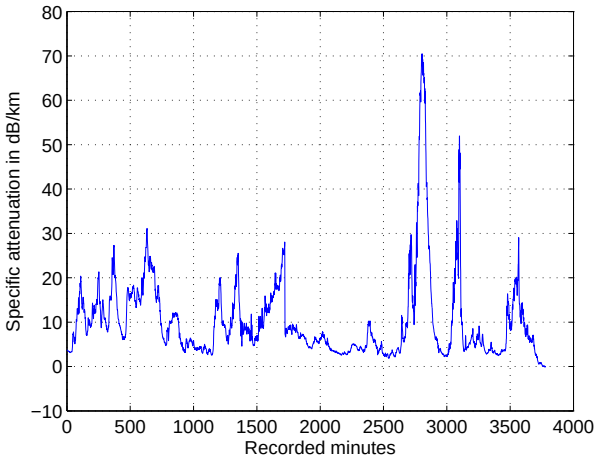

Figure 3.30: Attenuations of a dry snow event at Graz (Austria) [70].

about 7 mm/hr against this dry snow event. The attenuations of GHz frequencies against this snowfall rate are simulated using Eq. 3.25. The corresponding simulation plot is shown in Figure 3.31 which showsimulation of specific attenuation for GHz frequencies up to 100 GHz against a snowfall rate of 7 mm/hr . It was found out that effect of GHz

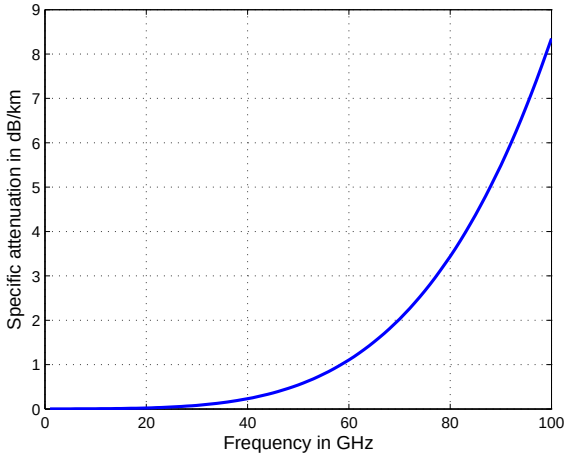

Figure 3.31: Attenuation of GHz frequencies for snowfall rate of 7 mm/hr [70].

frequencies below 25 GHz in terms of dry snow attenuations is insignificant when compared with dry snow attenuations by FSO link for the corresponding snow rate. Even the frequencies below 60 GHz do not exhibit considerable attenuations for such snowfall rates. The plot as shown in Figure 3.32 shows simulated specific attenuation of different GHz frequencies for a snowfall rate against snow event of 25.11.05 to 28.11.05 at Graz (Austria). The simulations for wet snow are not performed here as wet snow has negligible effect in terms of snow attenuations on the performance of FSO link. From the plot as shown in Figure 3.32, it can be observed that as GHz frequencies increase the corresponding specific attenuations also increase with the same instantaneous snowfall rate.

A comparison of Figure 3.30 and Figure 3.32 suggest that the specific attenuations intro-

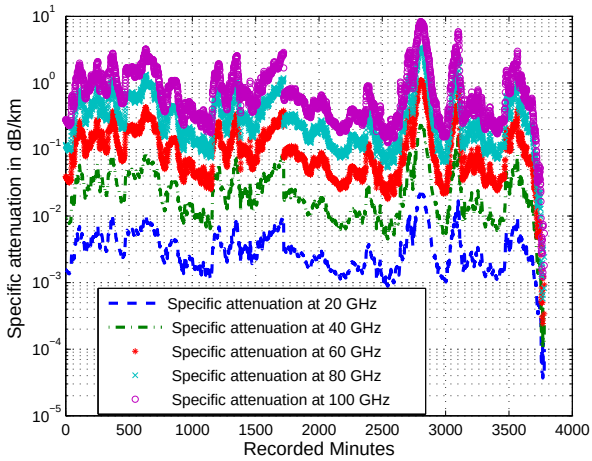

Figure 3.32: Attenuation of GHz links for Graz snow event [70].

duced by 100 GHz link are almost 9 times lesser than the specific attenuations introduced by FSO link for the same snowfall rate. Figure 3.32 simulations further suggest that only 100 GHz link has considerable specific attenuations for 7 mm/hr snowfall rate and the GHz frequencies lower than 60 GHz are not affected significantly by the snowfall rate. These observations suggest that for a location having a high frequency of snowfall events, back up link up to 60 GHz can be the optimal choice.

The availability analysis simulation was also performed for the dry snowfall event case as shown in Figure 3.33, corresponding to the snow attenuations as shown in Figure 3.30. Figure 3.33 shows the specific attenuations and corresponding link state values of a hybrid (850 nm FSO/40 GHz) link, 850 nm FSO and 40 GHz links. The availability criterion for the dry snow event case is the same as that was considered for the fog and rain events case i.e., a BER of 10^{-9} with the OOK modulation of FSO.

The link state values of 60, 45 and 30 are represented for hybrid (FSO/40 GHz) link, 850 nm FSO and 40 GHz links, respectively, when these links are in operationally active state.

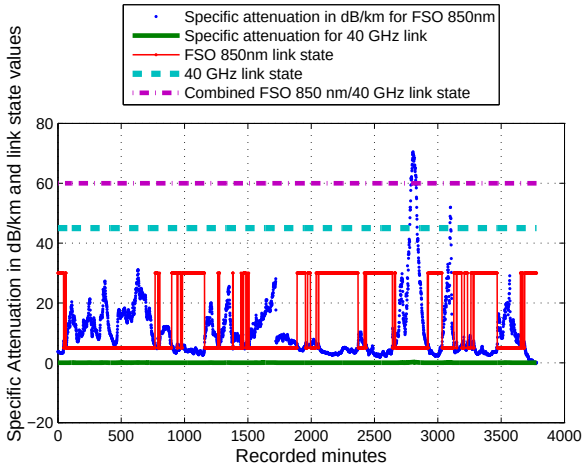

Figure 3.33: Attenuation and link state for FSO /40 GHz for a snow event [70].

While link state values of 20, 15 and 5 represent when hybrid link, 850 nm FSO and 40 GHz links are in down state, respectively. The simulations on availability showed that 40 GHz back up link could help achieve 100% availability in case of dry snow events to the hybrid link despite the 39.49% availability that is achieved by FSO link only.
The comparison analysis of FSO 850nm/ 40 GHz hybrid system and FSO 850 nm/WLAN hybrid system was performed in [76]. It was observed that for a snow event availability improvement by both back up links is same and both hybrid networks achieve 100% availability despite the 39.49% availability for FSO link. In this case, 40 GHz back up link should be preferred as it can support higher data rated due to higher carrier frequency.

3.11.1 Comparison of FSO 10μm availability with the availability of FSO 850nm/WLAN hybrid system for snow event

The properties of FSO 850 nm/ WLAN hybrid sytems are mentioned in 3.1 where as the link budget summary of FSO 10 μm is based on a 500mW source, OOK modulation, 100mm Rx aperture and a 1km range link with at 155Mbps. The specific margin is 41 dB as mentioned in [91]. The simulation of WLAN attenuation and 10 μm wavelength are performed using the model mentioned in Eq. 3.25 and using the model mentioned in Eq. 3.24 respectively. The results were presented in [78]. Figure 3.34 shows comparison of the specific attenuation, availabilities for FSO 850 nm, WLAN, 10μm and Combined 850 nm/ WLAN availability for a snow event The simulations have been performed assuming that snow was dry. As wet snow attenuation is negligible for FSO, its impacts are not considered. In Figure 3.34 availability values of 65, 60, 45 and 30 represent when 10 μm, combined, 850 nm/ WLAN, WLAN link and FSO 850 nm link are available respectively whereas availability values of 25, 20, 15 and 5 represent when FSO 10 μm, combined 850

nm/WLAN, 4WLAN link and FSO 850 nm link are not available respectively depending on 10^{-9} BER criterion. It can be observed that availability improvement by FSO 850 nm/WLAN links reaches 100% availability despite the 39.49% availability for FSO 850 nm link whereas FSO 10 μm link availability is 76.83%. In this case, FSO 850 nm/ WLAN proves to be superior.

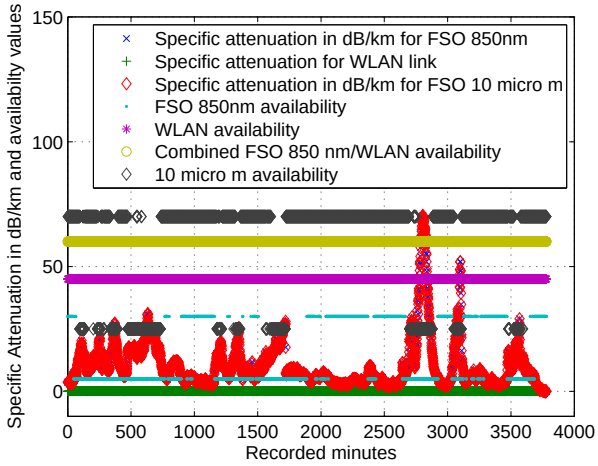

Figure 3.34: Availability of FSO 850 nm/ WLAN and 10μm for a snow event [78].

3.11.2 Monte Carlo simulation for FSO availability estimation under snow conditions

The snow attenuation simulations use measured data. However, the randomly varying dry snow rate motivates to use it as a random variable and perform Monte Carlo simulation to predict attenuation for this random occurrence of dry snow rate. The random values of dry snow rate between 1 mm/hr and 15 mm/hr were generated us-ing uniform distribution. The total number of values taken is 100000. From these dry snow rate values, the attenuation was evaluated using equation 9. These 100000 attenuation values and link budget consideration were used to find the status of reception of the optical signal. These 100000 optical signal reception status values were used to evaluate one availability value. The whole above process was repeated 100000 times to find 100000 availability values. These 100000 different availability values were used to make the histogram. The simulation was performed using Matlab. The results are presented in Figure3.35. The results show that availability of FSO link remains around 0.36% during different dry snow rate values.

The overall summary of availability analysis for measured data is presented in Table 3.2 showing availability of FSO 850 nm, 40 GHz, FSO 850nm/40 GHz,WLAN, FSO 850 nm/WLAN and FSO 10μm Systems under different weather conditions.

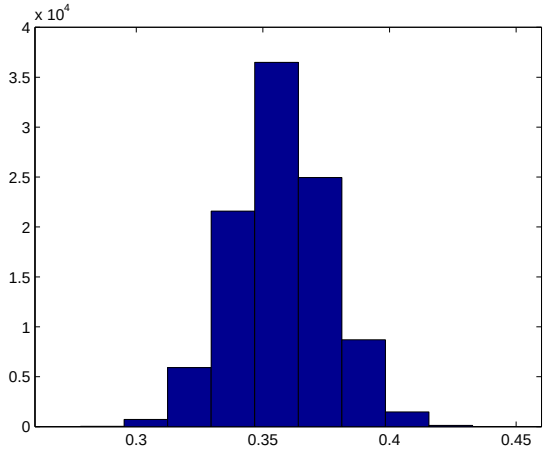

Figure 3.35: Histogram of FSO link availability for different dry snow rate values [71].

Table 3.2: Availability of different links under different weather conditions [70, 78]

System	Dense Maritime Fog	Rain	Snow
FSO 850 nm	0.51%	42.86%	39.49%
40 GHz	100%	14.29%	100%
FSO 850nm/40 GHz	100%	42.86%	100%
WLAN	100%	100%	100%
FSO 850nm/WLAN	100%	100%	100%
FSO 10μm	100%	100%	76.83%

3.12 Cloud attenuation of different optical wavelengths and GHz frequency range

Optical wireless communication provides link for uplink and downlink of satellite communication. Moreover these links can be used for intersatellite communication and High Altitude Platforms (HAP) communication. However cloud attenuation as high as several tens of decibels has been reported [40] for such optical wireless links. Consequently, clouds can completely block the optical beams passing through them.

3.12.1 Cloud attenuation of different optical wavelengths

The cloud attenuation of FSO link plays an important role as it causes link outage for several hours. The accurate estimation of cloud attenuations for real environment is ex-

tremely difficult due to heterogeneity of cloud particle density and diversity of cloud types. There are some empirical models that predict fog attenuation on a terrestrial optical wireless communication link in terms of visibility range. But such models are not applicable in order to estimate cloud attenuations considering vertical path length and elevation angle involved for ground-space link paths.
The clouds are formed by the condensation and deposition of water above the surface of the earth. The clouds can be characterised by several physical parameters such as cloud height, thickness, water content, droplet size, variability and horizontal extent. Water is the major constituent of all precipitation types including all types of clouds. Water droplet diameters in clouds, fog, and haze range from 0.1 to 100 μm and their density is from 1 cubic centimetre to 1000 cubic centimetre [2]. The nominal value of liquid water content varies between 3.128 x 10^{-4} g/m^3 for thin cirrus cloud type, to 1.0 g/m^3 for a cumulus cloud [97].
According to electromagnetic theory, each water droplet extinguishes the radiation with spectral features related to its radius and to the complex refractive index that varies with the wavelength. The cloud attenuation for FSO can be estimated by using three major physical parameters of cloud temperature, liquid water content and the cloud droplet size distribution. The behaviour of complex refractive index of water plays an important role in determining the FSO attenuations by absorption and scattering effects. The real part of complex refractive index depends on speed and propagation direction of optical wireless signal and is related to optical wave phase angle changes. Consequently it contributes towards the scattering of the optical beam. The imaginary part of complex refractive index helps in determining the attenuation contribution by absorption process. The Ray model [97] has been employed in [63] to find complex refractive index.
The cloud attenuation using Mie scattering theory can be estimated by considering the cloud drop size distribution parameter. Generally, the size distribution of atmospheric particulates is represented by two analytical functions, the lognormal distribution and the modified gamma distribution. Modified gamma distribution is generally considered best fit for fog and clouds case, whereas lognormal distribution is generally used to model rain and various atmospheric aerosols [97, 48, 59]. Modified Gamma distribution is represented by Eq. (3.28)

$$n(r) = Nar^{\alpha} exp^{-Br}, 0 \leq r < \infty. \tag{3.28}$$

with

$$B = \frac{\alpha}{\gamma r_{mod}^{\gamma}} \tag{3.29}$$

where n(r) is the volume concentration of cloud droplets per unit radius in $cm^{-3}\mu m^{-1}$ at radius r in μm and r_{mod} is the mode radius which is the radius of maximum frequency in μm. The constants α and γ describe the slope of the size distribution, while a is the normalisation constant ensuring that the integral over all radii yields N, the total number

density in cm-3. The value of the γ parameter is considered equal to one for all clouds. The parameters of size distribution of different clouds with their effective radius, number density N and the liquid water content are given in [97].
To apply Mie scattering theory, we assume cloud droplets to be spherical in shape and are suspended in space while acting independently with a complex refractive index [16]. Although in reality all the particles are not spherical in shape but this fact does not seem to have a large impact on the accuracy of the results calculated using Mie scattering theory [97]. The total expected specific attenuation (dB/km) can be estimated by Mie scattering as follows,

$$\gamma(\lambda) \cong 10^5 \int_0^\infty Q_d(\frac{2\pi r}{\lambda}, \acute{n})\pi r^2 n(r) dr \tag{3.30}$$

where r is the radius of the cloud particle in cm, λ is the transmission wavelength in μm, n(r) is the particle size distribution and Q_d is the Mie scattering efficiency [16] dependent on the size parameter $\frac{2\pi r}{\lambda}$ while $\acute{n}$ is the real part of the complex refractive index. Generally refractive index is complex and given by,

$$n = \acute{n} + i\acute{\acute{n}} \tag{3.31}$$

where $\acute{n}$ is the real part of the complex refractive index representing the scattering capacity of the particle and $\acute{\acute{n}}$ represents the absorption of the particle [16].
The extinction, scattering and absorption efficiencies can be obtained by normalizing the corresponding cross sections and are strongly dependent on the parameter $\frac{r}{\lambda}$,

$$Q_a = \frac{C_a}{\pi r^2}, Q_d = \frac{C_d}{\pi r^2}, Q_e = \frac{C_e}{\pi r^2} \tag{3.32}$$

where C_a, C_d and C_e are the absorption, scattering and extinction cross-sections respectively. According to the energy conservation principle,

$$Q_e = Q_d = +Q_a \tag{3.33}$$

Clouds attenuation for FSO links can be estimated by using Eqn. 3.30 by considering modified gamma distribution as given by Eqn. 3.28 and the extinction efficiency given by Eqn. 3.33.
Fog attenuation studies for different optical wavelengths have lead to the conclusion that usage of longer optical wavelengths is very advantageous in order to mitigate the fog effects.This motivated to study the effects of different optical wavelengths on clouds so that an optimal performance wavelength could be chosen for our future ground-space optical links. The results were presented in [63].

The simulations are performed for wavelengths of 650 nm, 750 nm, 850 nm, 1050 nm, 1550 nm, 3.5 μm and 10 μm. The Mie scattering efficiency is simulated for a temperature

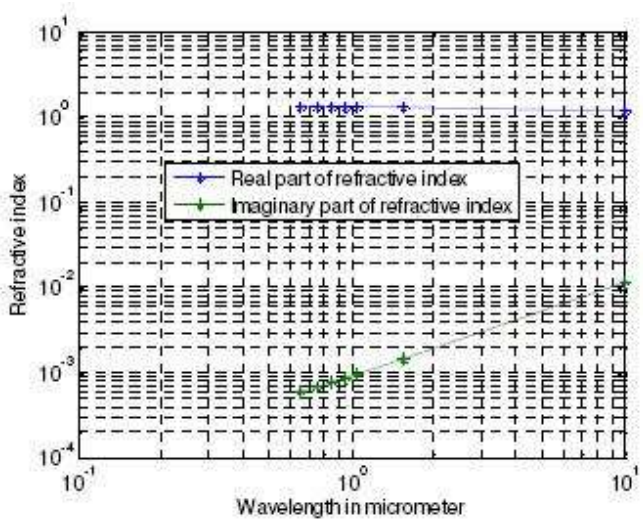

Figure 3.36: Complex refractive index for different wavelengths [63].

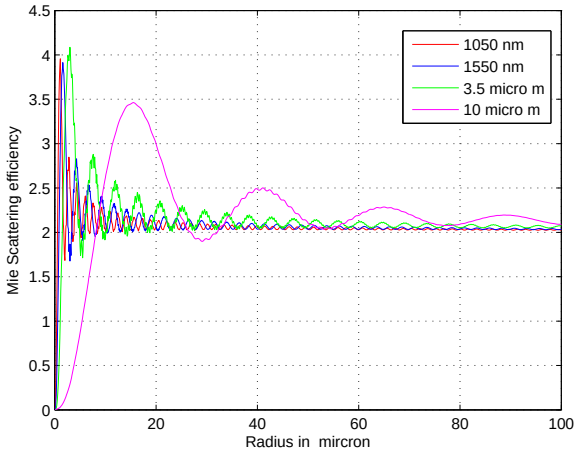

Figure 3.37: Mie scattering efficiency for different cloud particle radii [63].

of 0 °C. This temperature has been taken to calculate the complex refractive index for each wavelength using Ray model [97]. Figure 3.36 shows the complex refractive index for the above mentioned wavelengths. There is no significant difference in real part of the complex refractive indices at different wavelengths.

Complex refractive index calculated in the last step has been used to simulate Mie scattering efficiency. To avoid complexity in plot, only wavelengths of 1050 nm, 1550 nm, 3.5 μm and 10 μm are simulated in Figure 3.37.Figure 3.37 shows Mie scattering efficiency of different wavelengths for different cloud particle radii.

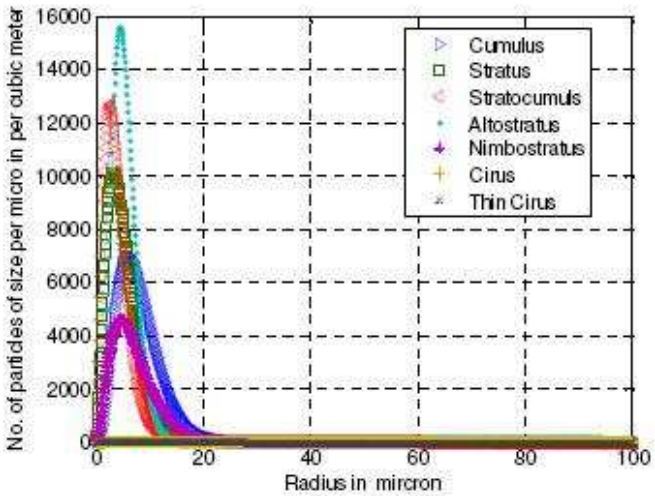

Figure 3.38: Modified Gamma distribution for different clouds [63].

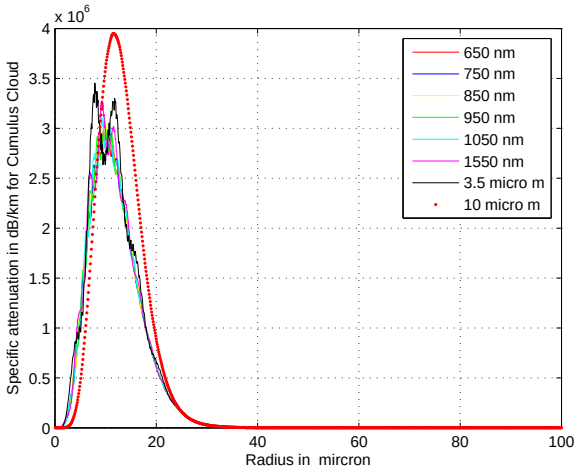

Figure 3.39: Specific attenuation for different wavelengths in Cumulus Cloud [63].

Modified Gamma distribution for different clouds is simulated in Figure 3.38. This figure shows that Altostratus cloud has highest volume concentration of cloud droplets. The volume concentration value obtained here using standard parameters for different cloud type is considered to find specific attenuation of the cloud droplets having radii up to 100 micron.

Figure 3.39 to Figure 3.45 show an approximate estimate of optical specific attenuation in dB/km for different cloud types at already mentioned optical wavelengths. It can be observed that for most of the clouds types, optical attenuation by longer wavelengths is comparatively very low.

As evident from plot in Figure 3.39, shorter wavelengths have lesser attenuation as com-

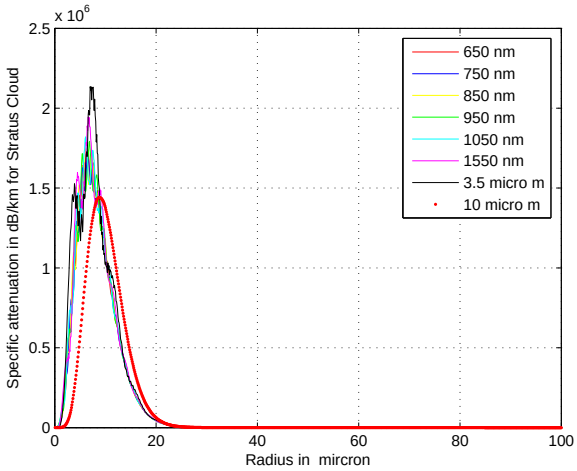

Figure 3.40: Specific attenuation for different wavelengths in Stratus Cloud [63].

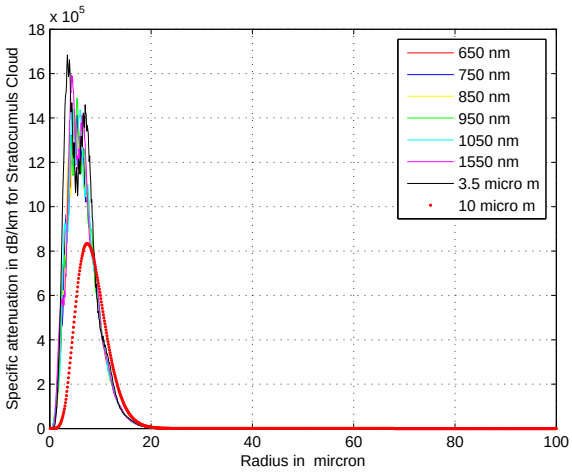

Figure 3.41: Specific attenuation for different wavelengths in Stratocumulus Cloud [63].

pared to longer attenuations for cumulus cloud droplets radii up to 20 micron. This same behaviour is evident in case of nimbostratus cloud for the same droplet radii as shown in Figure 3.43, below. But this trend of optical attenuations does not seem to follow in case of other cloud types like stratus, stratocumulus, altostratus and the thin cirrus cloud types in Figsure 3.40 , Figure 3.41, Figure 3.42 and Figure 3.45, respectively. A very different kind of optical attenuations behaviour is observed for the case of cirrus cloud as simulated in Fig. 9, below. The plot shows that almost the same level of attenuations is reached for the optical wavelengths considered, for cirrus cloud particle radii up to 60 micron. However, for cirrus cloud particle radii greater than 60 micron, the attenuation behaviour seems to follow the same trend as shown by cumulus and nimbostratus cloud types. This signifi-

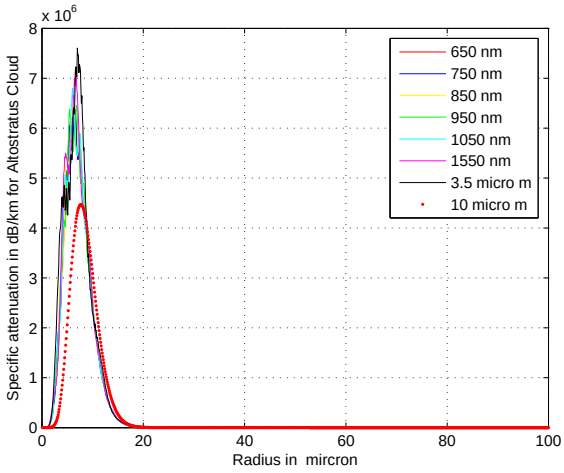

Figure 3.42: Specific attenuation for different wavelengths in Altostratus Cloud [63].

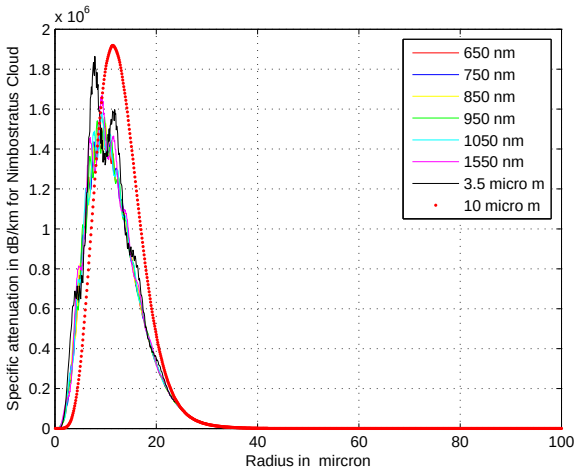

Figure 3.43: Specific attenuation for different wavelengths in Nimbostratus Cloud [63].

cant difference in the behaviour of optical attenuations in different cloud types suggests the variation in corresponding cloud type microphysics. This cloud particle microphysics plays a very decisive role in determining the corresponding attenuations reached when optical transmissions are made through a respective cloud.
The total specific attenuation is calculated using Eqn. 3.30 for the optical wavelengths and results are presented in Figure 3.46. It can be observed that 10 μm wavelength has much lesser specific attenuation for most cloud types. It is easily observable that the optical attenuation in thin Cirrus cloud seems to be very small when compared with other cloud types having very high attenuation. However, as evident from this plot, the optical attenuation in thin Cirrus cloud is much higher than fog and reach up to several ten thousand

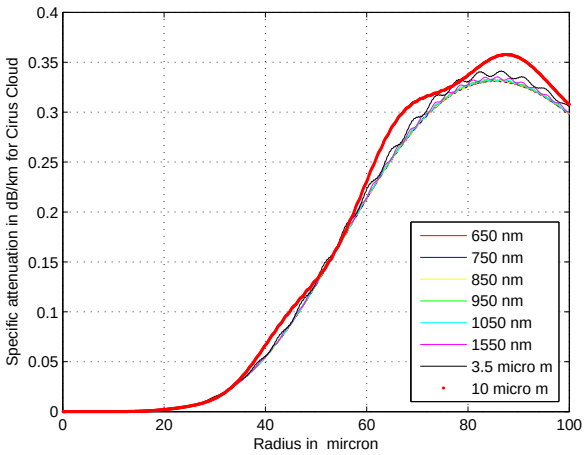

Figure 3.44: Specific attenuation for different wavelengths in Cirrus Cloud [63].

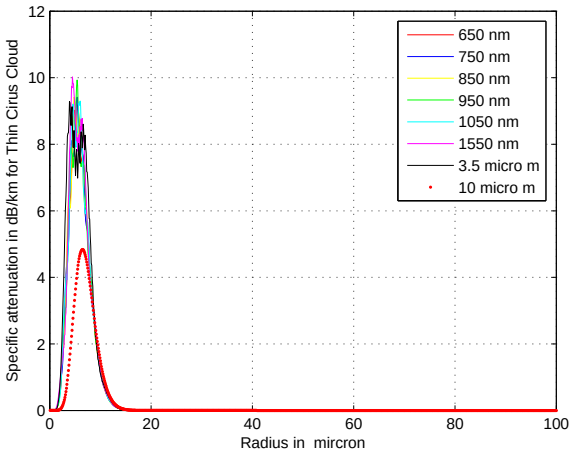

Figure 3.45: Specific attenuation for different wavelengths in Thin Cirrus Cloud [63].

decibels. Additionally, at 3.5 micron the attenuation is highest as compared to the other optical wavelengths considered but attenuation is lowest at 10 micron. The same trend follows in all other cloud types except cumulus and nimbostratus clouds as evident from Figure 3.46.

3.12.2 The cloud attenuation for GHz frequency range

The communication feeder links between gateways and telecom satellites will face rigorous requirement by the future broadband access missions. The presently used frequency

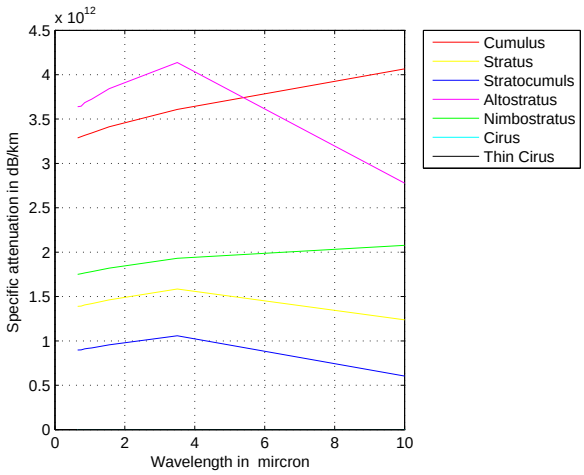

Figure 3.46: Total specific attenuation by different clouds at different wavelengths [63].

bands by feeder links for communication to GEO satellites are C, Ku and Ka bands. However, new microwave bands like Q and V bands can be explored for future bandwidth hungry applications. The atmospheric propagation effects on such high frequencies induce reduced availability due to signal degradation.Free space optical communications (FSO) is an attractive alternative to RF communication links with applications like Deep-space communications, Inter-satellite links, terrestrial long and short distance links and optical links between HAPs and UAVs .However the cloud attenuation of FSO causes complete blockage of the link.An alternate can be the combined FSOC/RF hybrid network. The GHz frequency range cloud attenuation is analysed here.
The specificcloud attenuation for GHz frequency range is given by [89]. This specific attenuation calculation along with liquid water content [97] for different clouds was used to simulate the attenuation suffered by different GHZ frequency ranges for different clouds. Simulations were performed for C band (4 GHz and 6 GHz), Ku band (10 GHz and 14 GHz), Ka band (20 GHz and 30 GHz), Q band (35 GHz and 50 GHz) and V band (55 GHz and 75 GHz). Figure 3.47 shows the Specific attenuation estimated for different clouds on log scale for different GHz frequency bands. The logarithmic results in Figure 3.47 do not show any huge difference between the specific attenuation of different frequencies.

Figure 3.48 shows the Specific attenuation estimated for different clouds on linear scale for different GHz frequency bands. Figure 3.48 shows that higher frequency bands suffer more attenuation by different clouds and the specific attenuation difference between 4 GHz C band frequency and 75 GHz V band frequency for Cumulus cloud is nearly 3 dB/km. For other clouds, this difference is even less and the difference for Cirrus and Thin Cirrus cloud is almost negligible. This advocates for the use of high frequency bands.

The high bandwidth hungry future communication applications pose the requirement to use FSO between optical ground stations and satellites. However strong cloud attenua-

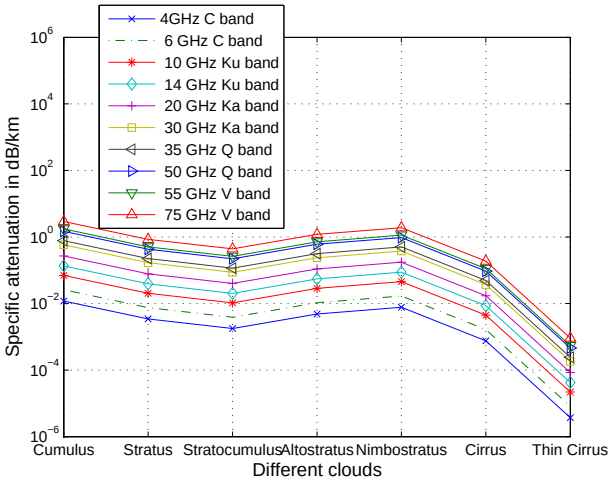

Figure 3.47: Log scale GHz attenuation estimated for different clouds [72].

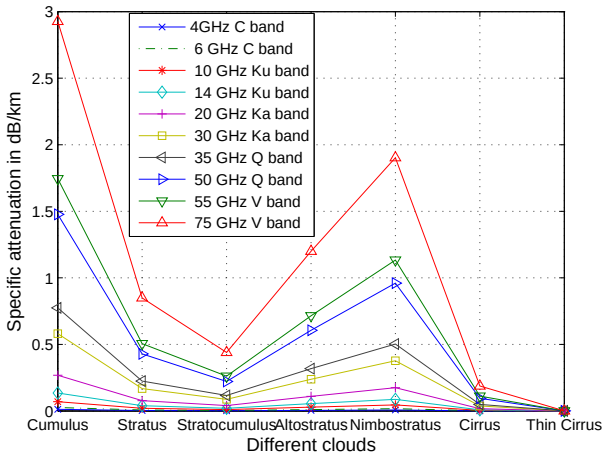

Figure 3.48: Linear scale GHz attenuation estimated for different clouds [72].

tion hampers to use this technology for the satellite communication. One solution is to use the FSO/RF hybrid network and utilize the RF bands when there is blockage of FSO link. The analysis show that 10 μm wavelength suffer the least attenuation among different FSO wavelengths. Among different RF frequency bands, the cloud attenuation is high for higher frequencies. However the difference of specific attenuation is not as significant as in case of FSO wavelengths. This advocates using high frequency RF bands along with large wavelength FSO link for high data rate demanding applications.

4 PROPOSED SWITCH OVER ALGORITHMS AND THEIR PERFORMANCE ANALYSIS

Free Space Optics (FSO) links provide usage of high bandwidth and the flexibility of wireless communication links. However, weather patterns like fog and heavy snow fall limit the availability of FSO. Another technology providing similar properties regarding offered data rates and flexibility of set up is Millimeter Wave Technology (mmW), operating at several tens of GHz. In this case, heavy rain limits mmW link availability. Another back up link technology WLAN can achieve better availability of hybrid network. A combination of FSO/mmW or FSO/WLAN technologies had been proved to be very effective to achieve very high availability. Different hybrid architectures of these two links and switch-over techniques are presented in this chapter and their prototype implementation and performance is analysed.

4.1 First version proposed switch-over algorithm and its performance

The first proposed switch over algorithm was for FSO and mmW systems and results were presented in [80]. The tested Free Space Optics equipment was a MultiLink system with 155Mbps data rate featuring a multiple beam system. The distance between the two setup FSO units was 2.7 km, connecting unit 1 at "Studienzentrum, Inffeldgasse 10" to unit 2 at the "Observatory Lustbühel". In order to get more information about the influence of the weather, the link distance was made longer than specified by the manufacturer for this system. A maximum range of 1 km is guaranteed for the MultiLink system.
The terminal station for the microwave communication system consisted of the outdoor equipment, which contained the upconverter with the power amplifier and the low noise amplifier with the downconverter. The indoor equipment consisted of an L-band converter and an access system . The received signal was shifted down from 40 GHz to 1 GHz, which was further converted down in the indoor equipment to 70 MHz. For the measurement setup a continuous mode modem was used to measure the receive power. Hence, the absolute measured power was an image of the channel influenced by weather conditions. As mentioned before, the main disturbance for the microwave link was rain. Therefore the rainfall was also required to be measured very accurately. On the bases of the available rain measurement data from the 2D video distrometer of cooperation partner "Institute of Applied Systems Technology (Joanneum Research)", the average rainfall can be calculated

over an arbitrary time interval. This 2D video distrometer measures the size, shape and the velocity of each raindrop.
The switch over algorithm was based on the following concept. Given the SNR the required power at the receiver, in order to produce a desired BER value, can be calculated for OOK modulation. Under different noise and atmospheric attenuation conditions, how much power must be transmitted can then be derived [8]. The signal level at the receiver should be checked for a certain threshold and when the received signal level falls below this threshold, there should be a switch over from FSO to MMW and whenever the signal goes above another higher threshold, there should be a back switch over from MMW to FSO. Thus system remains available despite the degradation in FSO link. The channel selection algorithm is shown in Figure 4.1.

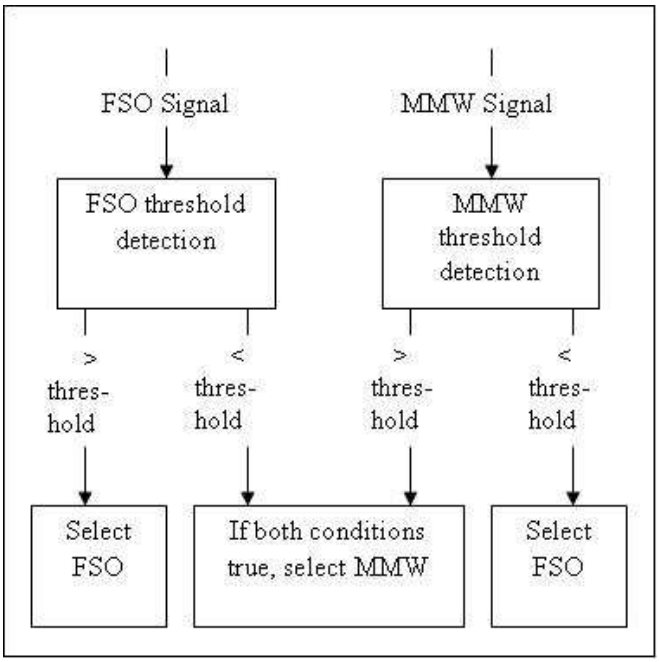

Figure 4.1: Channel selection by switch over [80].

4.1.1 Simulation results of first proposed switch over algorithm for one year availability data

The data for the analysis was taken from the measurement campaign. Basically two types of measurements were carried out. The first recorded the received power and the second observed the link at the network layer using the network program "PING". Each link of the point to multipoint network must have a line of sight with the according Fresnel zone. Concerning the link to the Observatory Lustbuehel, the clearance from the line of sight

was 6 times the first Fresnel zone [52]. The link budget for the long distance displayed a signal to noise ratio of 15 dB. The modems in use could lock at a SNR of 8 dB., hence the resulting margin for rain was 7 dB, which was much smaller than necessary for achieving a satisfactory availability. In the EU-project "EMBRACE" a margin of 18 dB has been proposed to obtain an availability of 99.95%. The following results of this switch over analysis were presented in [80].

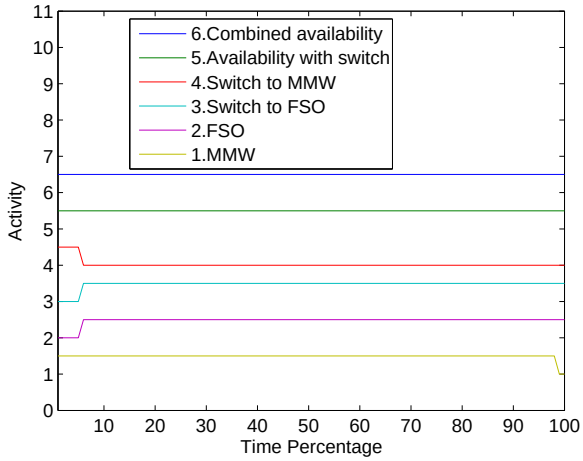

Figure 4.2: Mean year availability and switch activity for both channels [80].

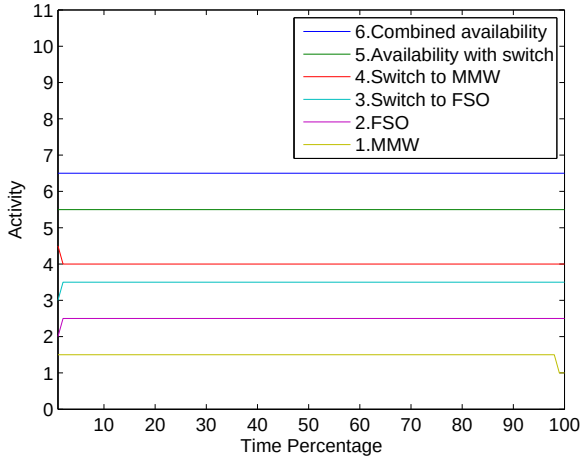

Figure 4.3: December 2001 availability and switch activity for both channels [80].

It can be seen from these graphs that switch over maintains availability of combined redundant links. The advantage of using switch over is that while maintaining the availability

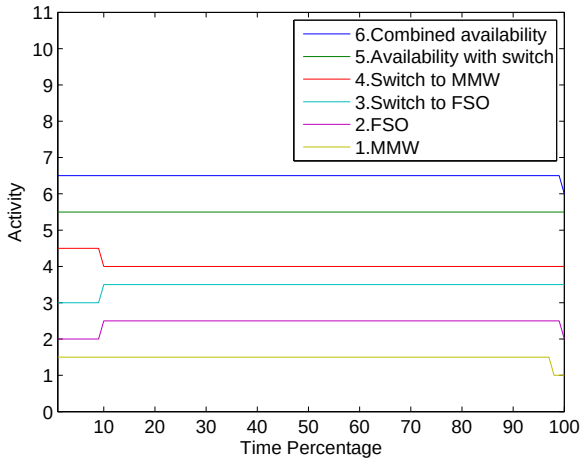

Figure 4.4: January 2002 availability and switch activity for both channels [80].

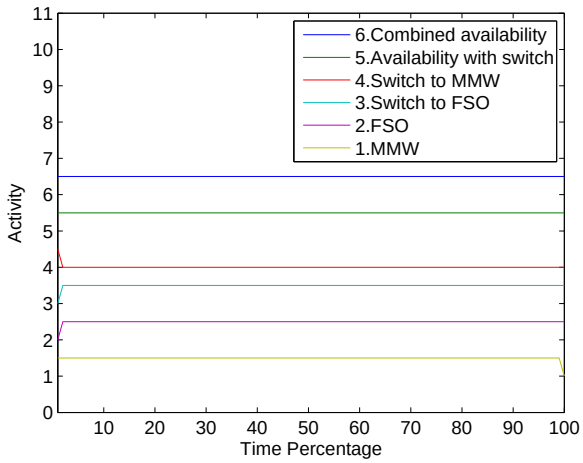

Figure 4.5: Availability and switch activity for maximum FSO availability month [80].

of combined redundant links, it avoids transmission of extra power for back up link when FSO link is available.

4.1.2 Performance of first proposed switch over algorithm for different weather conditions

The same switch over algorithm was analysed for one year measured availability data of mmW and for four years availability data of FSO [79]. Figure 4.7 shows the proposed switch over for FSO and mmW. FSO signal is continuously monitored against a threshold.

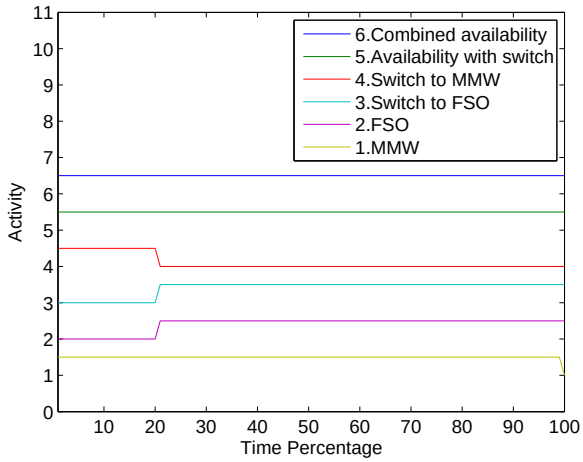

Figure 4.6: Availability and switch activity for minimum FSO availability month [80].

If FSO signal falls below the threshold, it switches to mmW signal. Then besides monitoring FSO signal, it starts monitoring mmW signal for a certain threshold. If mmW signal is above its threshold and FSO signal is below its higher threshold, it remains on mmW link. If FSO signal exceeds higher threshold, it keeps mmW active till FSO link becomes stable. Although main link FSO despite of being available is not used in this time but it helps in avoiding rapid switching. When both links are down, it keeps both active in order to detect the recovery of any link. By the use of this switch over availability of redundant links is maintained without wasting extra redundant transmission power. The switch over behaviour results were presented in [84] for different weather conditions. Figure 4.8 shows

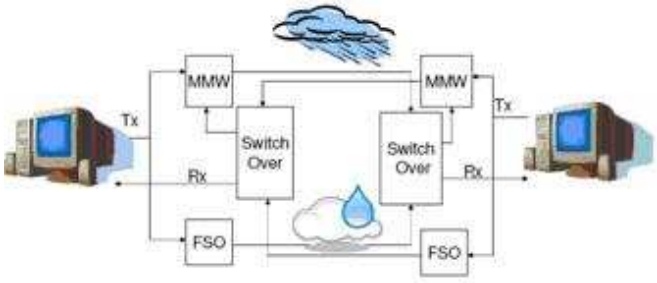

Figure 4.7: Physical view of the system with switch over [79].

the snow event recorded at Graz on 28.11.2005. Switch Over value of 90 represents the FSO usage whereas switch over value 5 represents the MMW usage only. The simulation of 40 GHz attenuation has been performed with the assumption of dry snow fall using [60]. The FSO link is operational for 39.49% of snow event.

The behavior of switch over is also simulated for a fog event measured on 25.10.2005 at Graz. Figure 4.9 shows the specific attenuation measurement for FSO 850 nm link. In

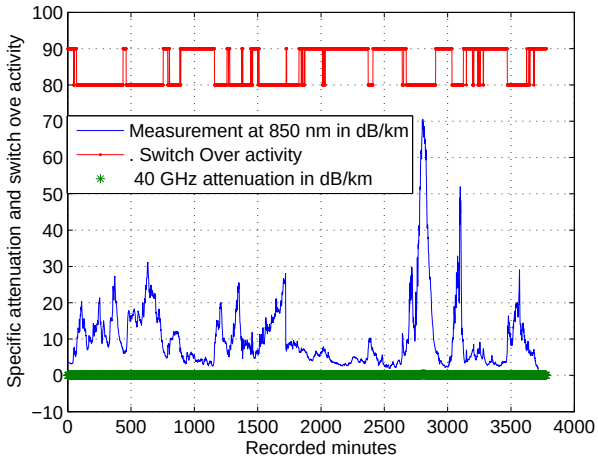

Figure 4.8: Switch Over activity for a snow event [84].

Figure 4.9 FSO measurement means FSO specific attenuation in dB/km. The switch over combined load balancing mode has been represented by a value of 40 whereas switch over value of 0 represents only MMW usage when FSO attenuation exceeds its specific margin of 7 dB/km. This shows that for a fog event with specific attenuation of 110 dB/km, switch over can use both links in load balancing mode for 39.14 % of total fog event time. The behavior of 40 GHz link has been simulated using [89] and [33].

Figure 4.10 shows the performance of switch over for a rain event in Prague. In Prague,

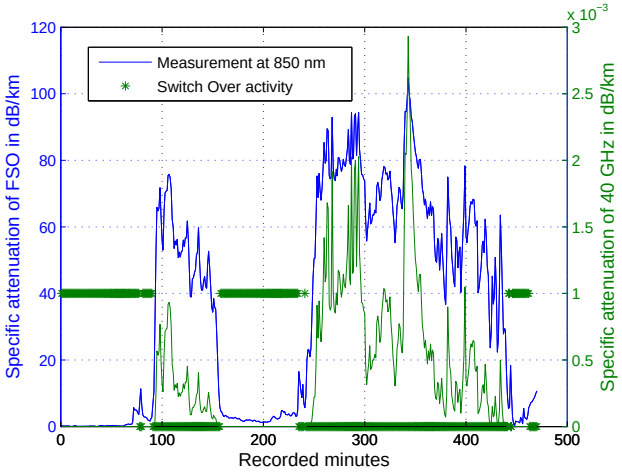

Figure 4.9: Fog event and switch over behavior [84].

FSO link at 850 nm has been operated on a path length of about 850 m. Transmitted power is +16 dBm, divergence angle is 9 mrad and optical receiver aperture is 515 cm. Rain rate was measured using two tipping bucket rain gauges with different collecting areas.

In Figure 4.10, switch over value 4 represents FSO usage which amounts to be 71.42%, whereas switch over value 0 represents either MMW usage or none of the link. In this event MMW has not been used at all and no link was available for 29.58% of time. This is due to the fact that the rain is highly detrimental for MMW and there is no such time in this rain event when 40 GHz link availability is better FSO. During this time as explained earlier, both links will be kept active till any of the link regains its operational status. This suggests that lower frequency back up links should be used in the regions with high rain rate. The behavior of 40 GHz link has been simulated using measured rain rate and [88].
The comparison of measured availability shows that fog has the most deteriorating effect

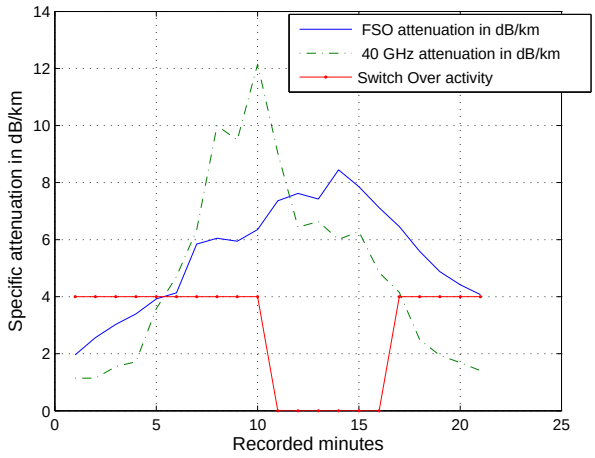

Figure 4.10: Rain event and switch over behavior [84].

on FSO availability. This fact had been observed in winter months especially in December in which minimum FSO availability was recorded. Snow also affected the FSO availability in these months. In the simulation of winter months, it shows that for worst case of FSO link availability, the backup link usage has been increased by switch over to maintain the availability. For the months of spring and summer, FSO availability is more than 99%. Causes of less than 1% failure in summer were heavy thunderstorms and mist in night [52]. Behaviour of switch over was simulated for the months of June and it has been shown that switch over tries to combat the effect of hailstorm and mist by activating mmW link during that time. However it restricts wastage of mmW usage when it is not required. Simulations were carried out for all 12 months of the year. The results are presented here in the form of chart. It shows that average usage of backup mmW link for the whole year was less than 15%.

Figure 4.11 shows comparison of average availability by combined redundant links and simulated availability with switch over for all months of the year. It can be seen by the Figure 4.11 that irrespective of different weather conditions of the year, switch over tries to maintain the availability achieved by using redundant links. Besides maintaining the availability of the link, switch over avoids unnecessary redundant use of back up link. In

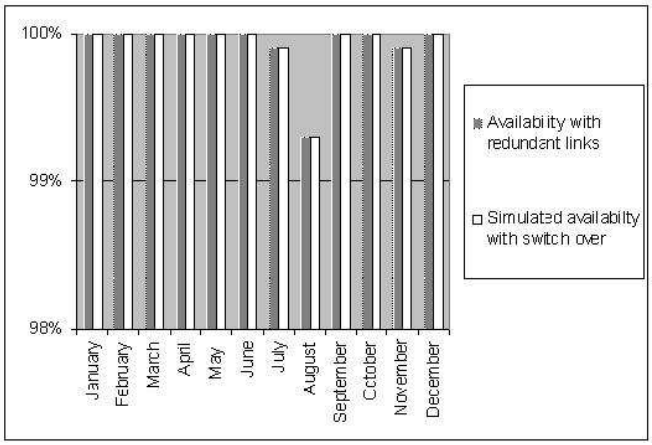

Figure 4.11: One year availability comparison of redundant links and switch over [84].

the Figure 4.12, MMW usage has been simulated for the exaggerated worst condition of FSO link establishing and breaking on alternate instants.
Figure 4.12 shows comparison of average mmW usage without switch over and simulated mmW usage with switch over for the whole year. Figure 4.12 shows the huge difference between mmW usage with and without switch over. It not only saves expensive semiconductor amplifier power but also improves aging. Here unavailability of FSO has been simulated with the exaggerated case of alternate available and unavailable events that would occur rarely in the reality. This exaggeration doubles mmW usage. In reality, approximately half of this usage is expected which further decreases the amplifier power usage.
It was concluded that the benefits of FSO motivate to use it as last mile access. However the deterioration of weather attenuation can be coped with backup link of comparable data rate. But use of back up link as continuously transmitting redundant link is not a good solution. The available power in semiconductor amplifier in the GHz range is small and expensive. Moreover greater usage of equipment causes aging. The switch over can help to increase the usage of FSO link while maintaining availability. By selecting one link, it avoids wastage of transmission power for redundant MMW channel when FSO link is available. The simulations show that average usage of back up link for maintaining the availability achieved by redundant link is 14.79%. It means switch over can provide the same availability by avoiding back up link transmission more than 85%.

4.2 Second version proposed Switch-Over algorithm: Self Synchronising approach

This algorithm was proposed for FSO and IEEE 802.11 standard. The IEEE 802.11 is an international standard of physical and MAC layer specifications for wireless local area

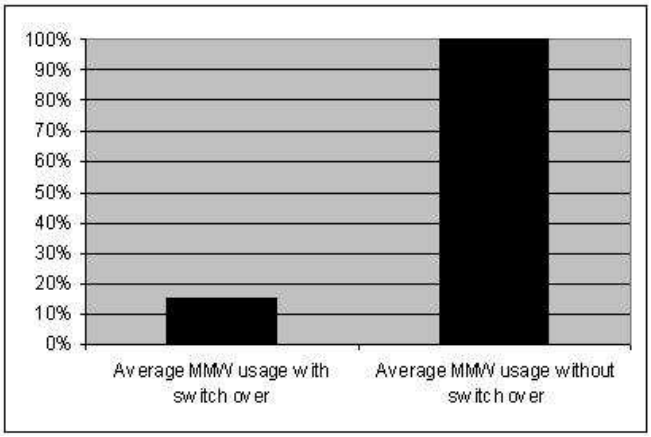

Figure 4.12: One year comparison of mmW usage with and without switch over [84].

networks (WLANs) in the 2.4 GHz public spectrum bands. Its original specification supports data rates of 2 Mbps. More recent amendments (IEEE 802.11a/b/g) allow higher data rates (11 Mbps and 54 Mbps, respectively) and exploit other frequency bands (5 GHz band with 54 Mbps). The selection of an IEEE 802.11a standard compliant backup link has been governed by different reasons: The major goal of the backup link is to maintain link availability when main link (FSO) is strongly affected by fog. Research studies have shown that frequencies below 10 GHz show negligible attenuation due to fog. Therefore, a hybrid wireless network built up of FSO and a 5 GHz WLAN link provides high availability regarding weather conditions. Another advantage of this link is the fact that it is using a license-free band at a relatively low frequency, where the technological problems of amplification, temperature drift and similar have mostly been overcome. The 5 GHz band is less populated and, thus, devices in this band are less susceptible to interference. A higher transmit power allows greater distances than IEEE 802.11b/g devices do. In addition to that, the emerging IEEE 802.11n standard allows for data rates up to 600 Mbps in a MIMO scenario. Thus, data rates comparable to the FSO link can be achieved with off-the-shelf equipment in WLAN scenarios as well. Future studies will show if this also holds for long-range directional links. The wireless optical communication system available at Technical University Graz is the GoC MultiLink 155/2 and supports data rates up to 155 Mbps over a distance of 2.7 km. The WLAN link was built with two embedded PCs using high-gain grid antennas and Ubiquiti XR5 miniPCI WLAN cards. These are getting used for further performance improvements since they provide fairly high receiver sensitivity and therefore are able to connect sites over up to 50km depending on the antennas used.

4.2.1 Proposed setup for installation

The properties of the FSO and the WLAN system are given in Table 4.1. The system proposed uses a hybrid link to interconnect two sites of the campus of the Technical University of Graz: The newest part of the campus bearing most developed lecture rooms and high speed internet access ("Inffeldgründe") and a remote observatory of the campus devoted to space research ("Observatorium Lustbühel"). Figure 4.13 shows the proposed link together with a map of the city of Graz. The distance of 2.7 km between these two parts exceeds the manufacturer's specification of the FSO system. Still, as it was proven in a test setup this increased link distance only reduces the error margin, while still making a undisturbed communication possible during acceptable weather conditions.

Table 4.1: Properties of FSO, WLAN Hybrid System [66].

System	FSO	WLAN
Tx Wavelength	850 nm	5.20-5.825 GHz
Tx Technology	VSCEL	Semiconductor Amplifier
Tx Power	2mW(+3dBm)	1.26mW (1 dBm)
Tx Aperture Diameter	4x25mm Convex lens	Antenna gain 30 dBi
Beam divergence	2.5 mrad	-
Rx Technology	Si-APD	Semiconductor Amplifier
Rx acceptance angle	2 mrad	10 degree
Rx aperture	4x25mm Convex lens	-
Rx sensitivity	-41 dBm	-94 dBm
Specific Margin	7 dB/km	14 dB/km

The idea of switch over is quite trivial. The FSO link is the default link, as it allows for a higher bandwidth. If the optical received signal strength (ORSS) on this link falls below a certain value, the multiplexer switches to the WLAN link [8, 80]. If the received signal strength on the FSO link goes up again, the system switches back. Therefore, it is only necessary to acquire the FSO link quality, which is measured in 10 levels. At level 0 the optical link completely breaks down, whereas all higher levels show little to no bit errors at all.

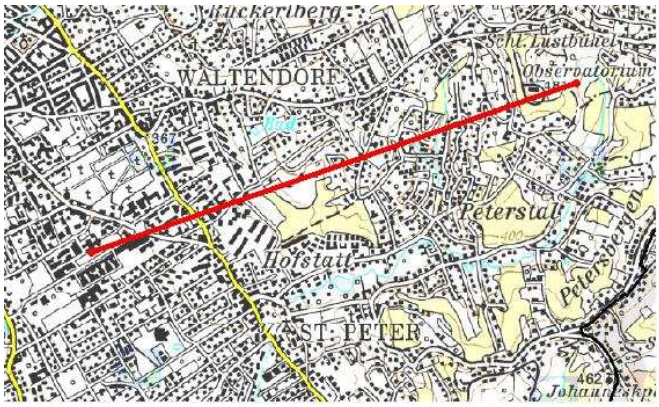

Figure 4.13: Link between different campus sites (2.7 km) [66].

In weather conditions unfavourable for FSO, transitions between optical signal strength levels occur at a quick succession. Therefore, without a hysteresis the switching rate of the multiplexing device could exceed the network's ability to adapt to a changing infrastructure. In fact, the RS232 interface of the GoC MultiLink 155/2 updates the link quality data every second. Hysteresis is ultimate solution to avoid rapid switching back and forth. A synchronization-efficient switch-over algorithm is implemented. The block diagram in Figure 4.14 shows the physical arrangement of the system. At one end there is a multiplexing device, while de-multiplexing on the other end is performed by any commercially available switch. As a multiplexing device, two possibilities were evaluated; A self-made PHY layer multiplexer and a Linksys WRT54GL, in which we exploited the virtual LAN (VLAN) capabilities to switch between the two links. The latter device operates on the MAC layer, but still provides transparency.

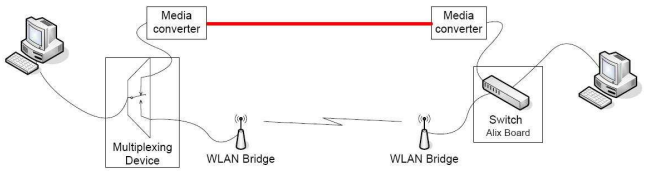

Figure 4.14: Physical arrangement of the system [66].

The transceiver on multiplexer-end always connects to the active link, i.e. either the FSO link with high bandwidth or the WLAN link with a lower bandwidth. The switch on the other end assumes both links active.
Since FSO is completely implemented on PHY layer and since the WLAN link is operated in switching mode, both links can be considered transparent to MAC layer. Therefore, the switch only receives packets with the MAC address from the multiplexer-end transceiver.

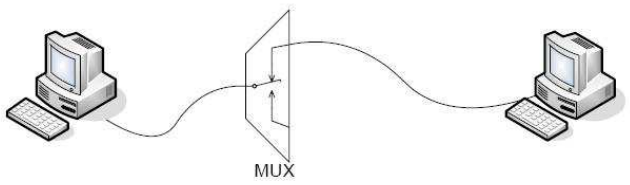

Figure 4.15: A first test of the MUX

This switch now maps MAC addresses to ports. If a packet with the MAC address from the multiplexer-end arrives at the switch, the port from which it came becomes the outgoing port for packets. If now, due to switch-over, a packet with the same source address arrives at another port, the MAC table gets updated, so that the new port is the destination for outgoing packets. Thus, this system is self-synchronizing. In addition to that, link speed is determined by the switch according to the capacity of the medium connected to the outgoing port. Therefore, the bandwidth on the main link is not limited by the redundant link bandwidth.
However, there may be packet loss if the multiplexer on the multiplexer-end side switches over but no packets are transmitted from the multiplexer-end. If now the switch-end transmits, these packets are lost at the multiplexer. This can be overcome with the ordinary TCP, which automatically transmits ACK packets and thus ensures a proper and fast switching table update. The following Lab. and simulation results were presented in [66].
A few tests were performed to evaluate the performance of the equipment, in terms of bandwidth and link loss time (LLT) during a switching event. Bandwidth and LLT were measured with Iperf 1.7.0 and WireShark 1.0.3. With a first test (depicted in Figure 4.15) of the determined the RF capabilities of the self-made Ethernet multiplexer (MUX). This and the following tests were performed with Iperf, a network analysis tool. This test revealed that the MUX is not a limiting factor in the overall network connection. For both lines a total TCP bandwidth of 94 Mbits/s was achieved. A UDP test showed that (with a default bandwidth of 1.05 Mbits/s) the datagram loss was 0% (0 out of 2676).

The scenario depicted in Figure 4.16 is similar to the actual scenario, with the difference that the two Ethernet cables are replaced by an FSO link and a WLAN link, respectively. This test showed that - speaking about the RF capabilities of the MUX - a significant amount of crosstalk is produced on the line which is not in use. If we now use a switch which does not shut off ports which are not in use but instead listens on them all the time, the damaged differential signals significantly reduce the overall bandwidth (to 15 - 25 Mbits/s). Therefore, a proper choice of the switch is absolutely necessary, until a complete re-design of the MUX PCB was done. A bridging module running on an Alix embedded PC seems to be an excellent choice, since TCP bandwidths of 94 Mbits/s and UDP loss of 0% (0 out of 893) could be achieved. The LLT during a switching event can be related to the auto-negotiation in which the participating devices exchange information about transmission parameters, such as speed or duplex mode. The MUX physically dis-

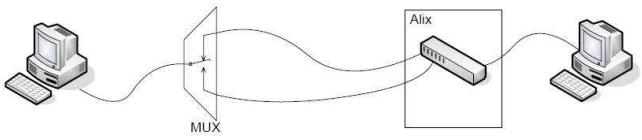

Figure 4.16: Using and appropriate switch for testing the MUX

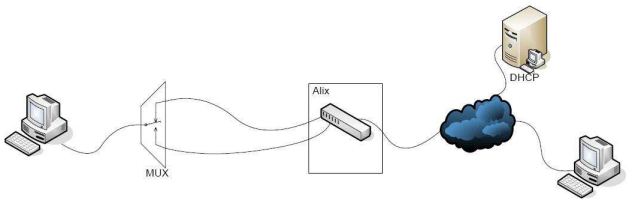

Figure 4.17: Testing the MUX in an DHCP environment

connects an Ethernet cable on one port and connects another cable at another port, making such a negotiation necessary. If Fibre-Ethernet media converters or WLAN access points are used the switch does not need to perform auto-negotiation, because the connections between the devices and the switch are not influenced. Instead, only a link negotiation at the multiplexer-end has to be performed. A test in which the MUX was clocked with a 2 s-periodic signal failed completely, because link negotiation could not take place. This, however, is a problem which should not occur in the final scenario, in which the switch never gets unplugged, because it is always connected to the FSO/RF equipment.

Finally, as it can be seen in Figure 4.17 we made a ping test, with which we determined the delay for packets to be redirected if at least one of the PCs acquires a new network address via DHCP - recall that the PC on the near-end briefly looses its connection and therefore has to reconnect to the network. We found out that over an interval of 18 s no ping packets could be transmitted.

In a final test scenario (Figure 4.18), we substituted the FSO link with a fibre cable, so that we could measure the effects of the media converters without the influence of weather. Although the FSO system allows bandwidths of up to 155 Mbps, we have used Fast Ethernet components with a nominal bandwidth of 100 Mbps only. This is due to the reason that

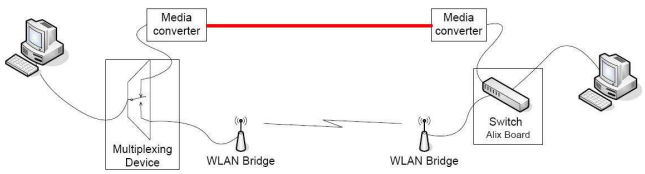

Figure 4.18: Actual Lab Test for Switch-Over System

Table 4.2: Bandwidth and UDP Datagram Loss (MUX and VLAN) [66].

	Fiber	WLAN	Fiber FDX	WLAN FDX
Bandwidth TCP (Mbps)	91.9	18.8	76 + 68	8.9 + 10.2
Loss UDP 1 Mbit	0.12%	0%	0%	0.23%
Loss UDP 10 Mbit	0.04%	0.024%	0.02%	0.059%
Bandwidth TCP (Mbps)	94.2	20.2	79.8 + 45.9	7.1 + 11.9
Loss UDP 1 Mbit	0%	0%	0%	0%
Loss UDP 10 Mbit	0%	0%	0%	0.08%

Table 4.3: Average Link Loss Time [66].

	MUX	VLAN
From WLAN to Fibre	1.62 s	1.54 s
From Fibre to WLAN	1.63 s	1.02 s

Fast Ethernet equipment is cheaper and more widespread, so a qualitative evaluation of different components can be done more easily. The WLAN link was built up of two Compex WP54AG Wireless Access Points in access point mode and wireless adapter mode, respectively.

In the first series we tested the self-made hardware multiplexer (MUX), which simply connects one Ethernet cable to any of two other cables on the PHY layer. First, all links were built up with category 5 cables in order to evaluate the bandwidth and crosstalk of the MUX. This test showed that attenuation can be neglected for Fast Ethernet, since we achieved bandwidths of 94 Mbps. The limiting factors in this case are most likely the network interface cards of the transmitters on both ends. The bandwidth of the overall infrastructure therefore is limited by the Fast Ethernet components and the WLAN devices.

Exact results of bandwidth tests can be seen in Table 4.2. However, another test revealed that the crosstalk cannot be neglected. The resulting LLT can be seen in Table 4.3.

Although the MUX does not influence the bandwidth, it introduces slightly more problems with UDP, resulting in a higher datagram loss, which may be due to a bad RF design of the PCB. Still, satisfying results could be achieved.

In a second series of tests the multiplexing device was a Linksys WRT54GL wireless router with OpenWrt 7.9 as an operating system. Switching between different ports was done by changing the configuration of the VLANs. This way, a switch can be logically divided into a series of switches, each one operating in a different VLAN. The actual VLAN in use was configured that way, so that it only contained the port connected to the switch-end transmitter and the port connected to the desired link, namely WLAN or Fibre, respectively. By changing the configuration i.e. removing the Fibre port and adding the

Table 4.4: Link availability and average bandwidth for different methods [66].

		Pure FSO	**TC**	**PT (T=60 s)**
Availability	%	67.43	98.62	99.37
Link Loss	%	32.57	1.38	0.63
Bandwidth (HDX)	Mbps	61.9	67.30	65.1
FSO underutilization	%	0	0.69	3.88

WLAN port for example, the Ethernet frames were now directed over the desired link. The re-configuration was done with a single command. Again, bandwidth and LLT were evaluated. As it can be seen in Table 4.2, half duplex bandwidth in VLAN implementation was increased in both WLAN and Fibre case compared to the MUX design. UDP datagram loss could be neglected. Table 4.3 reveals that LLT was much lower for all scenarios tested compared to the MUX design. Yet, since the switch of the Linksys WRT54GL uses a store-and-forward algorithm, a few packets are transmitted over the in-active link after VLAN re-configuration. If now such a re-configuration is done during a total link loss, these packets stored in the internal memory of the switch cannot be properly forwarded, resulting in a slightly higher LLT. The determination of this actual time is within the scope of future work, however. Despite this fact, VLAN switching definitely outperforms MUX switching, so the final measurement scenario will most likely use this mechanism.

4.2.2 Simulations and Validation

All Matlab simulations performed are based in a set of measurements from [38] at the Technical University of Graz. The campaign was started on September 29th 2005 and ended on March 1st 2006. The optical link was built up over a distance of 79.8 m between two buildings of the campus. 14 fog events were recorded during that time, among them the one used for simulations . Since the MultiLink 155/2 system allows for a per-second measurement, but only for a per-minute recording of the ORSS, a disrete ORSS signal was derived from the continuous one recorded by the above mentioned measurement campaign.

The data used for this set of information was recorded during a fog event on October 25th, 2005, between 03:00 and 11:00, as seen in Figure 4.19. During this event, FSO availability was reduced to 67.43%. This particular event was chosen instead of a long term period, since longer periods lack of a significant number of threshold crossings relative to the observation interval. That is, the FSO link may be available for weeks, succeeded by a day-long period of total link loss. On average, fog events like the one considered here, contribute little to a whole-year average. Considering these fog events separately helps to distinguish the advantages and disadvantages of different switch-over methods. Furthermore, extrapolating the measurement results to longer periods of time makes carrier class

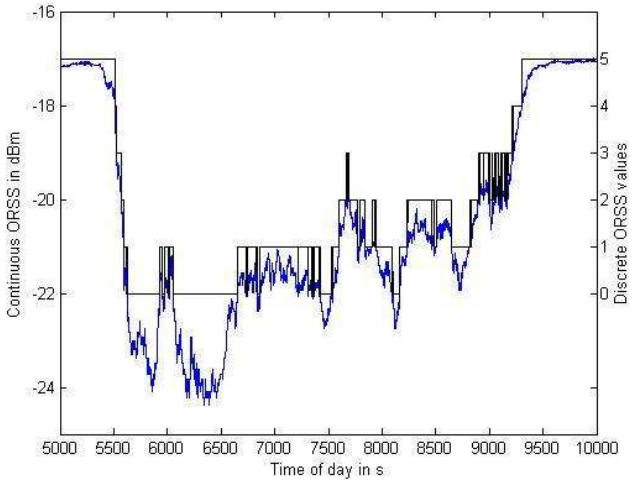

Figure 4.19: Comparison of discrete and continuous ORSS values [66].

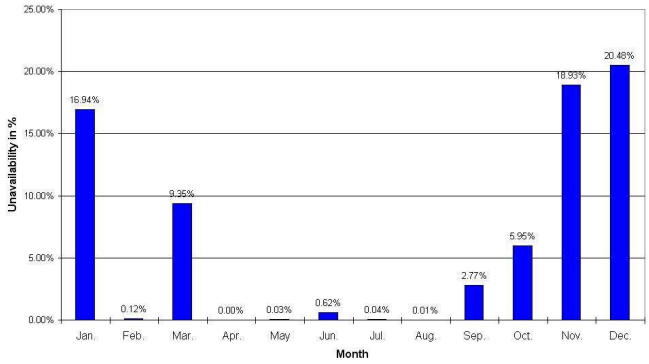

Figure 4.20: Average Unavailability from Oct. 2000 to Sep. 2001 [62].

availability of 99.999% achievable. For example, by looking at Table 4.4 one can verify that by taking the overall measurement campaign into account, the proposed methods can easiliy increase the availability to values exceeding 99.9%. Figure 4.20 on the other hand shows that the measurements were recorded during times of maximum FSO link failures. Therefore, an extension of these measurements to an all year average, assuming little FSO loss during the summer months would lead to an availability of 99.996%. To even further increase availability to carrier class, one would have to optimize the proposed algorithms with data from more than one single fog event. This, however, is within the scope of future work. For the simulations, an arbitrary receiver sensitivity of -22 dBm was assumed. This choice can be justified by the multitude of FSO equipment available, which in turn bears a variety of different transmitters and receivers, let alone link distances. Setting the receiver sensitivity to a particular value can therefore be done without loss of generality. In fact, the

choice of -22 dBm was governed by the reason that this value was crossed by the ORSS a certain number of times.

According to Table 4.3, LLT was set to 3 s to allow either of the discussed multiplexing devices and include an additional margin for eventually slow link establishment. The WLAN link was assumed to be available all the time, an assumption which can be justified by the fact that WLAN will only be used during fog events and that these events have little influence on the wavelengths used by WLAN. For bandwidth simulations FSO bandwidth was set to 91.9 Mbps and WLAN bandwidth to 18.8 Mbps according to Table 4.2. All methods employing a power hysteresis had an upper threshold exactly 1 dBm or 1 unit above the receiver sensitivity for the continuous or discrete case, respectively. Performance was tested by changing the value of the lower threshold only, while keeping the width of the hysteresis constant.

Pure threshold comparison (TC) yields an increase in availability to 98.62% while achieving best bandwidth performance for both continuous and discrete ORSS measurements. Since the focus of this work is put on availability, the following methods were optimized with that regard.
As one can imagine, finding the optimum switching methods together with its parameters means finding an acceptable trade-off between average bandwidth and availability. If the assumption would hold that the WLAN is available without interruption, transmitting on this link only would definitely ensure 100% availability. Yet, even if this assumption is justified by the fact that the WLAN link is only little affected by fog, the bandwidth is prohibitively low for that one. Pure threshold comparison (TC), as it was already mentioned, could provide an increase in performance in terms of availability and average bandwidth (see Table 4.4). Unfortunately, as Figure 4.21 shows, to increase the reliability of the overall link, pure TC cannot be used because of fluctuations causing too many switching operations. Table 4.4 compares the pure FSO solution to hybrid systems with different switch-over algorithms: TC and a combined power and time hysteresis (PT). Latter one will prove to perform best in terms of availability. The remainder of this section is devoted to a more complete evaluation of simulation results. An even more complete discussion of this topic can be found in [67].

4.3 Third version proposed Switch-Over algorithm: Filtering and time hysteresis approach

The main purpose of the switch-over algorithm is to cope with fluctuation noise. There are physical methods to reduce this noise, e.g. by using multi-link systems, wide apertures or saturated amplifiers [4]. Yet, long-distance links still suffer from fluctuation, and therefore switch-over methods have to be designed according to that. Pure threshold comparison (TC) would result in too many switching operations, which in turn decreases bandwidth

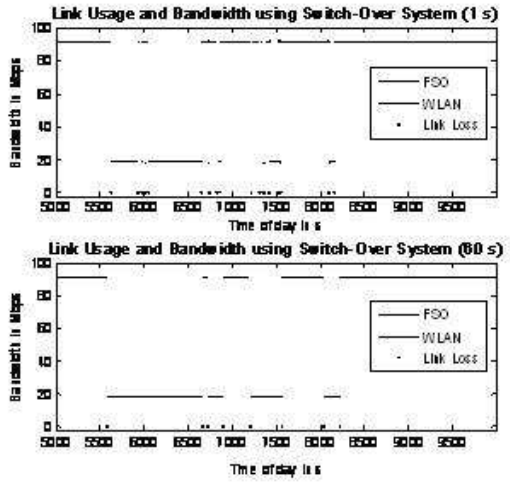

Figure 4.21: Bandwidth for different switch-over methods [66]

and availability by the occurring LLTs. Filtering and hysteresis would be possibilities to overcome fluctuation noise, to name only a few. It is the purpose of this section to introduce a few of these methods.

Finally, the designer has to take into account that changes in the average ORSS values as well as fluctuations strongly depend on the diurnal and seasonal time as well as on the geographic location. Thus, not only different devices but also different locations, sometimes even different seasons require separately designed algorithms.

4.3.1 Power Hysteresis (PH) and Time Hysteresis (TH)

Making use of a power hysteresis is a well-established method in wide fields of electronics, communications and signal processing and will be covered only briefly. Making use of PH has the purpose of getting hold of the unwanted variations of the ORSS by preventing to many switch-over operations. The design of the hysteresis is therefore strongly dependent on the amount of variations. Furthermore, since availability is the major concern of the proposed system, the lower threshold has to be set accordingly. At the least, the lower threshold has to be set to the receiver sensitivity; however, setting it to higher ORSS values leads to an increase in availability.
TH is another method which operates directly on the ORSS values but still prevents performance decrease due to numerous switch-over operations. Unlike PH, only one threshold is defined at a value higher than the receiver sensitivity. After crossing this threshold, the incoming ORSS values are evaluated for a certain wait period T. Only if they do not cross the threshold again in this given time (i.e. stays below or above), a swich-over operation

is performed. In order to optimize the design with respect to availability, this wait period is only employed for switching to the FSO link which is vulnerable to fog events and may loose its connectivity from time to time. Switching in the opposite direction is done immediately.

4.3.2 Filtering

Methods subsumed under filtering are performed directly on the ORSS values. Variations in these values are smoothed, so that simple threshold crossing algorithms can be employed. The threshold may be identical or greater than the receiver sensitivity - the latter choice providing higher availability values. Filters of different orders N and types can be considered; among them moving average (MA), triangular (TR) and exponentially weighted moving average (EWMA) filtering. Their impulse responses can be characterized as follows, each one for $n = 0..N-1$:

$$h_{MA}[n] = \frac{1}{N} \tag{4.1}$$

$$h_{TR}[n] = \frac{1-\frac{n}{N}}{\sum_n h_{TR}[n]} \tag{4.2}$$

$$h_{EWMA}[n] = \frac{e^{\frac{-n\ln 10}{N}}}{\sum_n h_{EWMA}[n]}, \tag{4.3}$$

where for EWMA the filter coefficient is defined by the order so that the last value is less than 10% of the first value. Filters have to be designed carefully in order to smooth the signal, but still allow for reacting timely on critical changes in the ORSS. As it can be seen in Figure 4.22, all filters applied to the ORSS signal provide smoothing of the unwanted variations. In terms of smoothing MA performs best; on the other hand, this filter lacks of the capability to react timely on critical changes in the ORSS. Especially higher filter orders suffer from that problem. TR and EWMA filters perform similar, since both of them fulfill the fading condition. Their smoothing capabilities are small compared to MA, but in turn allow for fast reactions on link loss. A trade-off has to be found, which filter type and filter order to take.

4.3.3 Combined Methods

Applying two or more of the methods mentioned above was a possibility which had to be evaluated as well. It might be interesting, for example, if the simultaneous employment of TH and PH yields any improvement on availability. Similarly, it might be the case that filtering beforehand improves the performance of hysteresis techniques.

Looking at Figure 4.23 one can easily see that PH is a powerful tool for increasing avail-

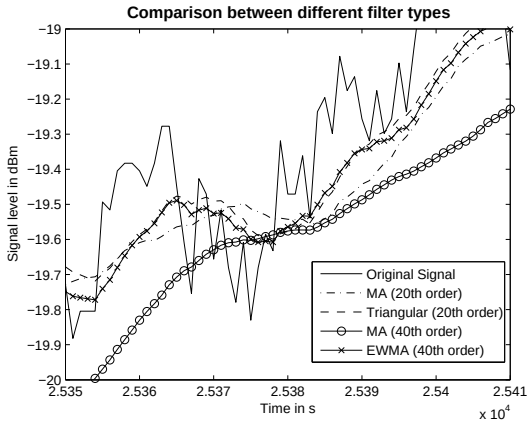

Figure 4.22: Comparison of filter properties [67].

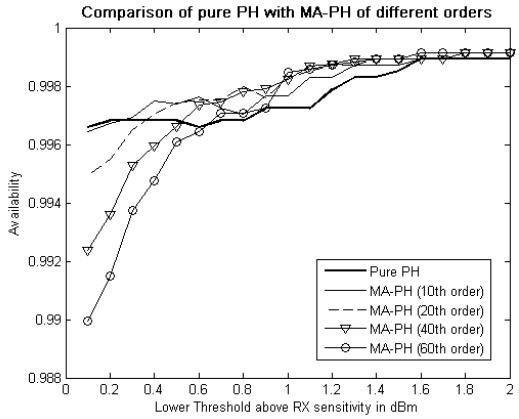

Figure 4.23: Availability for PH and filtered PH [67].

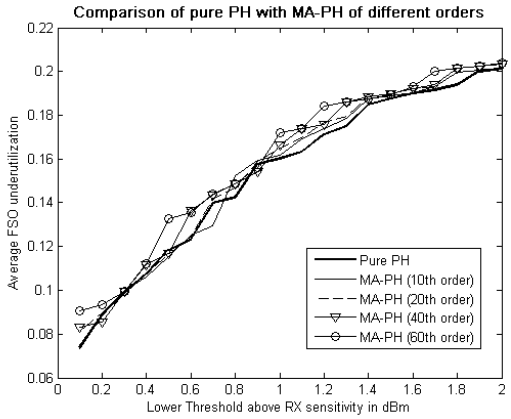

Figure 4.24: FSO underutilization for PH and filtered PH [67].

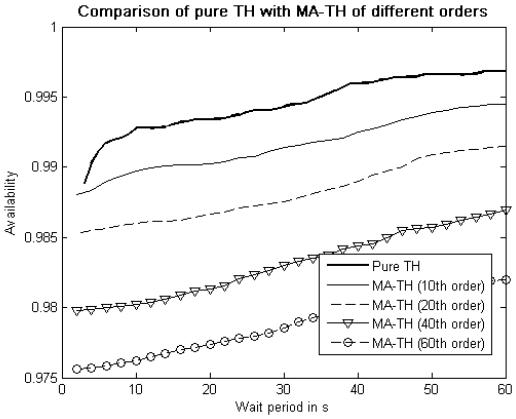

Figure 4.25: Availability for TH and filtered TH [67].

ability. Especially, if the lower threshold is reasonably larger than the receiver sensitivity, availabilities of 99.9% could be achieved. Even more so, if the signal was smoothed by MA filtering beforehand. Unfortunately, Figure 4.24 reveals that for these thresholds FSO underutilization is prohibitively large, which in turn leads to a decrease in performance in terms of average bandwidth. The introduced constraint therefore limits the lower threshold to values below -21.7 dBm. For these thresholds, on the other hand, MA filtering seems to reduce the overall availability. Moreover, higher filter orders even lead to worse availability values. This is due to the fact that both MA and PH are designed to mitigate the variations in the ORSS - combining these methods, on the other hand, only increases the time to react on changes of the link quality. As a result availability is decreased. Other filter types, like TR or EWMA perform better than MA, because these filters allow for faster reaction because of their forgetting factor. Still, pure PH cannot be outperformed by filtering beforehand.

4.3.4 Results by using Time Hysteresis

Figure 4.25 reveals that applying a temporal hysteresis cannot outperform PH in terms of availability. The threshold is set to the receiver sensitivity, and one may suggest that by setting the threshold to higher values (like it is done in PH) availability could be increased. Alas, this does not hold. Increasing the threshold to higher ORSS values only increases FSO underutilization (see Table 4.5). Still, PH provides a more reliable link. This also applies for MA-filtered TH, for the same reason as already mentioned above. TH and MA both cope with varying ORSS, a combination of these methods fails to react on decreasing link quality in a timely manner. Again, with increasing filter order availability values worsen, this time even more drastically. Although TR and EWMA filters perform better, pure TH still delivers best results. The advantage of TH can be seen from Figure 4.26, where one can see that the average bandwidth is relatively high. This is caused by a very

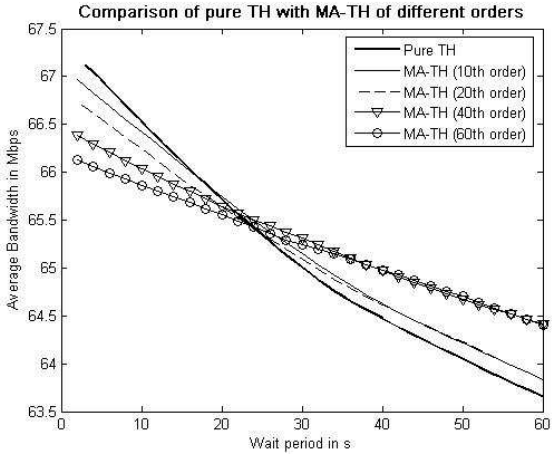

Figure 4.26: Average bandwidth for TH and filtered TH [67].

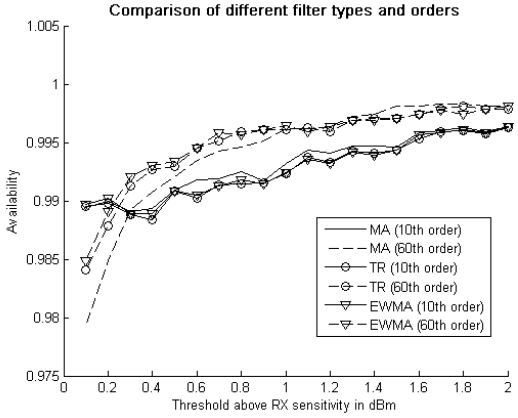

Figure 4.27: Availability for different filter types and orders [67].

small FSO underutilization, which indeed stays below 6% over all possible wait periods. Pure TH, compared to filtered TH, suffers from a higher dependency between wait period and bandwidth. In fact, for longer wait periods filtered TH provides higher bandwidhts as pure TH. Yet, this does not justify filtering because of availability concerns.

4.3.5 Results by using Filtering

Figure 4.27 shows that performance in terms of availability is increased by increasing the threshold, which is easy to comprehend. Interesting, though, might be the fact that higher orders perform better than lower ones, as long as the threshold is set to values high enough. Additionally, even more interesing is that for high orders MA performs worst, while its performance is best for lower orders. This can be explained easily by taking the fading

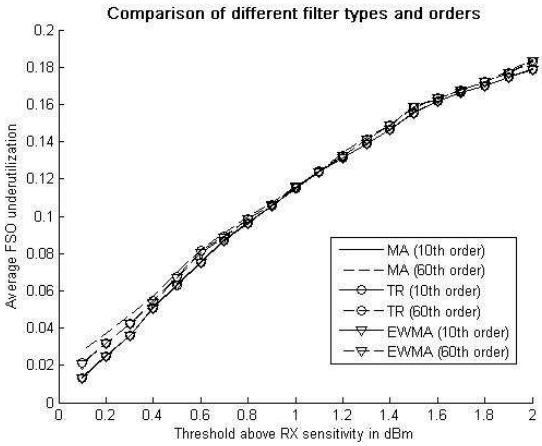

Figure 4.28: FSO underutilization for different filter types and orders [67].

properties of EWMA into account. High order EWMA filters perform smoothing, but also allow timely reaction on critical changes in the ORSS. Lower orders of EWMA or TR lack from these smoothing characteristics, therefore variations in the ORSS stay harmful. Low order MA copes better with these variations than TR or EWMA of the same order (see Figure 4.22). A look at Figure 4.28 on the other hand reveals that the increase in threshold compared to the receiver sensitivity is limited due to the FSO underutilization constraint. The threshold has to be below -21.2 dBm in order to keep underutilization below 10%. Another intersting point is illustrated in Table 4.5, where one can see that for both EWMA and TR higher filter orders not only perform better in terms of availability, but also in terms of bandwidth. This astonishes even more by taking into account that also the FSO underutilization is increased for higher orders. The reason for this can be found by looking at the relatively small guard band between receiver sensitivity and threshold. By switching over to WLAN too late, link loss is not only introduced by the switching operation itself, but also by FSO unavailability. Thus, by more efficient smoothing availability and bandwidth values can be improved, even if FSO underutilization is also increased.

4.3.6 Results by using Combined Methods

Since the previous sections revealed that a combination of filtering with whatsoever type and order with either TH or PH yields no improvement, the last thing to discuss is a combination of time and power hysteresis (PT). For this, we can also try to find out if filtering is sensible here. Again, the lower threshold was set to receiver sensitivity, whereas the higher threshold was 1 dBm higher. As Figure 4.29 shows, reasonable performance can be achieved by combining these two methods, as long as no filtering is involved. Unfortunately, simulation results show that the wait period is limited to less than 40 s, because for longer periods FSO underutilization is prohibitively large (Figure 4.30). It is interest-

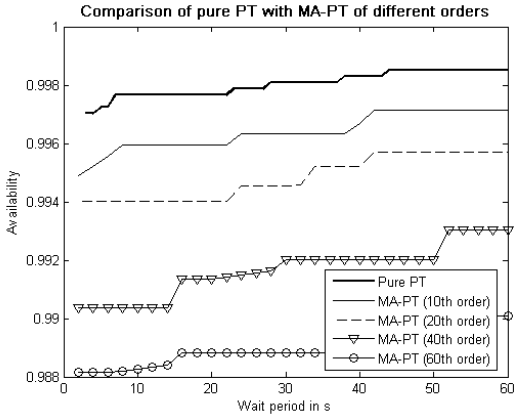

Figure 4.29: Availability for PT and filtered PT [67].

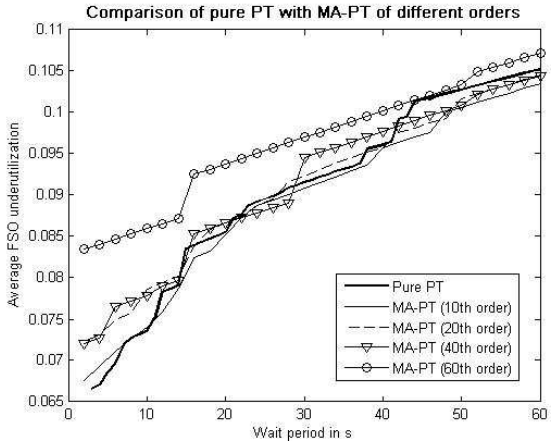

Figure 4.30: FSO underutilization for PT and filtered PT [67].

ing, though, that with increasing filter orders not only the availability is reduced, but also the average bandwidth decreases due to higher FSO underutilization. This can again be related to the fact, that both PH and TH already cope with variations in the ORSS, and applying filtering therefore is useless. Again, EWMA and TR perform better than MA, but still pure PT cannot be outperformed. By increasing the lower threshold to values above the receiver sensitivity, availability can be improved significantly. Yet, this method is not available because of its high FSO underutilization (Table 4.5). As the same table shows, best performance can be achieved with this method even for relatively short wait periods of 10 s.

Table 4.5: Comparison of different switch-over methods [67].

Method	LT dBm	UT dBm	T s	N -	Avail. %	BW Mbps	Under. %
TC	-22	-22	-	-	98.62	67.30	≈ 0
PH	-21.7	-20.7	-	-	99.69	60.65	9.93
TH	-22	-22	10	-	99.28	63.53	1.58
	-22	-22	60	-	99.68	63.63	5.82
	-22	-21	10	-	99.38	58.34	12.87
MA	-21.2	-21.2	-	10	99.25	60.60	9.66
MA	-21.2	-21.2	-	60	99.46	60.57	9.98
TR	-21.2	-21.2	-	10	99.15	60.56	9.65
TR	-21.2	-21.2	-	60	99.59	60.69	9.84
EWMA	-21.2	-21.2	-	10	99.18	60.59	9.64
EWMA	-21.2	-21.2	-	60	99.56	60.68	9.82
PT	-22	-21	10	-	99.77	62.58	7.35
	-22	-21	40	-	99.83	60.97	9.61
	-21	-20	10	-	99.83	55.66	16.87

4.4 Fourth version proposed switching algorithm: Load balancing approach

The redundant link usage of mmW along with FSO increases the availability up to 99.92%. However, the available bandwidth of mmW link was wasted redundantly during the operational time of main FSO link. Keeping in view these considerations, a bandwidth efficient switch-over has been proposed that will efficiently utilize the overall bandwidth of the hybrid system. The implementation strategy of the proposed switch-over is explained below. In default mode, FSO system is operational and mmW link can be used for sending additional data, hence the total bandwidth of the system is increased. The signal level at the receiver should be monitored for a certain threshold. When the FSO link received signal level falls below this threshold, the system should switch-over from FSO to mmW. Under this condition of switch-over, mmW sends the data whereas FSO transmit the test data so that receiver can monitor the FSO link for its recovery. The FSO received signal strength is continuously monitored and compared until it exceeds a certain higher threshold as an indication of its recovery so that there should be a return to load sharing on two independent data streams. In this way, system remains available all the time despite the degradation in FSO link under severe fog conditions. The same strategy is employed in case of mmW link failure by monitoring test mmW received signal strength against a higher threshold to avoid rapid back and forth switching. When both links are down, it sends test data on both links in order to detect the recovery of any of these links. The threshold for switching should be adjusted so that it should initiate and complete switching process before

the actual FSO or mmW link failure. The packets received should be acknowledged and when the receiver detects corrupted packets or low threshold level, it sends this information to the transmitter on both links. When the transmitter detects any link failure either by detecting threshold or retransmission request, it sends the packet next to the last acknowledged packet by the receiver on operational link and test data on the failed link. As the link between two communicating devices is the same, the threshold detection is expected simultaneously on both sides. In addition to threshold detection, retransmission request by the receiver on the basis of exceeding a certain acceptable BER is the second check for a link failure. The test data is used for monitoring the recovery of the failed link. Once both links regains their operational status, both sides perform handshaking for the link status information transfer and acknowledgement of last packet received by the active link and then both links start load sharing. Figure 4.31 and Figure 4.32 present logical block diagram and physical overview of the proposed Switch-over between FSO and mmW links respectively.

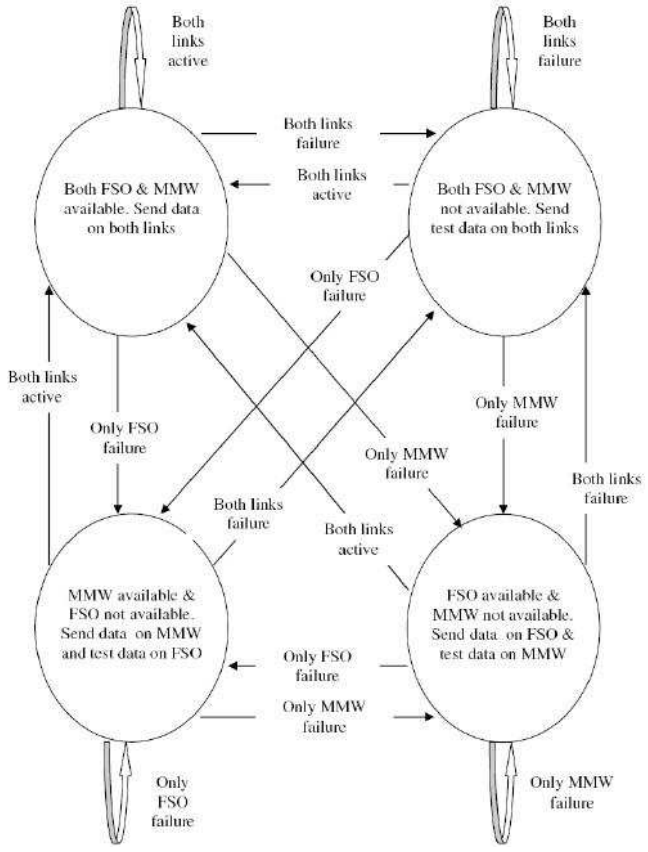

Figure 4.31: Channel selection by load balancing Switch over [65].

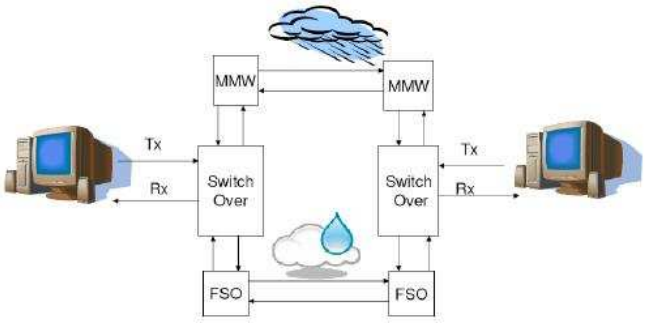

Figure 4.32: Physical view of load balancing Switch over [65].

4.4.1 The principles of Load sharing

The proposed switch-over greatly enhances the bandwidth utilization by employing the idea of load sharing during the time when both links are operational, which amounts to be more than 90% of the total measured time, This reduces the bandwidth wastage from 100% to less than 10% of the total measured time.
The availability data used for analysis was for FSO and mmW systems. The properties of two systems used for the experiment are presented in Table 4.6.
The following results were presented in [65]. Keeping in view the availability data mea-

Table 4.6: Properties of FSO, mmW Hybrid System [65].

System	FSO	mmW
Tx Wavelength	850 nm	40 GHz
Tx Technology	VSCEL	Semiconductor Amplifier
Tx Power	2mW(+3dBm)	EIRP 16 dBW
Tx Aperture Diameter	4x25mm Convex lens	Antenna gain 25 dB
Beam divergence	2.5 mrad	10 degree
Rx Technology	Si-APD	Semiconductor LNA
Rx acceptance angle	2 mrad	10 degree
Rx aperture	4x25mm Convex lens	-
Rx sensitivity	-41 dBm	Noise figure 6 dB
Specific Margin	7 dB/km	2.6 dB/km

sured during 2001-2003 for the hybrid system consisting of FSO and mmW links, availability of the two channels is simulated with and without switch-over. This availability data consists of a ping test such that each time two ping tests were performed to measure the availability of each link. Whenever less than 2 ping acknowledgements for any link were detected, it is assumed for the simulation that switch over will detect a threshold for switching. The principle utilized for a simulation of the proposed switch-over behaviour is mentioned in Figure 4.31 . Results for the whole year as calculated by simulation routines for switch-over are displayed in Figures 4.33, 4.34 and 4.35. Figure 4.33 shows comparison of average availability by combined redundant links and simulated availability with switch over for all months of the year. Figure4.34 shows comparison of mmW usage without Switch-over and simulated mmW usage with Switch-over for all the month of the year. Figure 4.35 shows comparison of average mmW usage without switch over and simulated mmW usage with switch over for the whole year.

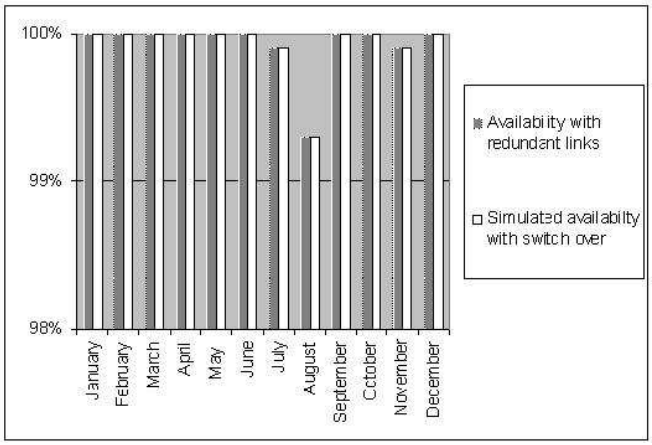

Figure 4.33: All months availability comparison with and without load balancing [65].

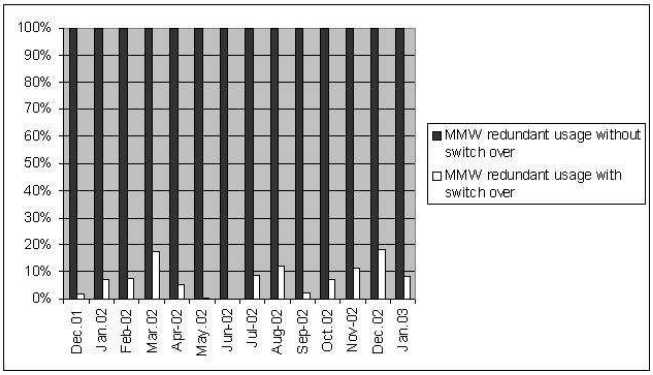

Figure 4.34: All months mmW usage comparison with and without load balancing [65].

It can be seen by the graph presented in Figure 4.33 that irrespective of different weather

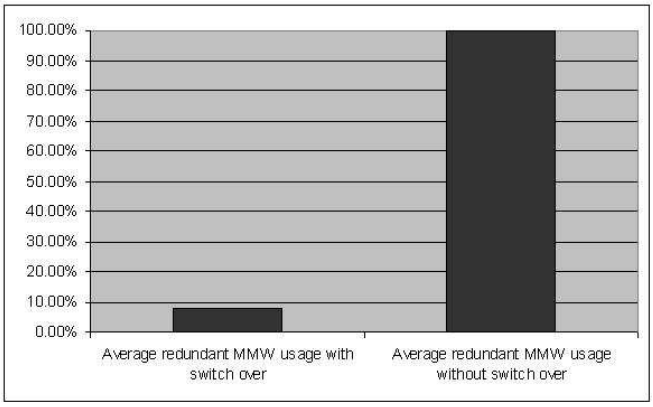

Figure 4.35: Whole year mmW usage comparison with and without load balancing [65].

conditions during the whole year switch-over tries to maintain the availability achieved by using redundant links. Besides maintaining the availability of the link, switch-over avoids unnecessary redundant usage of back up link. In the following graphs presented in Figures 4.34 and 4.35, mmW usage has been simulated for the exaggerated worst condition of FSO link failure and recovery on alternate instants. These results also show the significant difference between mmW usage with and without switch-over. It saves redundant transmission of mmW bandwidth which can be used to transmit useful additional data by load sharing.

In these simulations, switch-over is assumed to be fast enough to perform switching on the basis of threshold detection before the actual ping failure is received by any link. Finally, the availability reduction due to delay in switch-over is simulated and results are presented in Figure 4.36. In the simulation presented in Figure 4.36, a unit time is taken as the time delay between a transmission and acknowledgements of the ping. Simulation results show that if switch-over delay is very small, such that threshold detection and switch-over processes take place before the actual ping failure is detected; then switch-over maintains the availability achieved by continuous redundant link. The availability simulations with and without switch-over are based on the assumption that switch-over is fast enough to perform switching on the basis of threshold detection before the actual ping failure occurs.

The throughput improvement with this technique was presented in [82]. Based on the whole year measurement, it has been found by simulation that switch-over uses nearly 88% of the time for sending data on both links thus increasing the bandwidth utilization. The switch-over sends data, 2% of the time only on FSO and approximately 8% of the time only on mmW link. In comparison to this approach, redundant data approach sends same data at both links for the whole time. Moreover it requires high data rate FSO link to decrease to slow mmW data rate for synchronization.

Figure 4.37 shows the impact of switch-over for improving throughput. Ordinate shows the percentage of total time operation. It can be seen that combined data rate of both links can be obtained for 88% of total operational time with switch over. It also shows for com-

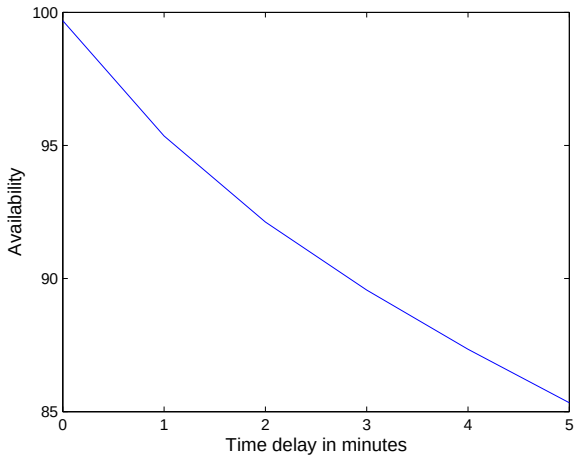

Figure 4.36: Availability reduction due to delay in switch over process [65].

parison that without switch-over, the maximum throughput will be the throughput of low throughput link for whole of the time.

In Figure 4.38, performance of switch-over is simulated for different throughput ratio

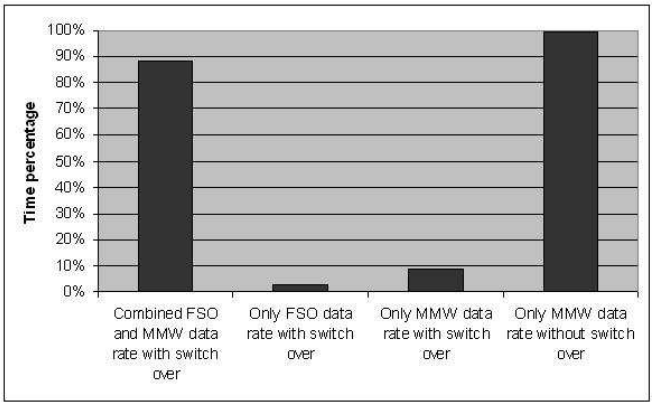

Figure 4.37: Comparison of two links usage with and without switch-over [82].

of FSO and mmW link. Thus a ratio of 1 means that the throughput of FSO and mmW are equal and a ratio of 10 indicates that throughput of FSO is 10 times the throughput of mmW link.Figure 4.38 shows that the performance of switch over increases significantly with the increases in difference of throughputs of two links. If there is a huge difference between, the throughputs of two links, switch-over exhibits many folds efficient bandwidth utilisation. Even if both systems have same throughput, throughput of the hybrid network with switch-over is 88% better than the throughput without switch-over. It was concluded that by selecting both links for information transfer, it avoids wastage of redundant transmission bandwidth of mmW channel when FSO link is available. The simulation shows

that if both links provide same throughput, the throughput of hybrid network with switch-over is 88% more than the throughput without switch-over. If the throughput of FSO is 10 times the throughput of mmW link, switch-over makes the throughput more than 10 times the throughput of hybrid network without switch-over.

Then switch over implementation prototype for load balancing of FSO and WLAN was

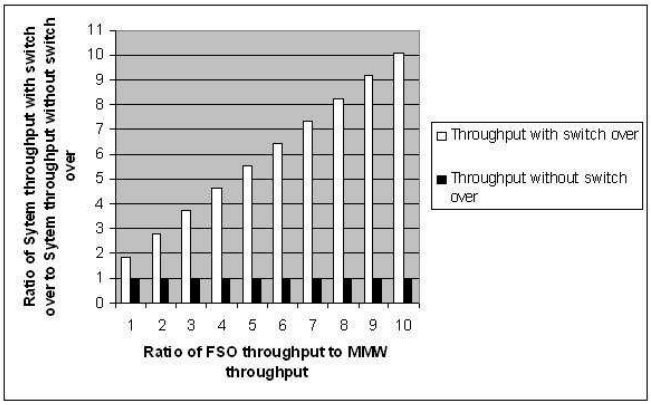

Figure 4.38: Comparison of throughput with and without switch-over [82].

presented in [69]. Essentially three cases have to be considered i.e. both, one or none of the links are operational. This leads to different strategies for each of the cases except the total failure where every system has difficulties. The second case, that only one of the links is available, implies a switch to the appropriate link or a redundant transmission on both channels. For the first case, that both are operational, it seems likely to use a load-balancing scheme for an utilisation of the complete available bandwidth. Thus the data is split into two independent data streams that are sent on two channels. This scenario improves the bandwidth utilisation of both links and back up link is not wasted for redundant transmission when the other link is operational.

For a load-balancing system a common problem arises by the fact that the receiving side gets packets out of order. There are two possibilities to avoid this impact on bandwidth with the use of TCP. One possibility is to use a UDP-based or UDP-tunneling protocol for connection-based purposes like Stream control transmission protocol (SCTP). The other option is the setting of the reordering threshold accordingly but it provides only a small improvement either due to management overhead or increased retransmission. Nonetheless this option is chosen because of the relatively good reordering algorithm of the Linux TCP/IP stack and the opportunity of a transparent communication channel regarding Ethernet traffic.

4.4.2 Hardware Setup

The whole system is built up according to Figure 4.39. The first requirement for a dynamically adapting load-balancing is the measurement of the link quality indicating values. This determines the ratio of usage for the two links which has to be easily adjustable. The link quality of the FSO system can be monitored through access of the Optical Management Interface (OMI). In addition to data channel fiber, there is provision of another fiber that can access OMI. It poses the requirement of another special media converter for the OMI fiber that converts from optical signal to RS232 standard output. Regarding the WLAN the SNR or RSSI as indicator for the link quality can be used. This leads to a WLAN device which provides a driver where the signal quality parameters can be easily accessed like Atheros based chipsets. The chosen WLAN device is an Ubiquiti XR5 miniPCI card.
The time to determine the signal levels of the connected devices is mainly dependent on

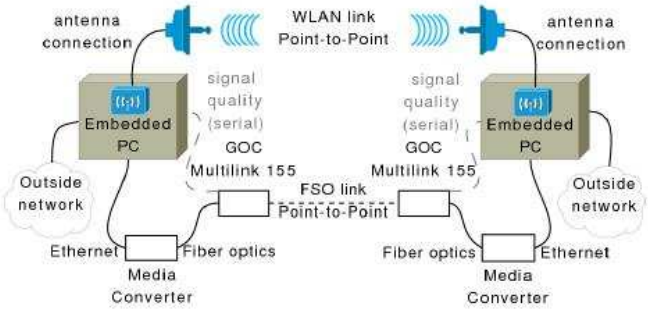

Figure 4.39: Physical arrangement of the system References [69].

the time required till the measured physical condition will be transmitted and received. For the WLAN interface it is a relatively small amount of time because of the direct access to the driver module and the possible measurement for every received beacon. From the GOC Multilink 155 the link quality can be queried at least every 700ms.
Additionally the FSO system data interface has to be connected to the load-balancing system. To accomplish this one media converter is needed for each FSO system. The converted interface is then connected to one of the Ethernet ports of the system.
The whole scenario shows rather high demands for fast decisions, short packet routing times and good programming capabilities. Thus the decision for an embedded PC seems very likely. Therefore two PC Engines Alix 2C3 Boards were chosen which incorporate an AMD Geode (500MHz) CPU, 256 MB RAM, a VIA VT6105M Ethernet with 3 Ethernet ports, two USB 2.0 ports, a serial port (RS232) and a miniPCI slot. This provides a sufficient amount of computing power and enough interfacing capabilities while having a small and power-efficient system. As it is convenient for the kernel messages to keep a working system console on the serial port the RS232 output from the FSO system is converted from RS232 standard to USB standard and connected to one of the USB ports of the system board.

4.4.3 Software Setup

The current choice of equipment makes it quite likely to use an embedded Linux distribution as operating system to have a stable and extensible platform. The provided source code helps to do extensions to the internal network data processing rather easy. In the actual installation the Atheros driver (WLAN) has to be included as well and a software tool would be used to monitor and set the parameters for load balancing. The time to take an appropriate decision depends on the load of the system which is influenced by multitasking and the efficiency of the implementation. For a rather simple algorithm and an efficient (CPU) load-balancing a decision time of 0.3 s to 0.5 s seems reasonable.
Furthermore this software tool has to change the load-balancing parameters. Hence these should be easily accessible from user space to have an easy programming interface while still providing the setting to occur in less than 1.5s.
Different approaches can be used to perform load balancing between FSO and wireless LAN. In layer 2 approach, load-balancing problem gets solved on the data link layer and is by definition transparent to the upper layers including the network layer. To accomplish the task with Linux a so-called "bonding device" is needed. This bonding device can use a variety of modes including a round-robin mode which uses each of the bonded interfaces equally on a by-frame basis. The module source has therefore to be extended to use the module with the unequal links.
Another approach is to use the traffic control framework under Linux. Linux uses independent queuing disciplines (qdisc) for every accessible interface. These qdiscs are getting filled with actual data to be transmitted and are getting emptied by the device driver for the specific interface. Therefore a qdisc has full control over the data being sent. In effect this technique gives a high efficiency which is mainly dependent on the scheduling algorithm. Anyway a physical failure or any other decrease in bandwidth can not be detected by the qdisc itself.
These qdiscs can also be used for data distribution among several interfaces like the True or Trivial Link Equalizer (TEQL) which is an already working and efficient implementation of this concept. In contrast to the mentioned goal TEQL is doing an "equalization" of all attached interfaces which means that each interface gets the same amount of data. An efficient alternative would be the alteration of this module to have a weighted distribution over the interfaces which is adjustable at runtime. A good choice for the used algorithm seems to be a deficit weighted round-robin scheduling because of the fast operation.
These qdiscs can also be used for data distribution among several interfaces like the True or Trivial Link Equalizer (TEQL) which is an already working and efficient implementation of this concept. In contrast to the mentioned goal TEQL is doing an "equalization" of all attached interfaces which means that each interface gets the same amount of data. An efficient alternative would be the alteration of this module to have a weighted distribution over the interfaces which is adjustable at runtime. A good choice for the used algorithm seems to be a deficit weighted round-robin scheduling because of the fast operation.

Another way to do a load distribution is the definition of a multi-path route with different weights for the specific links/routes to the same destination. The weight factor influences the ratio of distribution on these different routes. Nonetheless it was not possible to get an acceptable result with this technique and the distribution was not working on a per-packet basis because of route caching for a point to point link prevents a weighted distribution. An already working implementation and a straight-forward setup look advantageous.
Additionally to the load-balancing mechanism also a "bridging interface" (Linux module "bridge") is needed to establish a transparent connection between the outside networks on both ends and the bonded interfaces. Those bridging interfaces are only limited in throughput by the processing speed of the CPU. If there is no CPU limitation they are achieving a performance which is nearly equivalent to a commonly available switch. The advantages of this approach are that it is transparent to Ethernet traffic and nearly immediate reacts to a link failure.
Thus the chosen operating system is Voyage Linux v0.5.2 (Kernel 2.6.23) distribution which is lightweight and easily extensible. A good load-balancing implementation will be a modified version of the bonding device because of its widespread use and long development time. The modification includes a deficit weighted round-robin (DWRR) scheduler which requires only constant computing time to process a packet and does a fair distribution regarding the throughput.

4.4.4 Test results and measurements

A few tests were performed to verify the performance of different techniques. The testing scenario is built up to compare different load-sharing mechanisms which are already available in the Linux kernel. As the goal is only the possibility of an efficient operation, the achievable bandwidth holds as an appropriate indicator. The concrete behavior is figured out by different bandwidth test tools. For this scenario a bad interoperability gets minimized by using two equivalent systems with the same Fast Ethernet chip sets.
Therefore the scenario consists of two interconnected system boards as indicated in Fig-

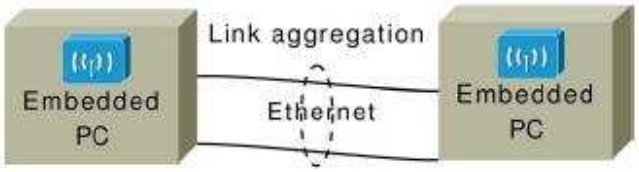

Figure 4.40: Schematic test setup [69].

ure 4.40. Two crossover cables are connecting the two boards such that each board has two used Ethernet ports.
The components used to test are two Alix 2C3 Boards, AMD Geode (500MHz) CPU, 256 MB RAM, VIA VT6105M Ethernet, two crossover Ethernet cables and Ubiquiti XR5

WLAN. The operating system is Voyage Linux v0.5.2 (Kernel 2.6.23). The used bandwidth test software is iperf version 2.0.2 (03 May 2005) pthreads and NPtcp (NetPipe) version 3.6.2.
As a first test the simplest solution gets tested: The operation of the two links is completely independent and no load-sharing at all is done. For completeness there are also the test results for the WLAN link included. As setup the links are just getting IP addresses for a point-to-point link.
During this test a simple round-robin scheduling for each frame is used so that every following packet gets transmitted over the next connection. Two separate tests were performed with a bridging or bonding of the two connections on the receiving side.
It can be seen in Figure 4.41, Table 4.7 and Figure 4.42 that the combined speed of the separate interfaces can nearly be reached with the chosen equipment. Anyway the already mentioned problem of out-of-order packets persists but it can be seen as well that the chosen software configuration can cope with this impact as the TCP tests show.

The results were presented in [69]. The data measured in 2002- 2003 for hybrid system

Table 4.7: Bandwidth results tested with Iperf [69].

	TCP Mbps	**UDP Mbps**	**Out of order packets**
Separate IF1	94.2	95.6	1
Separate IF2	94.3	95.6	1
WLAN	32.1)	37.5	1
WLAN Turbo	55.5	70.7	1
Bond-Bridge	187	190	38322
Bond-Bond	187	190	30322
TEQL	185	191	136492

consisting of FSO and mmW was used for simulation of the behaviour of load balancing switch-over. The measured ping test availability data is such that two pings for each link were used. Whenever less than 2 ping acknowledgements for any link were detected, switch over will detect a threshold through RS232 interface. The availability data was taken by two pings every minute. If the previous measurement detects a threshold, the maximum estimated delay a switch over takes to switch from load balancing on both links to only one link is less than 3 seconds. This delay time shows that switch over takes place much before next ping acknowledgements if threshold condition has been detected. In one simulation, load balancing switch over behaviour has been simulated for a fog event. As the maximum measured time for resumption of communication after switching from load balancing situation to only one link was measured as 2 seconds, this 2 seconds time has been considered as switch over delay in the simulations.

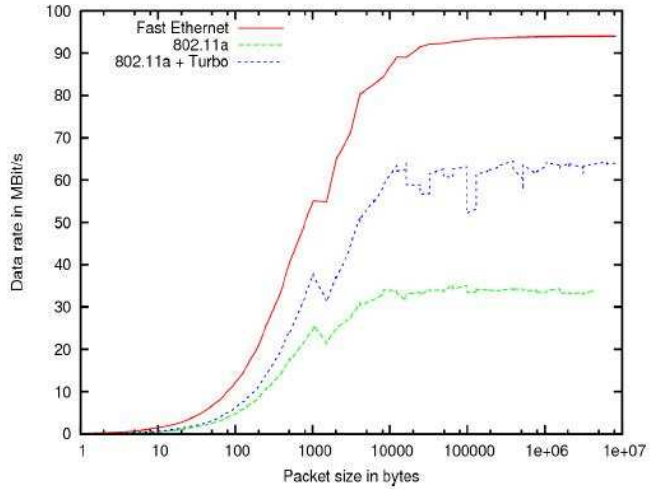

Figure 4.41: Bandwidth over different packet sizes (NPtcp) [69].

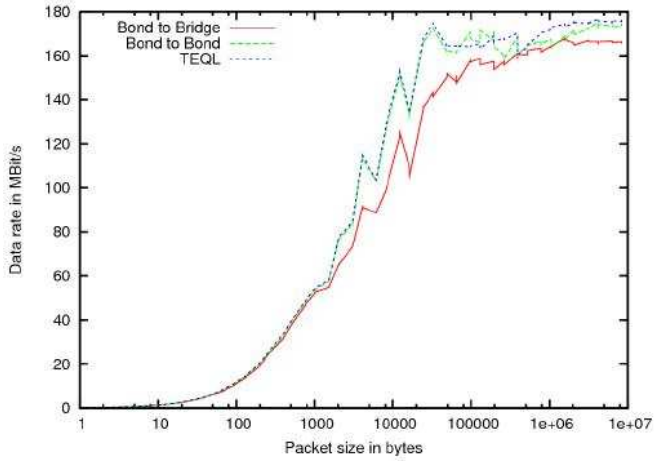

Figure 4.42: Aggregated bandwidth over different packet sizes (NPtcp) [69].

Simulations show that if switch-over delay is 3 seconds, switch-over process takes place much before the actual ping failure was detected. Consequently switch over maintains the availability achieved by continuous redundant link.

The load balancing switch over performance is also simulated to compare the usage of two links with and without switch over as shown in Figure 4.43. In these simulations it is assumed that WLAN will not suffer the unavailability as measured for MMW as weather effects below 10 GHz are negligible. It can be noticed that load balancing switch over can optimize the hybrid network with combined throughput of both links for more than 90% of the time.

More precise performance of switch over can be analysed by simulating its behaviour for a fog event. The optical received power was measured for this event on 31.01.06 for 80m

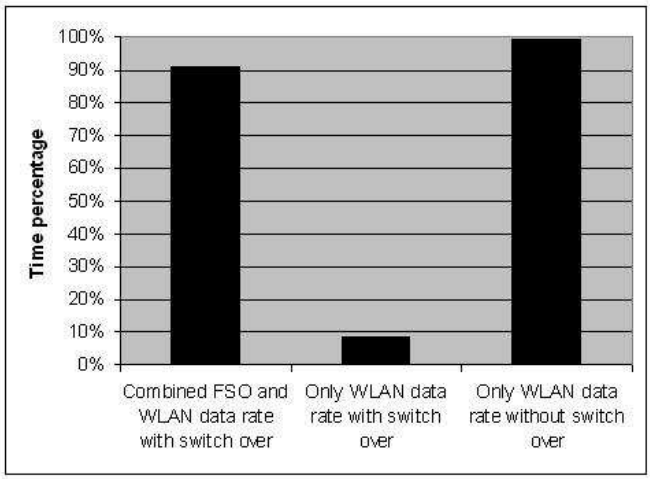

Figure 4.43: Comparison of two links usage with and without switch over [69]

link. Figure 4.44 shows the received optical power measured at different minutes of the day. In this event optical power attenuates below -35 dBm. The FSO receiver sensitivity is -41 dBm. The received optical power of -35 dBm is taken as threshold for switching to WLAN link in the simulation. For hysteresis, -34 dBm is taken as threshold for switching back to FSO link. The measured switch over delay of 2 seconds is taken as the time required to complete the switching from one link to other.

Figure 4.45 shows the switch over behaviour for this fog event. Switch value 1 indicates

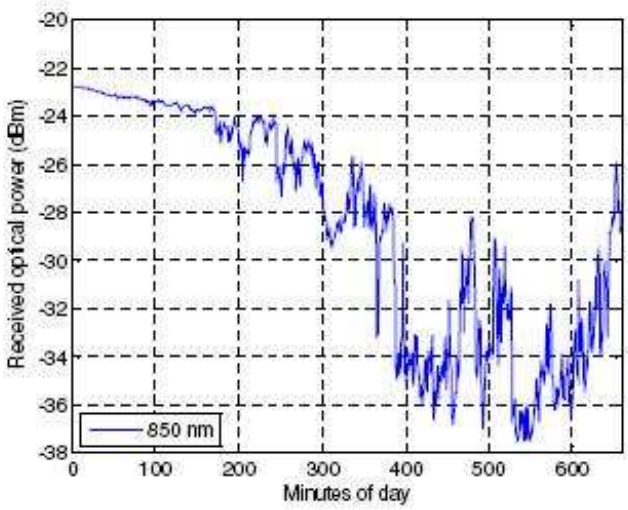

Figure 4.44: Received optical power measured at different minutes of the day [69].

switch to combined throughput load balancing mode whereas switch value 0 indicates switch over to WLAN link only.

It was concluded that the limiting factor causing reduced availability for FSO is weather

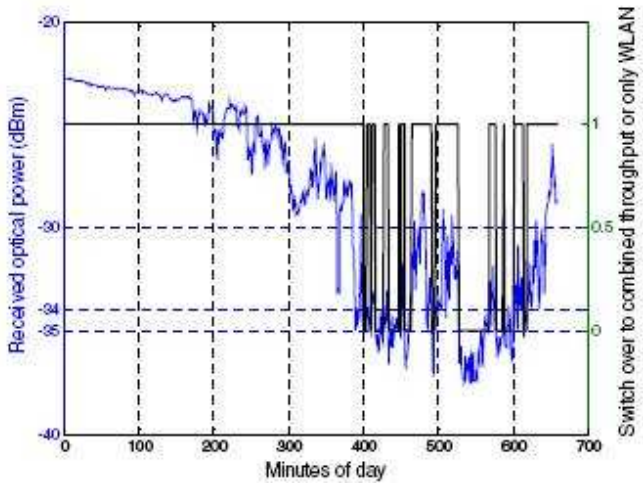

Figure 4.45: Switch over behaviour for fog event at time resolution of one minute [69].

attenuation. A back up link like unlicensed IEEE 802.11a has the potential of withstanding weather effects specially fog. Due to unlicensed nature, it can suffer interference by nearby users. However, the directional antenna can reduce this impact. This can improve the overall availability of hybrid network. The prototype of load balancing switch over is developed for hybrid wireless network. The performance of prototype has been evaluated by Laboratory tests and analysed by simulating for more than one year measured data. The simulation shows that switch over provides combined throughput of two links for more than 90% of the time while maintaining the availability measured by redundant transmission on both links. The fog event simulation also shows that switch over can adopt to the real world fog event. However, the key to the success of switch-over is to reduce switch over delay that must avoid any link availability loss.

5 IMPLEMENTATION AND APPLICATIONS

The comparison of different algorithms showed that load balancing approach can provide higher throughput than other approaches. The load balancing approach was considered for implementation.The current switch over techniques rely on the current received signal [52, 105, 31, 30, 15, 47, 32, 8, 96, 80, 45]. It has been analyzed that by this technique, switch over from one link to other may produce link loss time of a second [66]. However, the prior estimation of received signal strength can improve the performance of switching between two links by avoiding this link loss. The prior estimation based on LMS algorithms has been analysed.
The applications of hybrid FS/RF networks like data traffic over hybrid network, application in wireless sensor network are analysed. The future application in satellite and HAPS is also discussed.

5.1 Implementation

The foremost requirement for a dynamically adapting load-balancing is the measurement of the link quality indicating values. This determines the ratio of usage for the two links which has to be easily adjustable.

5.1.1 Hardware Setup

The whole system was built up according to Figure 4.39 as discussed in chapter 4.The link quality of the FSO system can be monitored through access of the Optical Management Interface (OMI). In addition to data channel fiber, there is provision of another fiber that can access OMI. It poses the requirement of another special media converter for the OMI fiber that converts from optical signal to RS232 standard output. Regarding the WLAN the SNR or RSSI as indicator for the link quality can be used. This leads to a WLAN device which provides a driver where the signal quality parameters can be easily accessed like Atheros based chipsets. The chosen WLAN device is an Ubiquiti XR5 miniPCI card.
The time to determine the signal levels of the connected devices is mainly dependent on the time required till the measured physical condition will be transmitted and received. For the WLAN interface it is a relatively small amount of time because of the direct access to the driver module and the possible measurement for every received beacon. From the GOC Multilink 155 the link quality can be queried at least every 700ms.

Additionally the FSO system data interface has to be connected to the load-balancing system. To accomplish this one media converter is needed for each FSO system. The converted interface is then connected to one of the Ethernet ports of the system.
The whole scenario shows rather high demands for fast decisions, short packet routing times and good programming capabilities. Thus the decision for an embedded PC seems very likely. Therefore two PC Engines Alix 2C3 Boards were chosen which incorporate an AMD Geode (500MHz) CPU, 256 MB RAM, a VIA VT6105M Ethernet with 3 Ethernet ports, two USB 2.0 ports, a serial port (RS232) and a miniPCI slot. This provides a sufficient amount of computing power and enough interfacing capabilities while having a small and power-efficient system. As it is convenient for the kernel messages to keep a working system console on the serial port the RS232 output from the FSO system is converted from RS232 standard to USB standard and connected to one of the USB ports of the system board.
Additionally a DFC77 receiver was attached to one of the devices to provide an accurate time source for the whole setup.
The Alix 2C3 boards were attached inside a box that is originally designed for electrical outdoor wiring. Additionally a plastic front and back plane was constructed to prevent accidental touching or contact to other devices located in the same case as shown in Figure 5.1 and Figure 5.2.

The actual distribution is done by kernel module. This kernel decides for each packet,

Figure 5.1: Alix board with open front plane.

which path it will take. For the efficient implementation, several issues have to be taken into account.
The load balancing has to be dynamically adjustable during the operation so that ratio of load balancing matches the current link properties. Another point is the switching of the operation mode. In case of probable failure of one link, the operation mode should change from load distribution to broadcasting mode where each interface is transmitting the same

Figure 5.2: Alix board with open front plane.

information. This can greatly improve the availability.

5.1.2 Measurement of WLAN and FSO bandwidths

The GoC system was used to measure the actual bandwidth of FSO system. The FSO throughput measurements in the range of 10 Mbps to 120 Mbps were considered as valid measurements. Figure 5.3 shows the results.

The two WLAN systems used for measurement included Alix boards communicating over a distance of approximately 2.7 km via WLAN IEEE 802.11 compliant devices operating in the 5 GHz range. One of the endpoints were located at Inffeldgasse and other at Observatorium Lustbuehel. The two WLAN interfaces were configured to act in WDS mode that allows a transparent communication for layer 2 of OSI model. The measured throughput values were considered valid if these values lie between 15 Mbps and 50 Mbps. Figure 5.4 shows the results.

The combined usage of both systems showed the enhancement in bandwidth. The WLAN system was used in managed mode in combined setup. Figure 5.5 shows the results.

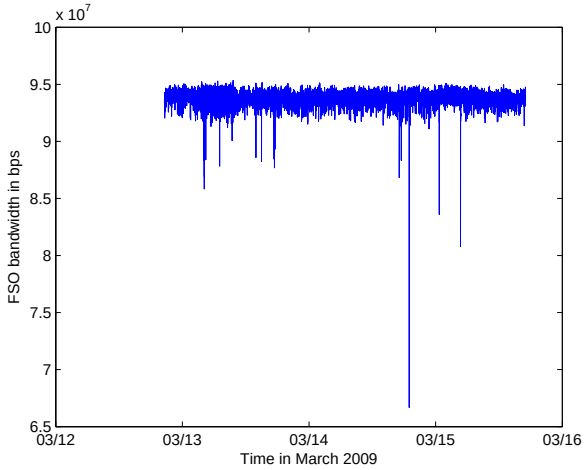

Figure 5.3: Measured FSO bandwidth.

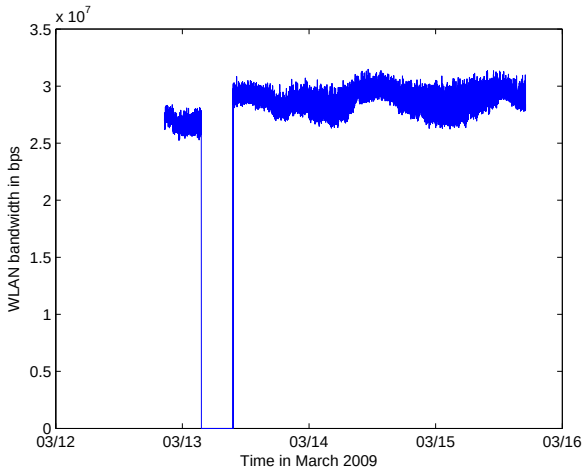

Figure 5.4: Measured WLAN bandwidth.

5.2 Forward Prediction of attenuation as a solution to avoid link loss

The tracking of terrestrial optical signal attenuation was analyzed for different weather conditions of fog, snow and rain [73]. The LMS algorithm has been used for forward prediction of the signal status. The Least Mean Square algorithm was introduced by Widrow and Hoff in 1959 [103]. It is an adaptive algorithm that uses the estimates of the gradient vector from the available data. It uses an iterative procedure that makes successive corrections to the weight vector in the direction of the negative of the gradient vector which eventually leads to the minimum mean square error. The LMS algorithm is most commonly used adaptive algorithm because of its simplicity and a reasonable performance.

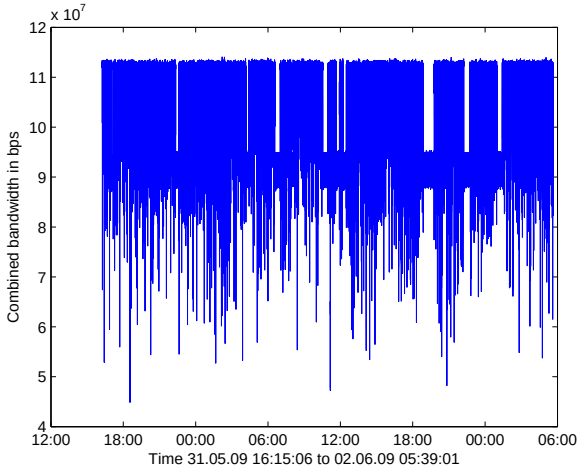

Figure 5.5: Measured Combined bandwidth.

Since it is an iterative algorithm it can be used in a highly time-varying signal environment. Keeping in view this feature of LMS algorithm, it has been used to track the signal status of FSO link. If y(n) is the output at time instant n, x(n) is input at time instant n, d(n) is the desired response at time instant n, e(n) is the error at time instant n, μ is the step size and w(n) is the tap weight vector at time n, the LMS algorithm can be summarized by the following equations.

$$y(n) = w^h(n)x(n) \tag{5.1}$$

$$e(n) = d(n) - y(n) \tag{5.2}$$

$$w(n+1) = w(n) + \mu x(n)e^*(n) \tag{5.3}$$

The results are presented for the combination of all the fog events in Figure 5.6. The tracking is done for future one minute signal value. Mean square error is mean square value of the difference between actual attenuation and predicted attenuation.

As the Figure 5.6 does not show the time in which MSE has been reduced, the magnified portion up to 500 seconds has been presented in Figure 5.7. This shows that this algorithm tracks in 250 seconds to acceptable MSE and the tracking continues successfully up to the end of measured approximately 35000 seconds. Moreover the one minute predicted value seems to be quiet sufficient for switching to other link.

Figure 5.8 shows the actual tracking of the signal for one of the fog event. The solid line is the actual attenuation whereas broken line shows the LMS algorithm tracking. As indicated by MSE, the algorithm starts tracking the attenuation in relatively less time.

The similar analysis is also performed for snow event of November 2005. The tracking is done for future one minute value. The results are presented in Figure 5.9. The magnified view of this tracking is shown in Figure 5.10. It shows that the same algorithm takes more time to track attenuation as compared to fog attenuation tracking. However once it reaches

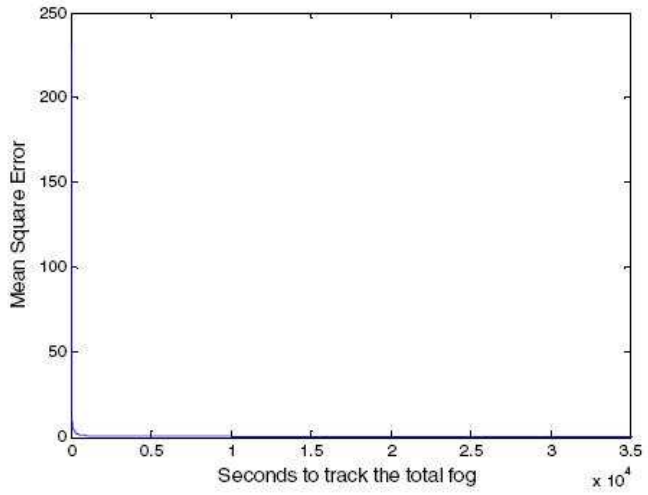

Figure 5.6: The tracking of all fog events [73].

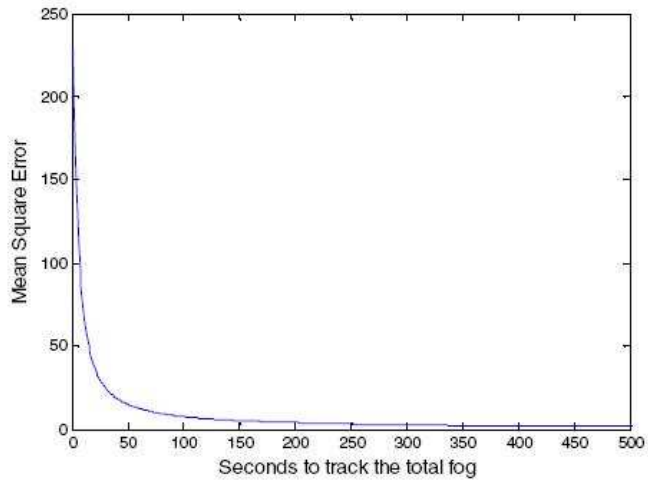

Figure 5.7: The tracking of all fog events up to 500 seconds [73].

the minimum MSE, it continues to track the signal attenuation. This can greatly help in switch over process.

The actual tracking of signal is presented in Figure 5.11. The solid line is the actual attenuation whereas broken line shows the LMS algorithm tracking. As indicated by MSE, the algorithm starts tracking the attenuation in relatively less time.

The tracking of rain event was also performed for the rain event of September 2007. The results are presented in Figure 5.12.The tracking in Figure 5.12 was performed for future signal value of one minute. The magnified view of this tracking is presented in Figure 5.13. It can be observed that tracking of rain attenuation is much better than fog and snow. Figure 5.12 shows that MSE does not approach global minimum in this time. However,

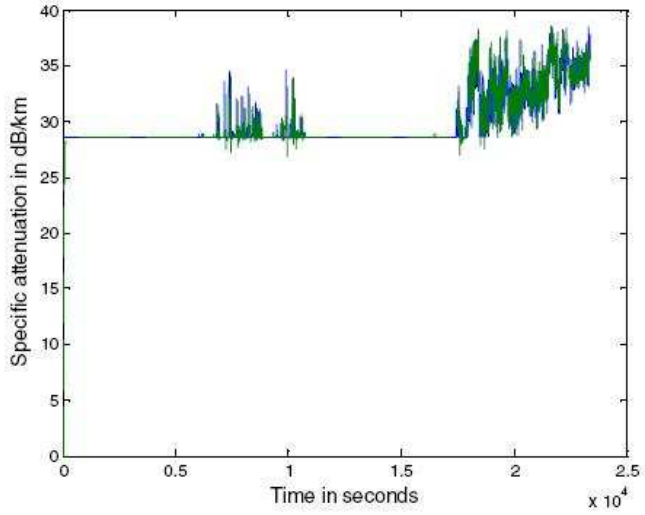

Figure 5.8: The actual tracking of optical signal attenuation for fog event [73].

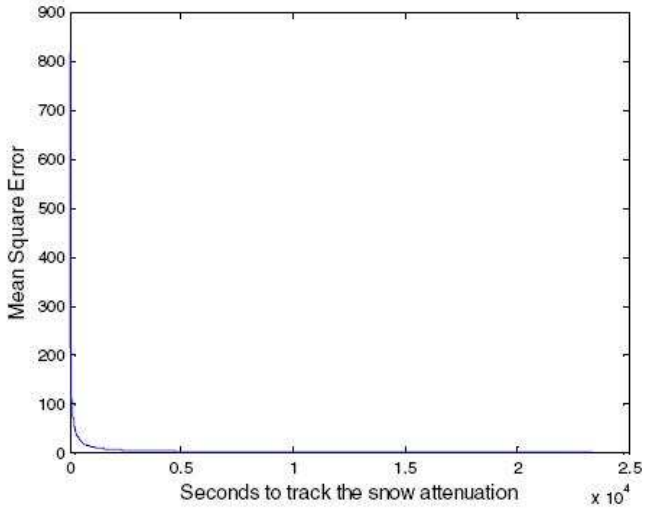

Figure 5.9: The tracking of a snow event [73].

the MSE reaches to acceptable limit and switch over process can be performed efficiently.

The actual tracking of signal is presented in Figure 5.14. The solid line is the actual attenuation whereas broken line shows the LMS algorithm tracking. As indicated by MSE, the algorithm starts tracking the attenuation in relatively less time.

It was concluded that LMS algorithm reaches acceptable minimum MSE in less time and starts predicting one minute forward value. Such a one minute forward prediction can greatly enhance the performance of switch over used to switch between FSO and back up RF link. The previous study shows that switch over takes some time to switch from one link to other. This time can be compensated by forward prediction of the attenuated

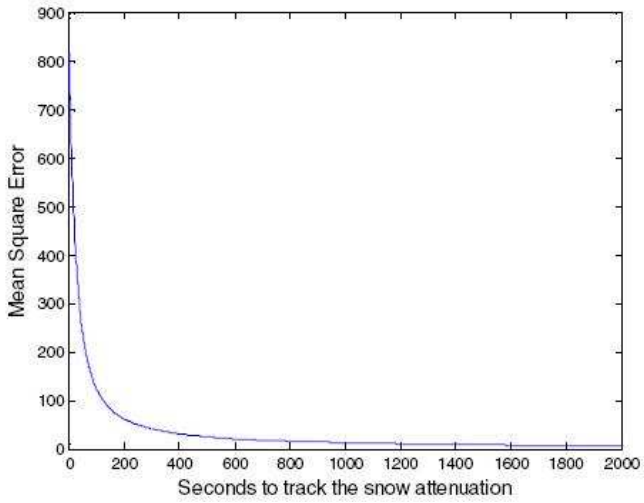

Figure 5.10: The tracking of snow event up to 2000 seconds [73].

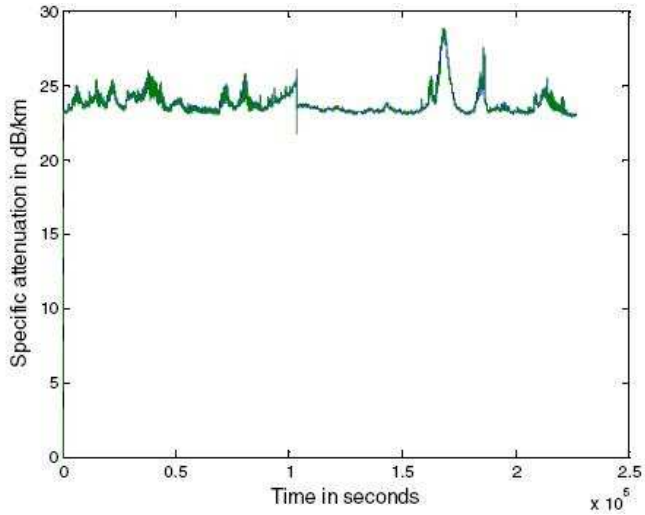

Figure 5.11: The actual tracking of optical signal attenuation for snow event [73].

signal.

5.3 The comparison of Traffic data and availability data

Connecting different sites of campuses is a popular and widely used application scenario [8, 90]. However, previous studies did not take traffic demands of the different sites into account. Not only availability has to be maintained, but also bandwidth requirements have to be considered. Since the availability issue was discussed in the previous sections

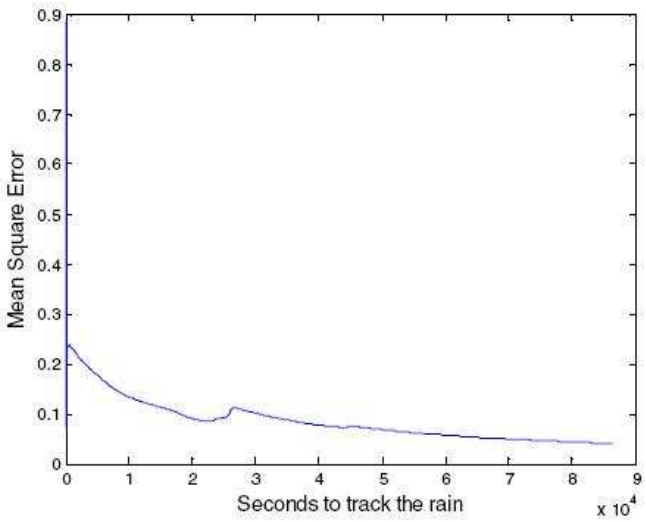

Figure 5.12: The tracking of a rain event [73].

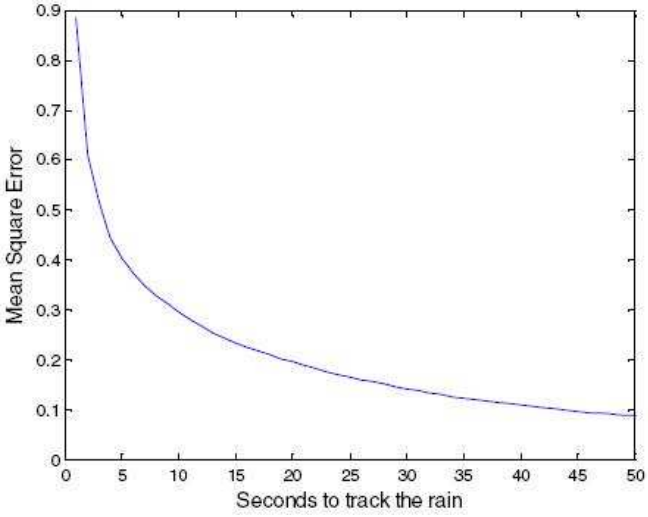

Figure 5.13: The tracking of rain event up to 50 seconds [73].

extensively and since one may state that this problem has been overcome to a certain degree we now want to focus on bandwidth considerations. For this purpose traffic statistics for the three main campuses of the Technical University of Graz were collected. Furthermore, relying on data from a measurement campaign from December 2000 we compare these traffic requirements to FSO availability, which almost exclusively determines the achievable bandwidth. The month of December was chosen because during that month the FSO availability is lowest, as it can be seen in Figure 4.20 [62]. Moreover, it is obvious that availability of the FSO link is especially high during the daytime, whereas link failure is almost exclusively restricted to dusk, dawn and the nighttime. This may stem from the

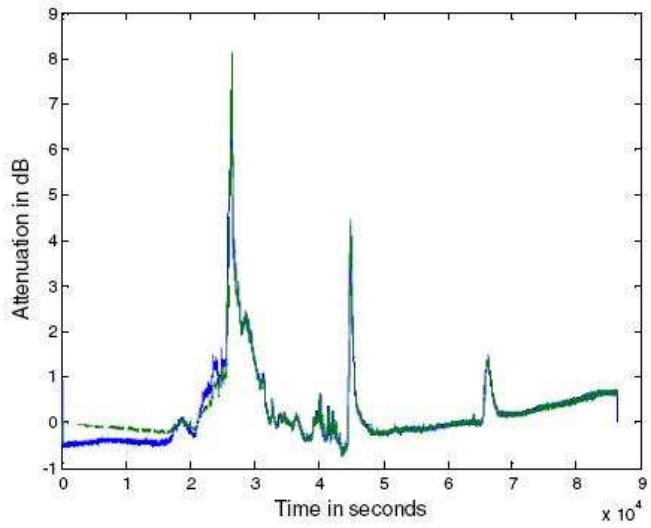

Figure 5.14: The actual tracking of optical signal attenuation for rain event [73].

fact that fog and haze, which have proven to be the most harmful conditions for the FSO link occur at precisely these times of day. At least, one can assume that this holds for the continental climate of Graz, which furthermore is influenced by the fact, that Graz is at the bottom of a large valley.

5.3.1 Scenario and Link Description

In Figure 5.15 one can see the location of the main sites of the campus of the Technical University of Graz, which are known as “Alte Technik”, “Neue Technik” and “Inffeldgründe”. The latter one of these campuses is the newest and most sophisticated one, bearing most of the offices and computer rooms accessible for students. Therefore, one may assume that this campus site has the highest traffic requirements.

In addition to that, one can see in Figure 5.15 that the distance between these sites is smaller than 2 km, even if a direct link between “Alte Technik” and “Inffeldgründe” had to be established, resulting in a mesh architecture.

The link itself should be built up with equipment already available, that is, using the MultiLink 155/2 FSO equipment and commercial IEEE 802.11a transceivers with high-gain grid antennas for the WLAN link. As abovely mentioned, the MultiLink 155/2 is specified for distances up to 2 km and has proven to work for even larger distances [53]. The specified distance of the WLAN link is strongly dependend on the antenna gain – in any case, a distance of less than 2 km should be no problem for either the FSO or the WLAN eqipment.

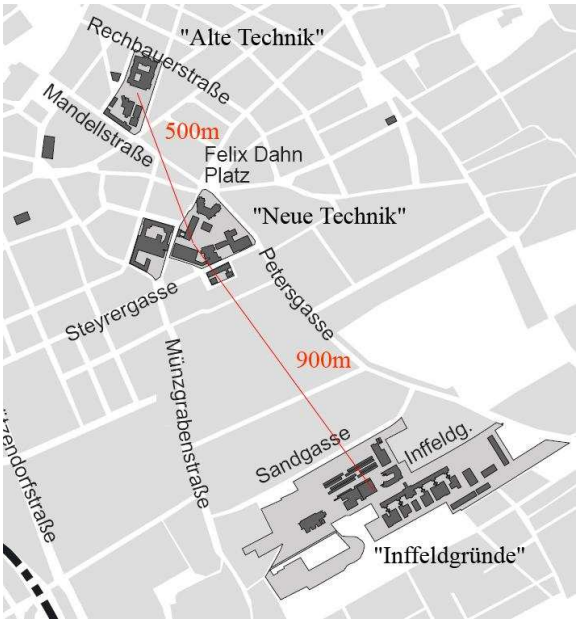

Figure 5.15: Map of the campus of the Technical University of Graz [68].

A more complicated problem arises from the question if the link can be made operational. That is, the line-of-sight has to be unobstructed for the FSO link, whereas at least the first Fresnel zone has to be free for the WLAN link. For this study, we assume both requirements fulfilled, although there may arise difficulties depending on the actual geographics of the campus.

5.3.2 Traffic Analysis

The traffic analysis results were presented in [68]. In order to make any comparison between bandwidth demands and available bandwidth possible, the recorded traffic data for the whole campus was used. The following pictures were automatically generated by the Multi-Router-Traffic-Grapher (MRTG), where green bars indicate incoming and blue lines indicate outgoing traffic. The recordings were done during December 2008, and as an example December 3rd was chosen. Figure 5.16 shows the overall internet traffic of the whole university between the December 1st and 3rd 10 am. As it can be seen, the major amount of traffic is caused between 10 am and 4 pm. Medium traffic occurred from 8 am to 10 am and from 4 pm to 7 pm, respectively. Comparably low traffic was recorded during the night time, that is between 7 pm and 8 am. Obviously, the major traffic reqúirements coincide with office and lecture hours. Figure 5.17 shows that these considerations not only hold for one particular day. In fact, every workday shows the same behaviour in terms of traffic requirements. Lower traffic was recorded on weekends, holidays, naturally.

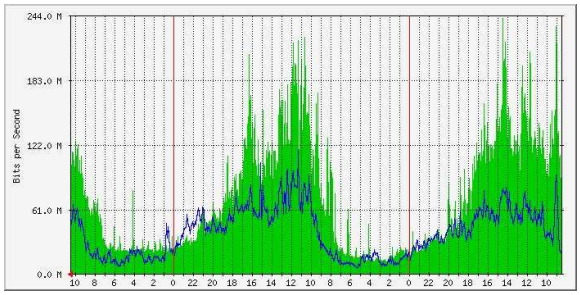

Figure 5.16: Internet traffic recorded for 48 hours (5 min average) [68].

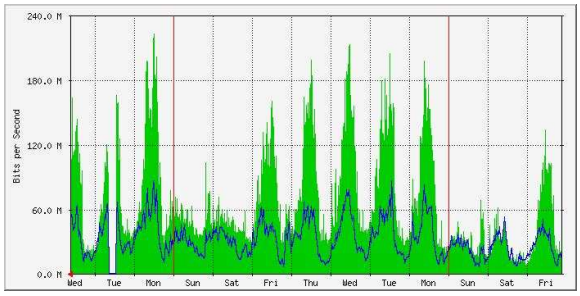

Figure 5.17: Internet traffic recorded for 13 days (30 min average) [68].

Furthermore, during the summer and spring breaks, traffic is also reduced a bit, because internet traffic caused by students is minimal during that time.

Furthermore, also the traffic between the main server of the Technical University of Graz and the three main sites of the campus was recorded. Figure 5.18 shows the traffic for campus “Inffeldgasse” as an example. In addition to the well-known average behaviour, there are certain peaks of traffic load during the nighttime. These peaks are most likely related to automatically performed client-server operations, such as automatic updates or daily back-ups.

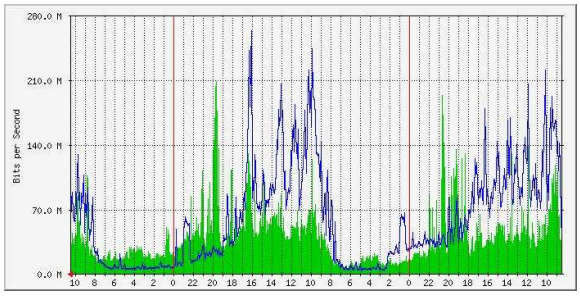

Figure 5.18: Traffic data recorded for “Inffeldgasse” [68].

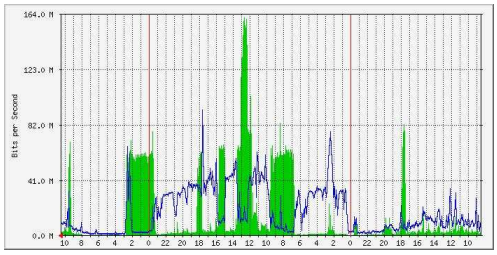

Figure 5.19: Traffic data recorded for "Neue Technik" [68].

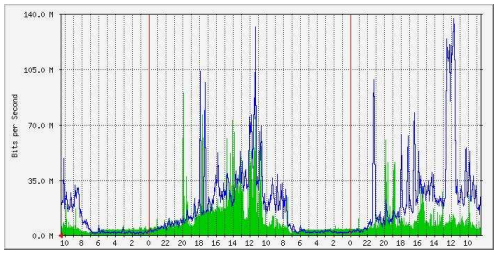

Figure 5.20: Traffic data recorded for "Alte Technik" [68].

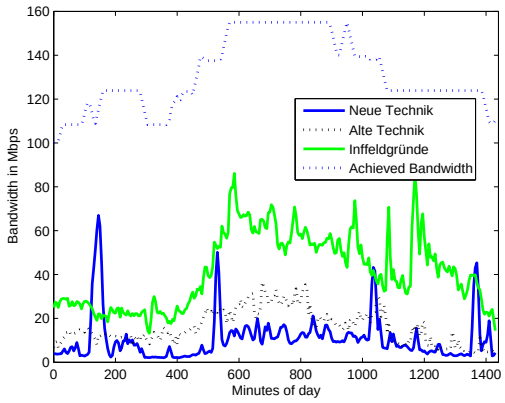

Figure 5.21: Average required and achieved bandwidth [68].

5.3.3 Simulations and Results

Simulations were performed using a set of measurements of the years 2000 and 2001 [99]. In this measurement setup, the link distance of 2.7 km clearly exceeded the manufacturer's specifications. Therefore, this analysis presents some worst-case-scenario, where one can assume that availability is increased for shorter link distances. Link bandwidth was set to 155 Mbps for FSO and to 15 Mbps for WLAN, respectively. The WLAN link was assumed to be available all the time. Link loss time during switching operations could be neglected in this discussion, since it affects average bandwidth only very little. Availability, on the other hand, is not a major concern in this study, since the methods proposed earlier tend to guarantee 99.999% availability throughout the year. For the whole month of December 2000 the average daily bandwidth was computed. Furthermore, relying on traffic data recorded during workdays in December 2008 the average daily bandwidth requirement was calculated as well. Bandwidth requirements were computed between each of the three sites and the main server. Both incoming and outgoing traffic was taken into consideration. Comparing Figure 5.21 with Figure 5.18, the diurnal changes in the traffic requirements are reflected in the average as well. Furthermore, one can see from Figure 5.21 that the pro-

posed hybrid FSO/WLAN switch-over system can satisfy traffic demands *on average*.

Still, obtaining these bandwidths on average may not be satisfactory for many applications. That is, even if we guarantee availability, it can be seen that alone the site "Inffeldgasse" exceeds the maximum available bandwidth from FSO from time to time (see Figure 5.18). Furthermore, during times of heavy fog and subsequent FSO unavailability, the achieved WLAN bandwidth of 15 Mbps does not even satisfy nighttime traffic for "Inffeldgasse".

Still, there may be solutions for that problem. For one, a simultaneous use of multiple FSO/WLAN hybrids could be employed, using a load sharing mechanism as it was introduced in [69]. Moreover, other FSO equipment could be used which allows higher data rates. Also the WLAN equipment could be modified so that it uses multiple channels simultaneously. Furthermore, the WLAN link itself could be built up in a multiple-input multiple-output (MIMO) manner, as it is suggested in the IEEE 802.11n draft. Studies will show if this indoor short distance technology can be exploited for long range directional links as well. Finally, automatic bandwidth consuming tasks could be timed properly in order to reduce peak bandwidth requirements and spread resulting traffic over a certain amount of time.

As a conclusion one can say that high bandwidth requirements coincide with times of FSO availability, making an FSO/WLAN switch-over system a promising method to interconnect different sites of a campus. Still, there are a few problems to be overcome, such as peak bandwidths and proper load distribution.

5.4 Application of FSO/RF hybrid network for power consumption optimisation of Wireless Sensor Network

Wireless sensor networks (WSN) are a technology suitable to monitor a wide range of environmental parameters such as pressure, temperature, acceleration, chemical composition or any other parameter for which the sensors have been manufactured. The idea of wireless sensor networks has been realized by integrating the functions of sensing, computation and communication, into smart sensor nodes. Wireless sensor networks are used for battlefield surveillance, habitat monitoring, home automation and health-care applications [14, 25, 95]. With the advent of robust distributed sensors, WSN can be deployed in inaccessible environments and harsh weather conditions [35, 19]. However, the rising demand of WSN for physical environments monitoring has raised increased interest in long lasting wireless sensor networks. In fact, long time period operation of a sensor has to rely on its battery, which also limits the long lasting performance of the whole WSN. Therefore the problem of efficient use of the energy budget of the sensors is a major issue. The battery power is consumed by all the sensors' activities: sensing, processing, storing and communication, however the optimization of the energy spent in the communications is one of

the most important problems in energy efficiency [11], in fact, the radio consumes a significant part of the energy budget of the sensors, furthermore the major energy savings are achieved by turning off the radio, which however means disconnecting the sensors from the rest of the WSN. Under this respect a promising approach is to base communications on FSO links [106]. Hybrid WSN having both RF and FSO links for communications are known to survive up to twice as long as WSN with only RF links in indoor environments [98].

When used in outdoor WSN, the FSO links are however subject to some limitations. In fact the weather can significantly affect optical wireless terrestrial communications. Among different weather conditions, rain, fog, and snow are known as the most important attenuating factors of optical communications. This motivates the need for including the effect of such weather conditions on optical communication applied to long lasting, terrestrial WSN applications. In [64] different weather effects on hybrid FSO/RF WSN were considered.In particular, considering a pair of sensors connected by both an RF and an FSO link, [64] gives two main contributions: (i) it provides a scheme based on three thresholds for switching among FSO and RF links for the communications (one to activate the RF link, other one to switch from RF to FSO, and last one to switch from FSO to RF), and (ii) it evaluates the performance in terms of energy efficiency of the proposed switching scheme, by considering FSO links availability measurements obtained during long experiments in Graz. The result is that the switching schema based on three thresholds reduces significantly the use of the RF link, thus providing better performance than the case in which only two thresholds (one to switch from FSO to RF and the other to switch from RF to FSO) are used. Furthermore the proposed method doubles the sensors lifetime as compared to the case where the sensors use only RF for communications.

A hybrid WSN was considered where the sensors are equipped with both RF and optical interfaces. In particular, to the purpose of analysis of weather effects, a pair of nodes was considered with the potential to communicate on both RF and FSO links. Regarding the alignment and acceptable attenuation, the FSO links are assumed to have reasonable transmission and receiver diameters. However, for the sake of simplicity, we also assume that each sensor can communicate through line of sight FSO link with only one other sensor. In our analysis and experiments we assume that the FSO links use transmission wavelength of 850 nm. The motivations behind selecting this transmission length are readily commercial availability of Vertical Cavity Surface Emitting Laser (VCSEL) and the high response of silicon photodiodes at this wavelength [27]. The FSO link consists of VSCEL driver, VCSEL Laser diode, PIN photodiode and corresponding Transimpedance and limiting amplifiers.

On the other hand it was assumed that the RF links are omni directional and based on transceivers compliant with the standard IEEE 802.15.4. Thus all the nodes are assumed to have RF communication capability with 2.4 GHz carrier frequency and data rate of 250 kbps. Finally, we assume to have a receiver sensitivity of -90 dBm as provided by some commercially available WSN.

The sensor nodes can store small amount of energy due to their small size [93]. The energy

per bit for FSO communications is set to 1.48x10-7 mJ/bit [27].
In the actual communications between a pair of nodes, the nodes use as long as possible the FSO link (that ensures the highest energy savings), however waether dependent attenuation requires switching back and forth to RF or FSO. A simple way of such switching consists of using two thresholds on the FSO attenuation: one to switch from FSO to RF (once the signal on the FSO links is close to the receiver sensitvity), and the other to switch from RF to FSO (once the signal on the FSO is again strong enough). In order to avoid continuously switching back and forth between FSO and RF, the two thresholds are kept separate, and the second is higher than the first. This because switching off and on the RF link takes time that may result in periods of link unavailability. However, to take into account this fact, we introduce an additional intermediate threshold that is used to turn on the radio (to keep it ready), but to continue to use the FSO link. Therefore our switching schema uses three thresholds on the received signal strength of Free Space Optics link. At one threshold level, called RF activation, the RF link is activated but the transmission continues on the optical link. The criterion for selecting FSO link is that the received signal strength should be 3 dB above the receiver sensitivity to ensure bit error rate 10^{-9}[8]. The fog measurements that we conducted in Graz (Austria) show that the specific attenuation of the optical link changes at the rate of 10dB/km in one second [38] in the case of snow events. At the second lower threshold level, called RF transmission, the transmission on the optical link is stopped and the transmission on the RF link is started. The third threshold level called FSO Switch back is used to deactivate the RF link and to restart the transmission on the optical wireless link.
The PING replies over FSO link were recorded in 2003-2004 at Technical University Graz, Austria for availability measurement. These PING replies have been used to simulate the wireless sensor network behaviour for the measured availability of FSO link. This availability measurement shows the effects of all weather influences like fog, snow and rain. Although the availability was measured for longer distance FSO link powered by 220 V ac but it can be used as coarse estimate of battery powered short range FSO link availability.
Figure 5.22 shows the simulation of wireless sensor network behaviour for selecting FSO or RF link for communication depending upon the one year measured availability of FSO. The wireless sensor node selects either FSO or RF link depending upon the recorded ping reply. If there is a recorded ping reply it selects FSO link otherwise it selects RF link for communication. Link selection value of 1 indicates selection of FSO link for communication whereas value of 0 indicates selection of RF link for communication. The simulation shows that FSO link can be used for 92.0995% of the time. The reduced availability is consequence of fog, rain and snow attenuations.
The behaviour of wireless sensor network has been simulated for a measured snow event. This event took place on 02.02.2009. The snow is assumed to be dry and the attenuation of 2.5 GHz link is ignorable. That is why attenuation of 2.5 GHz link is not considered in simulation for snow. On the other hand, wet snow attenuation for optical signal is not significant and is not taken into account in simulations. Figure 5.23 shows snow event of 02.02.2009 and behaviour of wireless sensor network for selecting communication link.

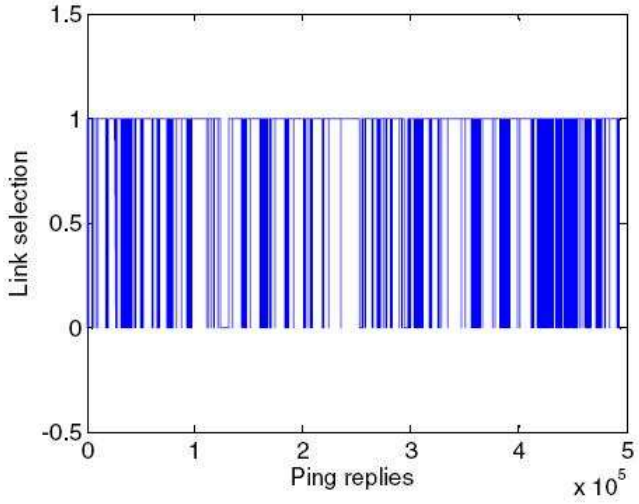

Figure 5.22: Behaviour of WSN for link selection for one year availability [64].

The received optical power of -21.5 dBm has been used as RF activation threshold and it has been represented by a switch over value of 0.5 in simulation. The received optical power of -22 dBm has been used as RF transmission threshold and the corresponding value of switch over is 0 in simulation. The value of 1 for switch over corresponds to either normal operation on FSO or switch back to FSO from RF link on regaining the received optical power of -21.4 dBm i.e. FSO switch back threshold. This simulation shows that by using this switching scheme, FSO link can be used for 68.335% time of this snow event whereas RF remains in active mode and transmission mode for 15.91% and 31.664% time respectively. The RF active mode time percentage of 15.91% mean 2291 seconds for the given event. It means the energy saving equal to difference of energy consumption between RF transmission mode and RF active mode for this time. It highlights the benefit of using three thresholds, otherwise with two thresholds RF will be used 2291 seconds in addition to 31.664% time use with three thresholds.

The behaviour of wireless sensor network has also been simulated for another measured snow event. This event took place on 28.11.2005. Figure 5.24 shows the snow event of 28.11.2005 and behaviour of wireless sensor network for selecting communication link. In order to show the effective switch over behaviour, this time the received optical power of -24 dBm has been used as RF activation threshold and it has been represented by a switch over value of 0.5 in simulation. The received optical power of -25 dBm has been used as RF transmission threshold and the corresponding value of switch over is 0 in simulation. The value of 1 for switch over corresponds to either normal operation on FSO or switch back to FSO from RF link on regaining the received optical power of -23.9 dBm i.e. FSO switch back threshold. This simulation shows that by using this switching scheme, FSO link can be used for 73.52% time of this snow event whereas RF remains in active mode and transmission mode for 0.9337% and 26.47% time respectively. The RF active mode

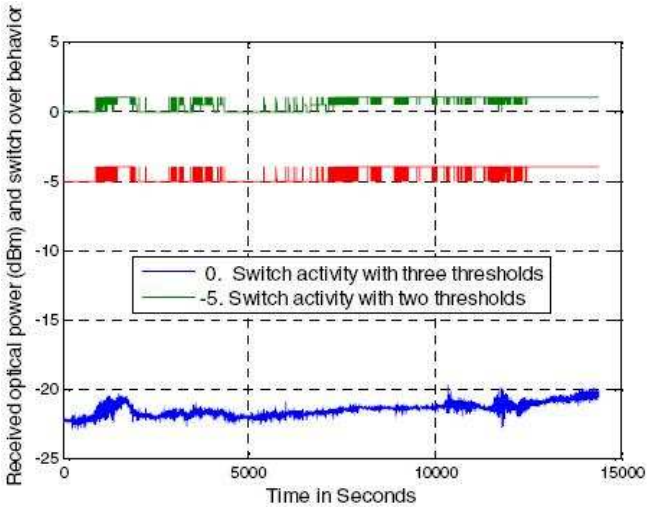

Figure 5.23: Link selection behaviour of WSN for Feb. 09 snow event [64].

time percentage of 0.993% mean 2118 seconds for the given event. It means the energy saving equal to difference of energy consumption between RF transmission mode and RF active mode for this time. It highlights the benefit of using three thresholds, otherwise with two thresholds RF will be used 2118 seconds in addition to 26.47% time use with three thresholds.

The behaviour of wireless sensor network has also been simulated for another measured

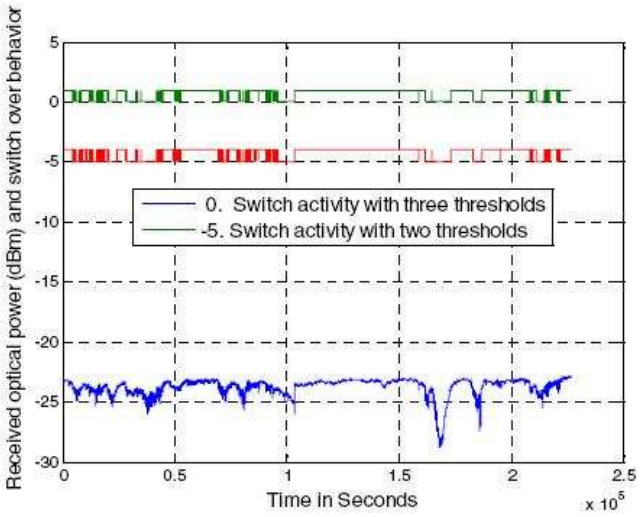

Figure 5.24: Link selection behaviour of WSN for Nov. 05 snow event [64].

rain event in May 2002. Figure 5.25 shows the simulation of wireless sensor node behaviour for this rain event. The receiver sensitivity is assumed to be 20 dB and the specific attenuation of 16 dB/km has been used as RF activation threshold and it has been rep-

resented by a switch over value of 40.5 in simulation. The received optical power of 17 db/km has been used as RF transmission threshold and the corresponding value of switch over is 40 in simulation. The value of 41 for switch over corresponds to either normal operation on FSO or switch back to FSO from RF link on regaining the received optical power of 15 dB/km i.e. FSO switch back threshold. This simulation shows that by using this switching scheme, FSO link can be used for 94.28% time of this rain event whereas RF remains in active mode and transmission mode for 2.8571% and 5.7143% time respectively. The RF active mode time percentage of 2.8571% mean one minute for the given event. It means the energy saving equal to difference of energy consumption between RF transmission mode and RF active mode for this time. It highlights the benefit of using three thresholds, otherwise with two thresholds RF will be used one minute in addition to 5.7143% time use with three thresholds. The behaviour of wireless sensor network has also been simulated for another measured rain event of the whole year of 2002.

Figure 5.26 shows the simulation of wireless sensor node behaviour for the rain events

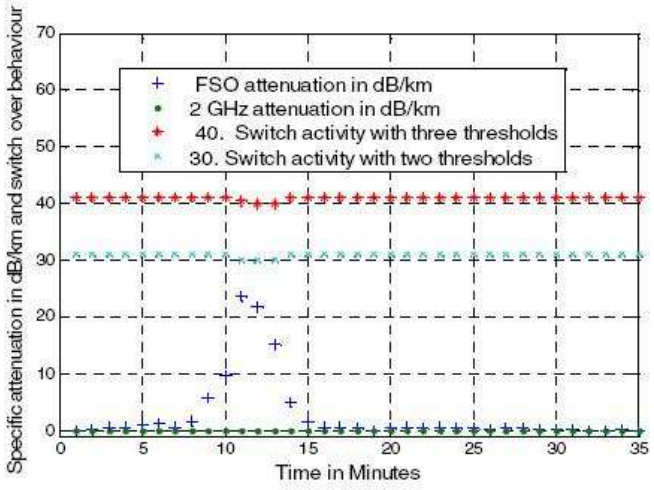

Figure 5.25: Link selection behaviour of WSN for May 02 rain event [64].

of the whole year of 2002.The receiver sensitivity, three thresholds and switch over representation use the same values as in Figure 5.25. This simulation shows that by using this switching scheme, FSO link can be used for 99.9735% time of all rain evens whereas RF remains in active mode and transmission mode for 0.0133% and 0.0265% time respectively. The RF active mode time percentage of 0.0133% means 360 second for the given event. It means the energy saving equal to difference of energy consumption between RF transmission mode and RF active mode for this time. It highlights the benefit of using three thresholds, otherwise with two thresholds RF will be used 360 second in addition to 0.0265% time use with three thresholds.

As a result of different weather influences, the minimum measured availability was 80%. The power consumption of wireless sensor with different duty cycles is also simulated for RF only and both RF and FSO communication links setup with three thresholds. The worst

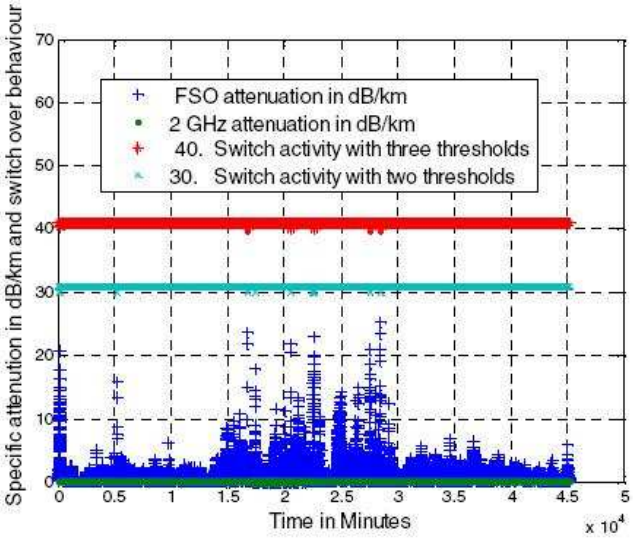

Figure 5.26: Link selection behaviour of WSN for 2002 rain events [64].

availability case of FSO i.e. 80% is used to simulate wireless sensor network using both links.

Micaz specification was used for simulation. FSO power consumption is simulated through values calculated in [27]. Figure 5.27 shows that power consumption improves twice even for the worst case of FSO availability.

Battery Life Time of 250 mAhr capacity battery is also simulated for RF only and both

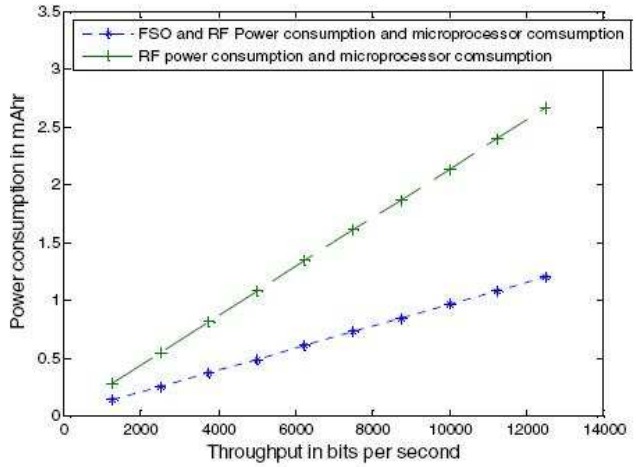

Figure 5.27: Power consumption of WSN using RF only and both RF and FSO [64].

RF and FSO links. Figure 5.28 shows the battery life time for both cases. The two times improvement can be observed. Moreover it can be observed that with the increase of throughput, improvement gets even better.

It was included that the reduced link availability of FSO due to weather effects urges to

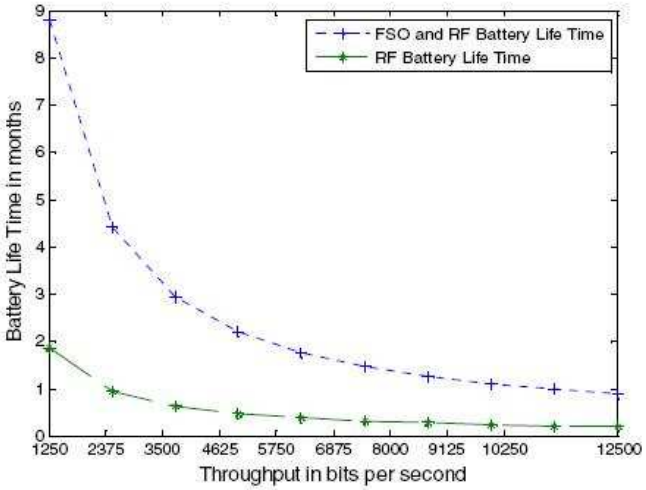

Figure 5.28: 250 mAhr WSN battery life time using RF only and both RF and FSO [64].

include the attenuation effects of rain and snow in analysis. Keeping in view the receiver sensitivity and change in attenuation, the optimal usage of power efficient FSO link can be achieved by using proper selection of threshold. The simulation results for recorded snow and rain events show that power consumption saving on RF transmission can be as high as 2291 seconds by using three threshold switching. An improvement of at least twice in the power consumption over only RF link usage can be achieved for the harsh outdoor terrestrial environment. The effect of low energy consumption per bit by FSO link becomes prominent with the increase of throughput.

5.5 Future applications of FSO/RF hybrid network in Satellites and HAPS

FSO offer a possibility of enhanced high data rate communication between flying vehicles and satellites due to their abundance of bandwidth. Optical communication terminals can be used for high capacity links between satellites and communication links from optical ground station to satellite. However the optical terminals are also suited for communication links between high altitude platforms. Within the General Studies Programme and ARTES-5 studies it was concluded that future development has to cope with the impairment by atmospheric effects to make the application of optical links an attractive alternative to microwave technology. Figure 5.29 shows a general overview of applications that use optical networking.
Among these applications hybrid network of FSO/RF can provide high availability while

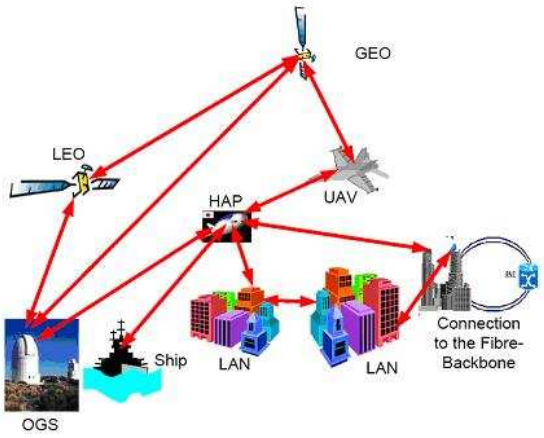

Figure 5.29: Optical Networking Applications [56].

exploiting the potentials of FSO. The main motivation for the potential use of optical communication links is the fastly increased bandwidth of these links which can be explained by the increase of the carrier frequency compared to todays state of the art RF links. Furthermore the high directivity of optical antennas allows for communication over huge distances while the antennas high directivity results in immunity to multi-user interference and therefore the absence of regulations for the electromagnetic spectrum at optical frequencies. The drawback of optical communications through the atmosphere is of course the atmospheric impairment of optical frequencies. For this reason tradeoffs of both technologies and possible hybrid RF/Optical solutions have to be carefully considered.

6 CONCLUSIONS

Due to capability of providing high data rate, Free Space optics has the great potential to grow out from a niche market. However, carrier class availability is the basic requirement of a communication link. This thesis analyses the availability of FSO and FSO/RF hybrid networks for different weather conditions of fog, rain, snow and clouds. The different switch over algorithms are proposed that try to achieve maximum throughput while maintaining the availability achieved by hybrid network.

6.1 Concluding summary

The analysis of different weather conditions of fog, snow and rain reveal that FSO 850 nm/ 40 GHz achieve the availability of 100% despite the 0.51% availability of FSO link alone for measured dense maritime fog event. Similarly for a measured snow event, addition of back up link of 40 GHz increase the availability from 39.49% of FSO link alone to 100%. However, for a rain event 40 GHz back up link does not help at all and the combined hybrid FSO 850nm/40 GHz link availability remains at 85.71% , the availability achieved by FSO link alone. The comparative analysis of FSO 850 nm/ WLAN link shows that this hybrid network achieves 100% availability not only for dense maritime fog and snow events but also for rain events. This strongly advocates for the use of FSO 850 nm/WLAN link if availability is the main concern. However, the use of WLAN link may be trade off in terms of data rate. The analysis of 10 μm shows some interesting results with 100% availability for dense maritime fog and rain events whereas 76.83% availability for snow event. A hybrid combination of FSO 10 μm / 40 GHz link can be the optimum in this case as we observe that 40 GHz link achieve 100% availability for snow event.
The use of FSO for satellite, intersatellite and High Altitude Platforms (HAP) links is strongly prohibited by cloud attenuation. The comparative analysis of different optical wavelengths exhibit that 10 μm perform better than other wavelengths. However, the addition of back up link can improve the situation. An alternate is to use the site diversity to mitigate cloud attenuation. Another solution is to use the FSO/RF hybrid network and utilize the RF bands when there is blockage of FSO link.Among different RF frequency bands, the cloud attenuation is high for higher frequencies. However the difference of specific attenuation is not as significant as in case of FSO wavelengths. This advocates using high frequency RF bands along with large wavelength FSO link for high data rate demanding applications.
The benefits of FSO motivate to use it as last mile access. However the deterioration

of weather attenuation can be coped with backup link of comparable data rate. But use of back up link as continuously transmitting redundant link is not a good solution. The switch over can help to increase the usage of FSO link while maintaining availability. By selecting one link, it avoids wastage of transmission for redundant MMW channel when FSO link is available. The initial results showed that average usage of back up link for maintaining the availability achieved by redundant link is 14.79%. It means switch over can provide the same availability by avoiding back up link transmission more than 85%.
The results of switch over algorithm shows that the self synchronising switch-over system increases availability as well as average bandwidth compared to a pure FSO system. However, switching should be fast enough to avoid any loss of link availability. The key to success is to reduce link loss time, a goal which can only be achieved by combining optimal switching methods. Pure threshold comparison (TC) yields an increase in availability to 98.62% while achieving best bandwidth performance. However, to increase the reliability of the overall link, pure TC cannot be used because of fluctuations causing too many switching operations. The different proposed algorithms are optimized with respect to maximum availability under the side constraint of limited FSO underutilization. This way, minimum bandwidth efficiency could be guaranteed. Different methods have different influence on availability and bandwidth. Filtering, as it turned out, yields only little improvement compared to threshold comparison, whereas it even delivers worse results in combination with either time or power hysteresis. The results show that time hysteresis (TH) and combined time-power hysteresis (PT) perform best, with emphasis on the latter one. PT even bears the possibility for carrier class availability of 99.999%.
The simulation results showed by performing load sharing, it avoids wastage of redundant transmission bandwidth of mmW channel when FSO link is available. The simulations showed that average redundant usage of back up link for maintaining the availability is reduced to less than 10% provided that switching is fast enough to avoid any link availability reduction. The key to the success of switch-over is such implementation that must avoid any reduction in link availability. Further results showed that the performance of switch over increases significantly with the increases in difference of throughput of two links. If there is a huge difference between, the throughput of two links, switch-over exhibits many folds efficient bandwidth utilisation. The simulation showed that if both links provide same throughput, the throughput of hybrid network with switch-over is 88% more than the throughput without switch-over. If the throughput of FSO is 10 times the throughput of mmW link, switch-over makes the throughput more than 10 times the throughput of hybrid network without switch-over.
The use of back up link like unlicensed IEEE 802.11a has the potential of withstanding weather effects specially fog. Due to unlicensed nature, it can suffer interference by nearby users. However, the directional antenna can reduce this impact. This can improve the overall availability of hybrid network. The prototype of load balancing switch over is developed for hybrid wireless network. The performance of prototype has been evaluated by Laboratory tests and analysed by simulating for more than one year measured data. The simulation showed that switch over provides combined throughput of two links for more

than 90% of the time while maintaining the availability measured by redundant transmission on both links. The fog event simulation also showed that switch over can adopt to the real world fog event. However, the key to the success of switch-over is to reduce switch over delay that must avoid any link availability loss.The actual bandwidth measurement shows that FSO bandwidth was around 94 Mbps whereas bandwidth of WLAN for WDS mode was around 30 Mbps .The loadsharing provided maximum bandwidth of 114 Mbps with WLAN in managed mode.
The comparison of mutirouter traffic grapher (MRTG) traffic data at Graz University of Technology and availability data showed that peaks in the bandwidth requirement coincide with peaks of achievable bandwidths. Therefore, an FSO/WLAN switch-over system can be seen as a successful way to provide internet access to office buildings and lecture halls, since bandwidth is limited in times of little usage mainly. Availability, however, is ensured almost throughout the whole time, and is only limited by the time required for detecting an FSO failure and reacting on it.
The tracking of optical wireless signal attenuation was also analysed for fog, snow and rain events. The tracking showed that LMS algorithm reaches acceptable minimum MSE in less time and starts predicting one minute forward value. Such a one minute forward prediction can greatly enhance the performance of switch over used to switch between FSO and back up RF link. The earlier results showed that switch over takes some time to switch from one link to other. This time can be compensated by forward prediction of the attenuated signal.
The Wireless sensor network power consumption of hybrid FSO/RF network was analysed for terrestrial environment of rain and snow. The reduced link availability of FSO due to weather effects urges to include the attenuation effects of rain and snow in analysis. Keeping in view the receiver sensitivity and change in attenuation, the optimal usage of power efficient FSO link can be achieved by using proper selection of threshold. The simulation results for recorded snow and rain events showed that power consumption saving on RF transmission can be as high as 2291 seconds by using three threshold switching. An improvement of at least twice in the power consumption over only RF link usage can be achieved for the harsh outdoor terrestrial environment. The effect of low energy consumption per bit by FSO link becomes prominent with the increase of throughput.

6.2 Future Work

The optical communication links are best served for short distance links in the troposphere but are successfully tested for links involving very long distances like, for example, between optical ground stations (OGS) and un-manned aerial vehicles (UAVs), OGS in the troposphere to the terminals in space like GEO/LEO satellites, and stratospheric or high altitude platforms (HAPs).The influences on hybrid network FSO/RF technologies for deep space communication is within the scope of the future work. This can help for the analysis

and link budget calculation for projects involving deep space communication.
The analysis of different coding schemes like Raptor Codes, LPDC and other coding schemes for hybrid network of FSO and RF technologies can be helpful for efficient implementation of hybrid network. The design of optimal coding scheme for throughput highly available hybrid network can be an area for future work.
The increased interest in long lasting wireless sensor networks motivates to use Free Space Optics (FSO) link along with radio frequency (RF) link for communication. Earlier results show that RF/FSO wireless sensor networks has life time twice as long as RF only wireless sensor networks. The power consumption of hybrid network has been analysed for terrestrial environment of rain and snow [64]. The practical implementation of wireless sensor network employing hybrid FSO/RF network and analysis of the measured data is also an area that can be explored.
The results show that switch over takes some time to switch from one link to other [66]. This time can be compensated by forward prediction of the attenuated signal. Such a forward prediction can greatly enhance the performance of switch over used to switch between FSO and back up RF link [73]. The implementation based on this idea and subsequent analysis can be a direction that can be investigated.

REFERENCES

[1] http://ww1.ucmss.com/books/lfs/csrea2006/icw4088.pdf.

[2] http://www.path.berkeley.edu/path/publications/pdf/prr/99/prr-99-11.pdf as seen on 12.07.09.

[3] Optical wireless communications using ultra short light pulses and pulse shaping, 2007.

[4] M. Abtahi and L. Rusch. Mitigating of scintillation noise in FSO communication links using saturatedoptical amplifiers. In *MILCOM*, pages 1–5, October 2006.

[5] A. Acampora. Last mile by laser. *Scientific American*, July 2002.

[6] M. Achour. Simulating free space optical communication; part i, rain fall attenuation. *Proc. SPIE*, 3635, 2002.

[7] M. Achour. Free-space optics wavelength selection: 10 micro versus shorter wavelengths. *Proc. SPIE*, 5160:234–246, 2004.

[8] A. Akbulut, H. Gokhan Ilk, and F. Ari. Design, availability and reliability analysis on an experimental outdoor fso/rf communication system. *Proc. IEEE ICTON*, pages 403–406, 2005.

[9] M. Akiba, K. Ogawa, K. Walkamori, K. Kodate, and S. Ito. Measurement and simulation of the effect of snow fall on free space optical propagation. *Applied Optics*, 47 No. 31:5736–5743, 2008.

[10] M. Akiba, W. Wakamori, and S. Ito. Measurements of optical propagation characteristics for free space optical communication during rain fall. *IEICE Trans. Commun.*, E87-B:2053–2056, 2004.

[11] I. F. Akyildiz, W. Su, Y. Sankarasubramaniam, and E. Cayirci. Wireless sensor networks: a survey. *Computer Networks*, 38:393–422, Mar. 2002.

[12] N. Araki and H. Yashima. A channel model for optical wireless communication during rainfall. *Proc. 2nd International Symposium on Wireless Communication Systems*, pages 205–209, 2005.

[13] D. Atlas and C.W Ulbrich. The physical basis for attenuation-rainfall relationships and the measurement of rainfall parameters by combined attenuation and radar methods. *Jornal Rech. Atmos*, 8:275–298, 1974.

[14] P. Baronti, P. Pillai, V. Chook, S. Chessa, Y A. Gotta, and Fun Hu. Wireless sensor networks: a survey on the state of the art and the 802.15.4 and zigbee standards. *Computer Communication*, 30(7):1655–6195, 2007.

[15] S. Bloom and W. S. Hartley. The last-mile solution:hybrid fso radio http://www.systemsupportsolutions.com/whitepapers.htm.

[16] C. F. Bohren and D. R. Huffman. *Absorption and scattering of light by small particles*. John Wiley and sons, New York, 1983.

[17] O. Bouchet, T. Marquis, M. Chabane, M. Al Naboulsi, and H. Sizun. Fso and quality of service software prediction. *Proc. SPIE*, 5892:01–12, 2005.

[18] G. Brussaard and P. A. Watson. *Atmospheric Modeling and Millimeter WavePropagation*. 1995.

[19] C. Chong and S. Kumar. Sensor networks: Evolution, opportunities, and challenges. *Proc. IEEE*, 91, no. 8:1247–1256, 2003.

[20] P. Clark and A. Sengers. Wireless optical networking: Challenges and solutions. *in MILCOM*, pages 416–422, October 2004.

[21] R. K Crane. Prediction of the effects of rain on satellite communication systems. *Proc. IEEE*, 65(3):456–474, 1977.

[22] R. K Crane. Prediction of attenuation by rain. *IEEE Trans. Commun*, COM-28, 1980.

[23] R. K. Crane. A two-component rain model for the prediction of attenuation statistics. *Radio Sci.*, 20, 1982.

[24] R. K. Crane and Horng-Chung Shieh. A two-component rain model for the prediction of site diversity performance. *Radio Sci.*, 24, 1989.

[25] D. Culler, D. Estrin, and M. Srivastava. Overview of wireless sensor networks. *IEEE Computer*, Vol. 37, Special Issue in Sensor Networks, No. 8,:41–49, 2004.

[26] C. C. Davis, I. I. Smolyaninov, and S. D. Milner. Flexible optical wireless links and networks. *IEEE Communication Magazine*, pages 51–57, March 2003.

[27] S. Deng, J. Liao, Z. Rena Huang, M. Hella, and K. Connor. Wireless connections of sensor network using rf and free space optical links. *Proc. SPIE*, 6773:677307–1–677307–11, 2007.

[28] IEEE Standards Department, Wireless LAN Medium Access Control (MAC), Physical Layer (PHY) specifications, Spectrum, and Transmit Power Management Extensions in the 5 GHz band in Europe. Amendment 5 to IEEE standard 802.11. 802.11h -2003, 2003.

[29] IEEE Standards Department, Wireless LAN Medium Access Control (MAC), and Physical Layer (PHY) specificationsIEEE standards. 802.11-1997, 1997.

[30] J. Derenick, C. Thorne, and J. Spletzer. Hybrid free-space optics/radio frequency (fso/rf) networks for mobile robot teams http://www.cse.lehigh.edu/ spletzer/publications/multibot05.pdf.

[31] J. Derenick, C. Thorne, and J. Spletzer. On the deployment of a hybrid free-space optic/radio frequency (fso/rf) mobile ad-hoc network. In *IEEE/RSJ International Conference on Intelligent Robots and Systems (IROS)*, pages 3990–3996, August 2005.

[32] A. M. Efe, A. M. Ceylan, F. Ari, Z. Telatar, H. Gokhan Ilk, and S. Tugac. An experimental hybrid fso/rf communication system http://www.actapress.com/paperinfo.aspx?paperid=13974&reason=500.

[33] R.G. Eldridge. Haze and fog aerosol distributions. *Journal of atmospheric sciences*, 23:605–613, 1966.

[34] Damosso et. al. A systematic comparison of rain attenuation prediction methods for terrestrial paths. In *Proc. open symposium on effects of lower atmosphere on radio frequencies above 1GHz, Lennoxville, Que*, 1980.

[35] J. Stankovic et. al. Real time communication and coordination in embedded sensor networks. *Proc. IEEE*, 91, no. 7:1002–1022, 2003.

[36] L. Castanet et al. Influence of the variability of the propagation channel on mobile, fixed multimedia and optical satellite communications. *ISBN-13: 978-3832269043, Shaker Verlag*, Feb. 2008.

[37] P.W. Kruse et al. *Elements of infrared technology: Generation, Transmission and Detection*. J. Wiley and Sons, New York, 1962.

[38] B. Flecker, M. Gebhart, E. Leitgeb, S. Sheikh Muhammad, and C. Chlestil. Results of attenuation-measurements for optical wireless channel under dense fog conditions regarding different wavelengths. *Proc. SPIE*, 6303, 2006.

[39] A. Geiger, C. Ting, E.J. Burlbaw, J. Ding, and S. Sheua. 3.5 micron free-space laser communications. *Proc. SPIE*, 6304:63041L1–L9, 2006.

[40] H. Hemmati. *Deep Space Optical Communications*. John Wiley &Sons, 2006.

[41] T.H. Ho, S. Trisno, A. Desai, J. Llorca, S. D. Milner, and C. C. Davis. Performance and analysis of reconfigurable hybrid fso/rf wireless networks. *Proc. SPIE*, 5712:119–130, January 2005.

[42] Z. Jia, F. Ao, and Qinglin Zhu. Ber performance of the hybrid fso/rf attenuation system. In *7th International Symposium on Antennas, Propagation & EM Theory, 2006. ISAPE '06.*, Oct.2006.

[43] H. Jiang, M. Sano, and M. Sekine. Weibull raindrop-size distribution and its application to rain attenuation. *IEE Proc. Microwaves, Antennas and Propagation*, pages 197–200, 1997.

[44] J. Joss, J.C. Thams, and A. Waldvogel. The variation of raindrop-size distribution at locarno. *Proc. of international conference on Cloud physics*, page 1967, 369-313.

[45] T. Kamalakis, I. Neokosmidis, T. Tsipouras, A. andSphicopoulos, S. Pantazis, and I. Andrikopoulos. Hybrid free space optical/millimeter wave outdoor links for broadband wireless access networks. In *PIMRC*, pages 1–5, 2005.

[46] A. Kashyap and M. Shayman. Routing and traffic engineering in hybrid rf/fso networks. *Proc. IEEE International Conference on Communications, ICC*, pages 3427–3433, May 2005.

[47] I. Kim and E. Korevaar. Availability of free space optics (fso) and hybrid fso/rf systems. *Optical wireless communication*, IV, August 2001.

[48] I. Kim, B. McArthur, and E. Korevaar. Comparison of laser beam propagation at 785 and 1550 nm in fog and haze for opt. wireless communications. *Proc. SPIE*, 4214:26–37, 2001.

[49] W. Kogler, P. Schrotter, U. Birnbacher, E. Leitgeb, and O. Koudelka. Hybrid wireless networks Ű high availability with combined optical / microwave links. *Beitrag zur Konferenz tcmc2003 (telecom. and mobile computing), Graz*, 11-12. March 2003 http://www.optikom.tugraz.at/content/view/32/61/lang,german/.

[50] J.O. Laws and D.A Parsons. The relation of raindrop size to intensity. *Trans. Am. Geophys. Union*, 24:452–460, 1943.

[51] P. P. Lawson, R. E. Stewart, and L. J. Angus. Observations and numerical simulations of origin and development of very large snowflakes. *Journal Atmos. Sc.*, 55:3209–3229, 1998.

[52] E. Leitgeb and M. Gebhart. High availability of hybrid wireless networks. In *Proc. SPIE*, volume 5654, pages 238–249, 2004.

[53] E. Leitgeb, S. Sheikh Muhammad, C. Chlestil, M. Gebhart, and U. Birnbacher. Reliability of FSO links in next generation optical networks. In *ICTON*, pages 394–401, 2005.

[54] J. Llorca, A. Desai, E. Baskaran, S. Milner, and C. Davis. Optimizing performance of hybrid fso/rf networks in realistic dynamic scenarios. *Proc. SPIE*, 5892:589207 1–9, August 2005.

[55] A. Mahdy and J. S. Deugon. Wireless optical communications: A survey. *in IEEE Wireless Communications and Networking Conference (WCNC)*, pages 2399–2404, March 2004.

[56] A. K. Majumdar and J. C. Ricklin. *Free-Space Laser Communications, Principles and Advances*. Springer Science LLC, 2008.

[57] J.S. Marshall and W.M.K Palmer. The distribution of raindrops with size. *Journal of Meteorol.*, 5:165–166, 1948.

[58] S. D. Milner and C. C. Davis. Hybrid free space optical/RF networks for tactical operations. In *MILCOM*, pages 409–415, 2004.

[59] S. Sheikh Muhammad, B. Flecker, E. Leitgeb, and M. Gebhart. Characterization of fog attenuation in terrestrial free space optical links. *Journal of Optical Engineering*, 46(6):066001, June 2007.

[60] S. Sheikh Muhammad, P. Kohldorfer, and E. Leitgeb. Channel modeling for terrestrial free space optical links. In *ICTON*, pages 407–410, 2005.

[61] M. Al Naboulsi and H. Sizunand F. de Fornel. Fog attenuation prediction for optical and infrared waves. *Optical Engineering*, 43(2):319–329, February 2004.

[62] M. Al Naboulsi, H. Sizun, F. de Fornel, M. Gebhart, and E. Leitgeb. Availability prediction for free space optic communication systems from local climate visibility data. *COST 270 Short Term Scientific Mission Report*, 2003.

[63] F. Nadeem, M.S. Awan, E. Leitgeb, S. Sheikh Mohammed, M.S. Kan, and G. Kandus. Comparing the cloud attenuation for different optical wavelengths. *accepted for ICET*, 2009.

[64] F. Nadeem, S. Chessa, E. Leitgeb, M.S. Awan, and G. Kandus. Comparing the life time of hybrid network using optical wireless and rf links to only rf link for terrestrial wireless sensor networks. *Proc. IEEE IWCMC, Cannes, France*, 2009.

[65] F. Nadeem, M. Gebhart, E. Leitgeb, W. Kogler, M. S. Awan, M. S. Khan, and G. Kandus. Simulations and analysis of bandwidth efficient switch-over between fso and mmw links. *Proc. IEEE SoftCOM, Split-Dubrovnik, Croatia*, 246-351, 2008.

[66] F. Nadeem, B. Geiger, M. Henkel, E. Leitgeb, M. Löschnig, A. Chaman Motlagh, and G. Kandus. Switch-over implementation and analysis for hybrid wireless network of optical wireless and ghz links. *Proc. IEEE WTS, Prague, Czech Republic*, 2009.

[67] F. Nadeem, B. Geiger, E. Leitgeb, M. Saleem Awan, and G. Kandus. Evaluation of switch-over algorithms for hybrid fso-wlan systems. *Proc. IEEE Wireless Vitae, Alborg, Denmark*, 2009.

[68] F. Nadeem, B. Geiger, E. Leitgeb, M.S. Awan, M. Gebhart, and G. Kandus. Comparison of wireless optical communication availability data and traffic data. *Proc. IEEE VTC, Barcelona, Spain*, April 2009.

[69] F. Nadeem, M. Henkel, B. Geiger, E. Leitgeb, M.S. Awan, and G. Kandus. Implementation and analysis of load balancing switch over for hybrid wireless network. *Proc. IEEE WCNC , Budhapest, Hungary*, 2009.

[70] F. Nadeem, V. Kviscera, M.S. Awan, E. Leitgeb, S. Sheikh Mohammed, and G. Kandus. Weather effects on hybrid fso/rf communication link. *accepted for special issue on "Optical Wireless Communication" of IEEE Journal of Selected Areas in Communication*.

[71] F. Nadeem and E. Leitgeb. *Book chapter "Availability Estimation via Simulation for Optical Wireless Communication" accepted for the book "Simulation Methods for Reliability and Availability of Complex Systems"*. Sprinnger-Verlag London.

[72] F. Nadeem and E. Leitgeb. Comparing the cloud effects on hybrid network using optical wireless and ghz links. *accepted for CSNDSP 2010, UK*.

[73] F. Nadeem, E. Leitgeb, M.S. Awan, and G. Kandus. Forward prediction of fso received signal for fso/rf hybrid network. *Proc. IEEE IWSSC, Siena, Italy*.

[74] F. Nadeem, E. Leitgeb, M.S. Awan, and G. Kandus. Comparing the snow effects on hybrid network using optical wireless and ghz links. *Proc. IEEE IWSSC, Siena, Italy*, 2009.

[75] F. Nadeem, E. Leitgeb, M.S. Awan, and G. Kandus. Comparison of different models for prediction of attenuation from visibility data. *Proc. IEEE IWSSC, Siena, Italy*, 2009.

[76] F. Nadeem, E. Leitgeb, M.S. Awan, and G. Kandus. Fso/rf hybrid network availability analysis under different weather condition. *Proc. IEEE NGMAST, Cardiff, UK*, 2009.

[77] F. Nadeem, E. Leitgeb, M.S. Awan, and G. Kandus. Optical wavelengths comparison for different weather conditions. *Proc. IEEE IWSSC, Siena, Italy*, 2009.

[78] F. Nadeem, E. Leitgeb, M.S. Awan, and G. Kandus. Comparison of fso 10 micrometer availability with fso 850 nm/rf hybrid network availability. *Proc. IEEE VTC, Alaska, USA*, September 2009.

[79] F. Nadeem, E. Leitgeb, M.S. Awan, and M.S. Khan. Simulation of switch over for fso and mmw for four years measured data of fso availability. In *DLR Institute of Communications and Navigation 2nd SatNEX JA2310 Workshop, Oberpfaffenhofen, Germany*, April 17-18, 2008.

[80] F. Nadeem, E. Leitgeb, M. S. Khan, and M. S. Awan. Availability simulation of switch over for fso and mmw. *Proc. IEEE International Conference on Information and Emerging Technologies, ICIET, Karachi, Pakistan*, pages 95–99, 2007.

[81] F. Nadeem, E. Leitgeb, M. S. Khan, M. S. Awan, and T. Javornic. Comparing the fog effects on hybrid network using optical wireless and ghz links. *Proc. IEEE CSNDSP, Graz, Austria*, pages 278–282, 2008.

[82] F. Nadeem, E. Leitgeb, M. S. Khan, M. S. Awan, and G. Kandus. Throughput efficient solution for hybrid wireless network. *Proc. IEEE IWSSC, Toulouse, France,*, October 2008.

[83] F. Nadeem, E. Leitgeb, O. Koudelka, and G. Kandus. Comparing the rain effects on hybrid network using optical wireless and ghz links. *Proc. IEEE ICET , Rawalpindi, Pakisatn,*, pages 156–161, 2008.

[84] F. Nadeem, E. Leitgeb, V. Kvicera, M. Grabner, M.S. Awan, and G. Kandus. Simulation and analysis of fso/rf switch over for different atmospheric effects. *Proc. IEEE Contel, Zagreb, Croatia*, 2009.

[85] T. Oguchi. Electromagnetic wave propagation and scattering in rain and other hydrometeors. *Proc. IEEE*, 71, No.9, September 1983.

[86] R.L. Olsen, D. V. Rogers, and D. B. Hodge. The a.rb relation in the calculation of rain attenuation. *IEEE Trans. Antenna Propag.*, AP-26(2):318–329, 1978.

[87] T. Oomori and S. Aoyagi. A presumptive formula for snowfall attenuation of radio waves. *Trans. Inst. Electron. Commun. Eng. Japan (in Japanese)*, S B:451–458, 1971.

[88] Recommendations ITU-R P.838-1. Specific attenuation model for rain for use in prediction methods.

[89] Recommendation ITU-R P.840-3. Attenuation due to clouds and fog.

[90] J.A.R. Pacheco de Carvalho, H. Veiga, P.A.J. Gomes, and A.D. Reis. Experimental development and study of Wi-Fi and FSO links. In *CSNDSP*, pages 137–141, July 2008.

[91] A. Pavelchek, R. Trissel, J. Plante, and S. Umbrasas. Long wave infrared (10 micro m) free space optical communication. *Proc. SPIE*, 5160:247–252, 2004.

[92] Pruppacher H. R.and R.L. Pitter. A semi empirical determination of the shape of cloud and rain drops. *Journal of Atmosph. Sc.*, 28:86–94, 1971.

[93] G. J. Pottie and W. J. Kaiser. Wireless integrated network sensors. *Commun. ACM*, 43:551–558, May 2000.

[94] T. C. Ramadorai. Rain attenuation and prediction in the satellite-earth path. *Proc. Workshop HF VHF and Microwave Communications, New Delhi, India*, February 1987.

[95] K. Roemer and F. Mattern. The design space of wireless sensor networks. *IEEE Wireless Communications*, 11, No. 6:54–61, 2004.

[96] A. Sana, H. Erkan, S. Ahmed , and M.A. Ali. Design and performance of hybrid fso/rf architecture for next generation broadband access networks. *Proc. of SPIE*, 6390:63900A, 2006.

[97] E. P. Shettle. Models of aerosols, clouds and precipitation for atmospheric propagation studies. *AGARD conference*, 454(15):1–13, 1989.

[98] S. Sivathasan and D. C. OŠBrien. Lifetime comparison of rf-only and hybrid rf/fso wireless sensor networks. *Proceedings of the International Conference on Computer and Communication Engineering , Kuala Lumpur, Malaysia*, pages 328–331, 2008.

[99] Jürgen Tanczos. Untersuchungen der Verfügbarkeit optischer Freiraumübertragungsstrecken. Master's thesis, Technical University of Graz, 2002.

[100] D.R. Wisley T.H. Carbonneau. Opportunities and challenges for optical wireless; the competitive advantage of free space telecommunications links in todayŠs crowded market place. In *SPIE Conference on Optical Wireless Communications, Masachusetts*, 1998.

[101] M. Toyoshima, W. R. Leeb, H. Kunimori, and T. Takano. Comparison of microwave and light wave communication systems in space applications. *Optical Engineering*, 46 (1):015003, 2007.

[102] K. Watabe, M. Akiba, N. Hiromoto, T. Hayashi, K. Wakamori, Y. Takabe, Y. Chigai, and S. Ito. Characteristics of optical propagation through rain for infrared space communications. *IEICE Trans. Commun.*, E86-B:852–864, 2003.

[103] B. Widrow and Jr. M.E. Hoff. Adaptive switching circuits. *IRE Wescon Conv. Rec.*, pt. 4:96–104, . 1960.

[104] H. Wu, B. Hamzeh, and M. Kavehrad. Availability of airborne hybrid fso/rf links. *Proc. SPIE*, 5819:89–100, June 2005.

[105] H. Wu and M. Kavehrad. Availability evaluation of ground-to-air hybrid fso/rf links. *International Journal of Wireless Information Networks*, 14 No. 1, March 2007.

[106] C. B. Yahya. The role of optoelectronics in enabling low power sensor networks. *9th international symposium on Signal Processing and its applications*, pages 1–4, 2007.

[107] S. E. Yuter, D. E. Kingsmill, L. B. Nance, and M. Loffler-Mang. Observations of precipitation size and fall speed characteristics within coexisting rain and wet snow. *Journal Appl. Meteorol.*, 45:1450–1464, 2006.

OWN PUBLICATIONS

The work presented in this thesis has been published, in part, in the following journals and refereed conference proceedings.

As a first author

1. **F. Nadeem**, E. Leitgeb, M. S. Khan, M. Saleem Awan, "Availability simulation of Switch over for FSO and MMW", pp.95-99, International Conference on Information and Emerging Technologies, ICIET 2007, Karachi, Pakistan. (IEEE)

2. **F. Nadeem**, E. Leitgeb, M. Saleem Awan, M. S. Khan, "Simulation of Switch over for FSO and MMW for four years measured data of FSO availability", presented at the 2nd SatNEx International Propagation Workshop 2008, Oberpfaffenhofen, Munich, Germany, April 2008.

3. **F. Nadeem**, B. Flecker , E. Leitgeb , M. S. Khan, M. S. Awan, T. Javornik. "Comparing the Fog Effects on Hybrid Network using Optical Wireless and GHz Links", pp.278-282, CSNDSP 2008, Graz, Austria, July 2008. (IEEE)

4. **F. Nadeem**, E. Leitgeb , M. S. Awan , M. S. Khan , G. Kandus, "Throughput efficient solution for hybrid wireless network", accepted for IWSSC 2008, Toulouse, France, October 2008. (IEEE)

5. **F. Nadeem**, M. Gebhart, E. Leitgeb, W. Kogler, M. S. Awan, M. S. Khan, G. Kandus, "Simulations and analysis of bandwidth efficient switch-over between FSO and mmW links", (SoftCOM), pp. 346-351, Split-Dubrovnik, Croatia, 25-27 September 2008 (IEEE) **Best Conference paper award**

6. **F. Nadeem**, E. Leitgeb , O. Koudelka, G. Kandus. "Comparing the Rain Effects on Hybrid Network using Optical Wireless and GHz Links", pp156-161, ICET 2008, Rawalpindi, Pakisatn, October 2008.

7. **F. Nadeem**, E. Leitgeb, "Using combined FSO / MMW link for improving the link reliability on HAPS" article has been accepted for joint document D4c by European Union (EU) framework 6 programme JA-2220 SatNEx.

8. **F. Nadeem**, B. Geiger, M. Henkel, E. Leitgeb, M. Löschnig, A. Chaman Motlagh, G. Kandus, "Switch-over implementation and analysis for hybrid wireless network of optical wireless and GHz links," presented at IEEE WTS 2009

9. **F. Nadeem**, B. Geiger, E. Leitgeb, M. Saleem Awan, G. Kandus "Evaluation of Switch-Over Algorithms for Hybrid FSO-WLAN Systems" Presented at IEEE Wireless Vitae 2009

10. **F. Nadeem**, M. Henkel, B. Geiger, E. Leitgeb, M.S. Awan, G. Kandus "Implementation and analysis of load balancing switch over for hybrid wireless network" Presented at WCNC 2009

11. **F. Nadeem**, B. Geiger, E. Leitgeb, M.S. Awan, M. Gebhart, G. Kandus "Comparison of wireless optical communication availability data and traffic data" Presented at VTC Spring 2009

12. **F. Nadeem**, E. Leitgeb, V. Kvicera, M. Grabner ,M.S. Awan, , G. Kandus," Simulation and analysis of FSO/RF switch over for different atmospheric effects" Presented at Contel 2009, Croatia

13. **F. Nadeem**, E. Leitgeb, M.S. Awan, G. Kandus," FSO/RF Hybrid Network Availability Analysis Under Different Weather Condition" accepted for NGMAST,09, (UK)

14. **F. Nadeem**, E. Leitgeb, M.S. Awan, G. Kandus," Comparison of FSO 10 micrometer availability with FSO 850 nm/RF hybrid network availability" accepted for VTC fall,09 (USA)

15. **F. Nadeem**, S. Chessa, E. Leitgeb, M.S. Awan, G. Kandus," Comparing The Life Time of Hybrid Network Using Optical Wireless and RF Links To Only RF link For Terrestrial Wireless Sensor Networks " accepted for IWCMC 09, (France)

16. **F. Nadeem**, E. Leitgeb, M.S. Awan, T. Javornik, G. Kandus," Comparing The Snow Effects on Hybrid Network Using Optical Wireless and GHz Links " accepted for IWSSC 09 (Italy)

17. **F. Nadeem**, E. Leitgeb, M.S. Awan, G. Kandus," Optical Wavelengths Comparison For Different Weather Conditions " accepted for IWSSC 09 (Italy)

18. **F. Nadeem**, E. Leitgeb, M.S. Awan, G. Kandus," Comparison of different models for prediction of attenuation from visibility data" accepted for IWSSC 09 (Italy)

19. **F. Nadeem**, E. Leitgeb, M.S. Awan, G. Kandus," Forward Prediction of FSO received signal for FSO/RF hybrid network" accepted for IWSSC 09 (Italy)

20. **F. Nadeem**, M. Gebhart, E. Leitgeb, M.S. Awan, B. Geiger, M. Henkel, G. Kandus," Performance Analysis of Throughput Efficient Switch-over between FSO and mmW Links" accepted for Journal of Communication Sytems and Software (JCOMSS)

21. **F. Nadeem**, V. Kviscera, , M.S. Awan, E. Leitgeb, S. Sheikh Mohammed, G. Kandus," Weather Effects on Hybrid FSO/RF Communication Link " accepted for special issue on " Optical Wireless Communication " of IEEE Journal of Selected Areas in Communication

22. **F. Nadeem**, E. Leitgeb,"Availability Estimation via Simulation for Optical Wireless Communication", accepted as a book chapter for "Simulation Methods for Reliability and Availability of Complex Systems" book by Springer

23. **F. Nadeem**, M.S. Awan, E. Leitgeb, S. Sheikh Mohammed,M.S. Kan, G. Kandus," Comparing the Cloud Attenuation for Different Optical Wavelengths " accepted for ICET 2009.

24. **F. Nadeem**, E. Leitgeb,"Comparing The Cloud Effects on Hybrid Network Using Optical Wireless and GHz Links", accepted for CSNDSP 2010 (UK)

25. **F. Nadeem**, E. Leitgeb,"Dense Maritime Fog attenuation Prediction from measured visibility data", accepted for Special issue on Free Space Optical Communication of the Journal of Radioengineering.

26. **F. Nadeem**, S. Chessa, E. Leitgeb et. al " The Effects of Weather on the Life Time of Wireless Sensor Networks Using FSO/RF Communication ", accepted for Special issue on Free Space Optical Communication of the Journal of Radioengineering.

27. **F. Nadeem**, B. Geiger, E. Leitgeb et. al " Comparison of Link Selection Algorithms for FSO/RF Hybrid Network ", accepted for IET Communication Journal.

As a coauthor

1. M. S. Awan, E. Leitgeb, **F. Nadeem** et al. "Analysis of Free Space Optical Links under Moderate Fog Conditions in Graz and Milan and Behaviour of the Drop Size Distribution Parameters", presented at 2nd SatNEx International Propagation Workshop 2008, Oberpfaffenhofen, Munich, Germany, 17-18 April 2008.

2. M. S. Awan, E. Leitgeb, **F. Nadeem** et al. "Distribution Function for Continental and Maritime Fog Environments for Optical Wireless Communication", CSNDSP 2008, pp. 260-264, Graz, Austria, 23-25 July 2008. (IEEE)

3. M. S. Awan, C. Capsoni, E. Leitgeb, **F. Nadeem** et al. "FSO-Relevant New Measurement Results under Moderate Continental Fog Conditions at Graz and Milan", ASMS 2008, pp. 111-115, Bologna, Italy, 26-28 August 2008 (IEEE)

4. M. S. Awan, E. Leitgeb, C. Capsoni, **F. Nadeem** et al. "Attenuation Analysis for Optical Wireless Link Measurements under Moderate Continental Fog Conditions at Milan and Graz", VTC 2008-Fall, pp. 1-5, Calgary, Canada, 21-24 September 2008 (IEEE)

5. M. S. Awan, E. Leitgeb, C. Capsoni et al. "Evaluation of Fog Attenuations Results for Optical Wireless Links in Free Space", IWSSC 2008, pp. 112-116, Toulouse, France, 1-3 October 2008. (IEEE)

6. M. S. Awan, C. Capsoni, O. Koudelka, E. Leitgeb, **F. Nadeem**, M. S. Khan, "Diurnal Variations Based Fog Attenuations Analysis of an Optical Wireless Link", presented at IEEE Photonics Global 2008, pp. 1 - 4, 8-11th December 2008, Singapore. (IEEE)

7. M. S. Awan, Marzuki, E. Leitgeb, **F. Nadeem**, M. S. Khan, C. Capsoni, "Weather Effects Impact on the Optical Pulse Propagation in Free Space", VTC 2009-Spring, 26-29 April 2009, Barcelona, Spain. (IEEE)

8. M. S. Awan, E. Leitgeb, R. Nebuloni, **F. Nadeem**, M. S. Khan, "Optical Wireless Ground- Link Attenuation Statistics of Fog and Snow Conditions", WOCN 2009, April 28 -30, 2009, Cairo, Egypt. (IEEE)

9. M. S. Awan, L. Csugai-Horvath, R. Nebuloni, P. Brandl, **F. Nadeem**, E. Leitgeb, "Transmission of high data rate optical signals in fog and snow conditions", Wireless Vitae 2009, 17-20 May, 2009, Aalborg, Denmark. (IEEE)

10. M. S. Awan, E. Leitgeb, **F. Nadeem**, Carlo Capsoni, "Results in an Optical Wireless Ground link Experiment in Continental Fog and Dry Snow Conditions", ConTel 2009, 8-10 June 2009, Zagreb, Croatia. (IEEE)

11. M. S. Awan, E. Leitgeb, **F. Nadeem**, Carlo Capsoni, "Spatial and time variability of fog attenuations for optical wireless links in the troposphere", accepted for VTC 2009-Fall, September 20 - 23, 2009, Anchorage (Alaska), USA. (IEEE)

12. M. S. Awan, E. Leitgeb, **F. Nadeem**, C. Capsoni, "A new method of predicting continental fog attenuations for terrestrial optical wireless link", accepted for NGMAST 2009, 15-18 September 2009, Cardiff, UK. (IEEE)

13. M. S. Awan, E. Leitgeb, **F. Nadeem**, Carlo Capsoni, "Path reduction factor concept in the prediction of fog attenuations for terrestrial optical wireless links", accepted for IWSSC 2009, 10-11 September 2009, Sienna, Italy. (IEEE)

14. M. S. Awan, R. Nebuloni, C. Capsoni, L. Csurgai-Horváth, S. Sheikh Muhammad, E. Leitgeb, **F. Nadeem**, M. S. Khan "Prediction of Drop Size Distribution Parameters for Optical Wireless Communications through Moderate Continental Fog", accepted for International Journal on Satellite Communications and Networks special issue.

15. M. S. Awan, **F. Nadeem** et. al., "Characterization of Fog and Snow attenuations for Free-Space Optical Propagation", an extended version submitted for publication at Journal of Communication special issue on Optical Wireless Communication.

16. M. S.Khan, M.S. Awan, E. Leitgeb, **F. Nadeem** ,I. Hussain, "Selecting a Distribution Function for optical attenuation in dense continental fog conditions" accepted for ICET 2009.

17. E. Leitgeb, M. S. Awan, P. Brandl, T. Plank, C. Capsoni, R. Nebuloni, T. Javornik, G. Kandus, S. Sheikh Muhammad, F. Ghassemlooy, M. Löschnigg, **F. Nadeem**, "Current Optical Technologies for Wireless Access", ConTel 2009, 8-10 June 2009, Zagreb, Croatia

18. E. Leitgeb, M. S. Awan, T. Plank, N. Perlot,**F. Nadeem** et. al, "Investigations on Free-Space Optical Links within SatNEx II" , Eucap 2009, 23-27 March 2009, Berlin, Germany